PAN-AFRICAN UNIVERSITY

INSTITUTE FOR WATER AND ENERGY SCIENCES

(including CLIMATE CHANGE)
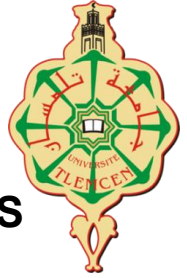
Master Dissertation

Submitted in partial fulfillment of the requirements for the Master degree in

ENERGY ENGINEERING

Presented by

Tariro Cynthia Mutsindikwa

TITLE: AN ASSESSMENT OF THE IMPACTS OF CLIMATE CHANGE ON HYDROPOWER POTENTIAL IN WEST AFRICA CASE STUDY: BAMBOI CATCHMENT (BLACK VOLTA)

Defended on 04/09/2019 Before the Following Committee

Chair	Abdellatif Zerga	Prof.	PAUWES, Algeria
Supervisor	Rabani Adamou	Prof.	University of Niamey, Niger
Co-supervisor	Yacouba Yira	Dr.	IRSAT/WASCAL, Burkina Faso
External Examiner	Amine B Stambouli	Prof.	University of Oran, Algeria
Internal Examiner	SM Chabane Sari	Prof.	PAUWES, Algeria

APPROVAL PAGE

AN ASSESMENT OF THE IMPACTS OF CLIMATE CHANGE ON HYDROPOWER POTENTIAL IN WEST AFRICA, CASE STUDY: BAMBOI CATCHMENT (BLACK VOLTA)

Submitted by

Tariro Cynthia Mutsindikwa   11 /09 /2019

 Student   Signature   Date

Approved by Examining Board

_____   _____   _____

Name of Examiner   Signature   Date

…………………………   _____   _____

Name of Advisor   Signature   Date

Prof Abdellatif Zerga
                                             _____   _____

Name of Director   Signature   Date

Pan African University

_____   _____   _____

Name of Rector   Signature   Date

DEDICATION

I dedicate this research to my beloved parents, siblings and all those who have an interest in Climate science.

Statement of the author

Name of student :   Tariro Cynthia Mutsindikwa

Signature: Date 12 /09 /2019

Supervisor

Name: Prof. Rabani Adamou (for and on behalf, Dr Yira)

Signature.. ... .   Date 16 /09 /2019

Co-Supervisor

Name**:** Dr. Yacouba Yira

Signature …. ..……….……   Date 16 /09 /2019

ACKNOWLEDGEMENT

LIST OF ABBREVIATIONS AND ACRONYMS

CC   Climate Change

WASCAL   West African science service centre on climate change and adapted land use.

CIREG   Climate Information for integrated Renewable Electricity Generation

DEM   Digital Elevation Model

GEF   Global Environment Facility

FAO   Food and Agriculture organisation of the United Nations

GLOWA   Global change and hydrological cycle

IWRM   Integrated water resources management

UNEP   United Nations Environment Analysis

NGO   Non –governmental organisational

UNFCC   United Nations Framework Convention on climate change

VRA   Volta River Authority

NSE   Nash–Sutcliff efficiency

KGE   Kling–Gupta efficiency

R^2   Correlation coefficient

REMO   Regional climate model

CORDEX   Coordinated Regional Climate Downscaling Experiment (Africa) project

WRF   Weather Research Forecast

MPI   Max Plankton Institute

GFDLESM   Geo physical fluid dynamics laboratory

LIST OF UNITS

MW	Megawatt
kW	Kilowatt
kWh	Kilowatt per hour
GW	Gigawatts
m^3	cubic meters
mm	millimeters
rpm	revs per minute
c/kWh	kilowatt-hour

TABLE OF CONTENTS

LIST OF FIGURES

LIST OF TABLES

RÉSUMÉ

En raison de sa faible capacité d'adaptation, l'Afrique de l'Ouest est l'une des régions qui seront durement touchées par le changement climatique. Cette étude est réalisée dans le cadre principal du projet CIREG, qui est centré sur le développement de la production d'énergie renouvelable dans des conditions climatiques changeantes en Afrique de l'Ouest. L'étude a évalué les impacts du changement climatique futur sur le potentiel hydroélectrique du bassin versant de Bamboi (Volta Noire) en Afrique de l'Ouest en utilisant un modèle conceptuel de ruissellement pluie-eau (modèle léger HBV). Le modèle hydrologique a été calibré et validé avec succès pour le bassin versant avec des coefficients (rendements de Nash-Sutcliffe, KGE, R^2) compris entre 0,59, 0,73 et 0,57 respectivement au cours des phases de calibration et de validation du modèle. Deux simulations climatiques MPI-ESM-REMO du projet CORDEX-Africa et GFDL-ESM2M-WRF de WASCAL sous RCP4.5 ont été appliquées au modèle hydrologique validé pour simuler le ruissellement du bassin versant. Une correction statistique du biais (cartographie quantile) a été appliquée pour corriger les biais inhérents aux données climatiques et deux périodes futures (2020-2049 et 2070-2099) ont été comparées à une période de référence (1983-2005). Les signaux du changement climatique entre différentes périodes ont été comparés et l'impact sur l'hydrologie du bassin versant a été analysé. Les données historiques et projetées sur les débits ont été converties en potentiel hydroélectrique selon une approche de production d'hydroélectricité au fil de l'eau. Les modèles prévoient une augmentation de la température de 0,8 et 2,8 ° C d'ici 2020-2049 et 2070-2099, respectivement. L'augmentation des précipitations de 11% et 6,6% pour la période 2020-2049 et de 10,9% et 3,7% pour la période 2070-2099 est projetée respectivement par l'ensemble de données climatiques WASCAL et CORDEX. Le débit suivra le modèle de précipitation. Il devrait augmenter de 11,4% pour la période 2020-2049 et atteindre 9,2% pour la période 2070-2099 pour les modèles climatiques moyens. Au contraire, une baisse globale de la production d'hydroélectricité de -8,9% et de -7,5% (ensemble moyen) a été projetée pour 2020-2049 pour les données corrigées et non corrigées par rapport à la période de référence. Malgré une légère augmentation de la production d'hydroélectricité vers la fin du siècle 2070-2099, par rapport à la période 2020 - 2049, elle reste inférieure à la période historique, avec une diminution globale de - 7,7% et -1% pour les données corrigées et les données non corrigées respectivement comparées à la période historique. Ces résultats s'expliquent par une augmentation des débits en saison des pluies non convertible en énergie hydraulique combinée à une diminution des débits en période sèche

entraînant d'importantes pertes d'énergie hydroélectrique. Mots-clés: changement climatique, hydroélectricité et correction des bias.

ABSTRACT

Due to its low adaptive capacity, West Africa is one of the regions which will be severely affected by climate change. This study is carried out in the main framework of the CIREG project, which is centered towards developing renewable energy generation under changing climate in West Africa. The study evaluated the impacts of future climate change on the hydropower potential of the Bamboi catchment (Black Volta) in West Africa using a conceptual rainfall-runoff model (HBV light model). The hydrological model was successfully validated for the catchment with coefficients (Nash-Sutcliffe efficiencies, KGE, R^2) ranging from 0.59, 0.73 and 0.57 respectively during the model calibration and validation phases. Two climate simulations MPI-ESM-REMO of CORDEX-Africa project and GFDL-ESM2M-WRF of WASCAL both under RCP4.5 were applied to the validated hydrological model to simulate the catchment runoff. A statistical bias correction (quantile mapping) was applied to correct the biases inherent in the climate data and two future periods (2020-2049 and 2070-2099) were compared to a reference period (1983-2005). The climate change signals between different periods were compared and impact on the hydrology of the catchment analyzed. Both historical and projected discharges data were converted to hydropower potential following a run-of-river hydroelectricity generation approach. The model mean ensemble projected a temperature increase of 0.8 and 2.8 °C by 2020-2049 and 2070-2099, respectively. Precipitation increase of 11% and 6.6 % for the 2020-2049 period and 10.9 % and 3.7 % for 2070 -2099 are projected by WASCAL and CORDEX climate dataset respectively. Discharge will follow the pattern of precipitation. It is projected to increase by 11 .4 % for 2020 - 2049 period and increase to 9.2% for the 2070-2099 period for climate models mean. On the contrary an overall decrease of hydropower production by -8.9 % and -7.5 (mean ensemble) was projected for 2020 -2049 for corrected and un corrected data respectively compared to reference period. Although, there is a slight increase of hydropower generation near end of the century 2070-2099, compared to the 2020 – 2049 period it is still lower than the historical period -7.7% and -1% for corrected and un corrected data respectively compared to the historical period. These results are explained by an increase in discharge in the rainy season not convertible into hydropower combined with a decrease in discharge during the dry months that leads to important hydropower losses.

Key words: Climate change, Hydropower and Bias correction

CHAPTER ONE: INTRODUCTION

1.1. BACKGROUND

Hydropower is a cheap, clean and environmentally friendly renewable energy source for power generation (Berga, 2016). It is often economically competitive and its role is expected to grow in the coming years because of its good synergies with other generation technologies. Currently hydropower contributes 16% of the world's generated electricity and 78% of the renewable electricity generation (Berga, 2016). Correspondingly, in West Africa hydropower is the leading source of renewable energy and it offers many benefits to the society which are water services, electricity and facilitates regional and economic development. It is reported that hydropower impedes the flow of 9% of global annual CO2 emissions by virtue of its nature (Berga, 2016). On the contrary it is reported that climate variabilities have caused fluctuations in world's precipitation making the hydropower industry more vulnerable (Khaniya et al., 2018).

Hydropower and climate change have a double relationship where by hydropower mitigates climate change by hindering the flow of greenhouse emissions into the atmosphere which causes global warming through the emission of heat trapping gases to the atmosphere (Berga, 2016). On the other hand, climate change is more likely to reduce the rainfall occurrence which decreases discharge evolutions in rivers. Decrease in discharge evolutions impact water availability there by affecting hydropower generation (Boadi et al., 2017). Quantitative estimation of the hydrological effects of climate change is therefore essential for solving future water problems. The dependency of renewable electricity on hydro-climatological conditions also exposes energy systems to the stochastic nature of climate variability and change. Given future climate variability and change the climate resilience of renewable electricity generation (REG) must be investigated; and science-based information on actual and future potential renewable electricity generation delivered to decision makers. This study is carried out in the main frame work of CIREG (Climate Information for integrated Renewable Electricity Generation) project, which is centered towards developing renewable energy generation under changing climate conditions in West Africa. The main goals of the CIREG projects in West Africa countries are to deliver demand-driven climate services to support renewable energy planning in West Africa and to support decision towards sustainable electricity generation with a high share of renewables. The purpose of this study is to assess the

impacts of climate change on renewable energy resources in the Black Volta basin by assessing how hydropower potential will be affected by climate change in future.

Definition of key terms

Climate change is a change of climate which is directly or indirectly caused by human activities that changes the state and composition of the global atmosphere. This change of state of global atmosphere will cause temperature to rise, glaciers to melt, and frequent droughts in some regions (IPCC, 2018) .

Climate models are mathematical representation of the climate system based on the physical, chemical and biological properties of its components, their interactions and feedback processes, and accounting for all or some of its known properties (Tirpack et al, 2006)

Hydropower is a renewable source of energy which derives its energy from falling water through a gradient to produce electricity.

1.2. PROBLEM STATEMENT

Due to its low adaptive capacity, West Africa is one of the regions which will be severely affected by climate change. Several studies have shown that discharge evolutions over the past decades in the Black Volta basin have been strongly affected by rainfall unreliability (Boadi et al., 2017). A strong rainfall deficit has been experienced since late 1960s in the Volta region with some dramatic droughts like the 1973/1974 and 1983/1984 ones (Boadi et al., 2017) .These rainfall variations have led to strong fluctuations in river discharge with a generally negative trend from 1960 to 2010 (Boadi et al., 2017). The decrease in discharge affects the hydropower potential of the region. The amount of precipitation in the region is expected to decrease by 0.5-40 percent by 2025, with an average decrease of 10-20 percent (USAID, 2017) . In addition, the majority of climate models in West Africa predicts an overall warming trend throughout the region with an estimated temperature increase of 0.5 ° C per decade (Sylla et al.,2016) . These rising temperatures increases the water evaporation causing a further decrease in the hydro power potential of the region. All the above aforesaid information gives a reason for assessing how these changing climatic conditions will affect hydropower potential which is one of the main sources of energy in the Volta Basin. Furthermore, scientific evidences about how climate change will affect hydropower generation in the catchment are less documented which creates a gap that need to be filled.

1.3. MAIN OBJECTIVE

The main objective of this study is to assess the impact of climate change on the hydropower potential of the Bamboi catchment in the Black Volta basin in West Africa.

1.3.1. Specific objectives

1. To set up the conceptual hydrological simulation model HBV light for the Bamboi catchment.
2. To assess the impact of future climate change on the hydrological regime of the catchment through scenario (RCP4.5) application comparing a reference period (1983-2005) to two future periods (2020-2049 and 2070-2099).
3. To assess the impact of climate change on hydropower potential of the catchment based on runoff data.

1.4. RESEARCH QUESTIONS

The study is designed to address the following research questions which will be explored throughout the thesis:

1. How efficient is the HBV hydrological model in simulating the hydrological regime of the Bamboi catchment?
2. What is the future climate change signal for the Bamboi catchment (comparing a reference period) 1983-2005 to two future periods (2020-2049 and 2077-2099)?
3. What is the expected impact of climate change on the hydropower potential of the Bamboi catchment?

1.5. HYPOTHESIS

H1: The HBV light model is able to simulate the hydrological regime of Bamboi catchment.

H2: Climate change will affect the hydrology of the Bamboi catchment.

H3: Climate change will impact the hydropower potential of the catchment.

1.6. LITERATURE REVIEW

Several studies have already assessed the impacts of climate change on water resources in West Africa although little work was done on Bamboi catchment in particular. Yira et al, (2017) carried out a study on the impacts of climate change on hydrological conditions in a tropical West African catchment using an ensemble of climate simulations. An ensemble of six RCM–GCM data all

derived from the CORDEX-Africa project was used as inputs to the hydrological model (WaSiM) in the Dano catchment. An assessment of historical runs of the models were done and a statistical bias correction was applied to the daily precipitation. Two periods were compared (1971–2000) as reference and (2021–2050) as future period to evaluate the impact of climate change under two greenhouse concentration pathway (RCPs) 4.5 and 8.5. The results showed an increase in temperature by 0.1 to 2.6 °C (Yira et al., 2017) . However, there is uncertainty in the precipitation and discharge evolvement in the future period as results of the models applied were contradicting. Another study was carried out in the Upper Senegal basin using REMO –MPI –ESMLR climate products under RCP4.5 and RCP 8.5 to assess the impacts of climate change on water resources. Two periods were compared 1971 -2000 and 2021 – 2100. The results indicate a decrease in the discharge by 80% (Mbaye et al., 2015) .

Obahoundje et al. (2015) undertook a research on potential impacts of land use, land cover change and climate change on hydropower generation at the Bui dam on the Black Volta. The study assessed the combined effect of climate and land use and land cover (LULC) changes, on the stream flow of the dam. The results showed that while climate change is predicted to decrease the power potential of Bui, LULC will reduce the impact of climate change. Climate change under the present conditions at Bui dam is predicted to reduce energy production by 23.2% with no LULC while it will reduce the hydropower by 0.5% taking into consideration LULC. Climate change under the dry scenario is predicted to decrease energy by 54% while under wet scenario is predicted to decrease the energy production by 0.15% (Obahoundje , 2015).

UNU WIDER and University of Ghana carried out a study on the assessment of the impacts of projected climate change on water availability and crop production in Volta Basin. Four climate change scenarios (two dry and two wet) were considered. The CliRun water model was used to simulate catchment runoff using forecasted rainfall and temperature under these scenarios. The WEAP model was used for water allocation. The results show that all the water demand be it hydropower, agriculture and municipal cannot be met under any of the scenarios used, calling for climate change mitigation and adaptation and integrated water resource management (Amisigo et al, 2014).

(Heinzeller et al, 2018) carried out an assessment on the WASCAL high-resolution regional climate simulation ensemble for West Africa which was developed at 12 km resolution. The

simulations cover the reference period 1980–2010 and the two future periods 2020–2050 and 2070–2100. From the results under RCP 4.5 scenario temperature is predicted to increase by 1.5∘C at the Guinea coast and by 3∘C in Northern Sahel. An increase in the precipitation by 300 mm along the coast of Guinea and by 150mm in the Soudano region and no change in precipitation in the Sahel region.

The current research attempts to assess the impacts of climate change on hydropower potential in the Volta basin by assessing the hydropower potential of the catchment based on runoff data. Many of the aforementioned studies assessed only the impact of climate change on water resources and not explicitly on the hydropower potential. Secondly, the studies that assessed the hydropower potential mainly focused on dam and not on run-off rivers systems. The current study combines climate impact assessment on water resources and hydropower potential of a run-of-river hydroelectricity system. Furthermore, the study applies a newly developed regional climate simulation product that has not yet been applied to climate impact assessment.

1.7. GENERAL METHODOLOGY

The diagram below fig 1.1 shows the general methodology to be applied in the current study in order to accomplish the objectives. The steps outlined will be followed in descending order. Detailed descriptions of each and every step is detailed in the next chapters.

Flowchart of the methodology
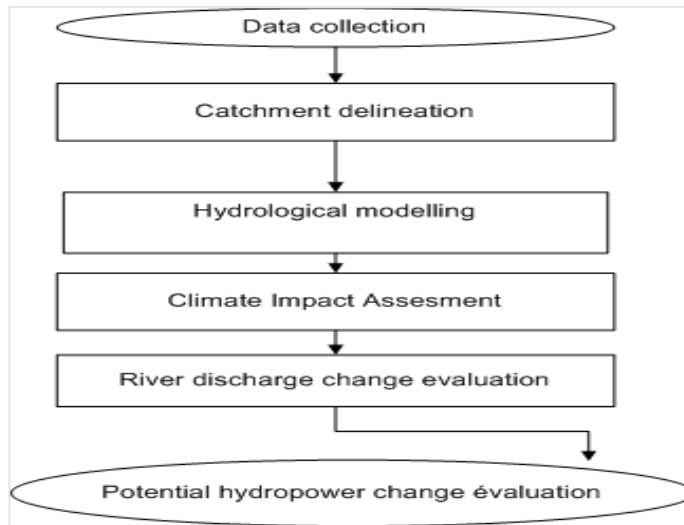
Figure 1.1 : Flow chart of the general methodology

How the objectives will be fulfilled?

Below is a brief summary of each objective and the method that will be applied to accomplish it.

Objective 1: To set up the conceptual hydrological simulation model HBV for the Bamboi catchment;

- The current research applied the HBV-light model to simulate the catchment hydrological regime.

Objective 2: To assess the impact of future climate change on the hydrological regime of the catchment through scenario (RCP4.5) application comparing three periods: (i) a reference period (1983-2005), (ii) the mid-century period (2020-2049), and (iii) the end of the century (2070-2099).

- The assessment will be done through the application of climate simulation products to the validated hydrological model. Climate simulations developed by WASCAL and CORDEX for the RCP4.5 scenarios will be applied and the mentioned three periods will be compared. The climate change signals between the three different periods will be compared and their impact on the hydrology of the catchment analysed**.**

Objective 3: To assess the impact of climate change on hydropower potential of the catchment based on runoff data.

- Historical and projected discharges data will be converted to hydropower potential following a run-of-river hydroelectricity generation approach. A hydroelectricity production model ($P0 = \rho g Q H n$) will be developed to simulate the energy production based on simulated discharge. Hydropower potential for historical and projected climate conditions will be compared to assess the climate impact on the hydropower generation potential of the catchment (Okot, 2013).

1.8. MOTIVATION OF THE STUDY

The main motivation of the study stems from the acknowledgement that hydropower is the major source of energy in Ghana contributing to over two thirds of its energy mix, therefore any change in the hydropower production in future will affect the economy of the country (Akpoti, 2016) .The study of climate change impacts on water availability and precipitation in the Volta basin is very important to the policy makers in the basin because the economy of the Volta basin countries depends on rain fed agriculture and hydropower generation (Neumann et al., 2010).

Summing up published work on climate change in the Volta basin few work has been done on assessing the impacts of climate change on Hydropower in Bamboi catchment, therefore creating the gap to carry out the research. This study is also motivated by the basis that rainfall is a key parameter in hydropower generation and understanding its present and future patterns which may be altered by climate change is necessary for planning. Several studies carried out in the Volta basin agree that the Volta basin is climate sensitive. Therefore, there is need to pay close attention to climate variability over the basin. This is important for planning of hydropower generation in the catchment.

1.9. PROJECT OUTLINE

The manuscript has seven chapters, the first chapter provides a general introduction, definition of the problem, historical overview and the research objectives and goals. The second chapter explores the relevant theories and published research work as well as the detailed explanations of the models to be used in the study. The third chapter describes the study area, climate and the geography of the area. Chapter four addresses the hydrological modelling (calibration and validation process and application). The fifth chapter presents the analysis of the projected climate

change signal in the catchment and their impact on its hydrological regime. Chapter 6 describes the hydropower generation model. Finally, chapter 7 provides an overall summary and the main conclusions derived from this study.

1.10. RELEVANCE OF THE STUDY

- This research is relevant because it is carried out in the main frame work of CIREG project area, which is centered toward developing renewable energy generation and climate change within West Africa with goals to foster demand-driven climate services to support renewable energy planning in West Africa and to support decision towards sustainable electricity generation.

- Predictions of climate change impacts on hydropower potential in the Black Volta is not absolute but it gives enough warning signs in the data that decision-makers need to be thinking of a more resilient mix of options for energy and agriculture to stand up to the climate challenge.

- This study is important to raise awareness on the climate change and strengthen the hydro-meteorological information.

- This study draws attention to the importance of considering climate vulnerability in energy planning now and in the future.

- The study is also very important because it assesses the impact of future climate change on hydropower and will help in developing strategies to adapt to future climate change.

- Hydropower contributes significantly to the reduction of GHG emissions and to energy supply security. Hydropower projects also have an enabling role beyond the electricity sector, as a financing instrument for multipurpose reservoirs therefore the impacts of climate change that may affect it must be investigated in time and possible solutions to be provided as an adaptive measure regarding the impacts of climate change on water resource.

CHAPTER TWO: LITERATURE REVIEW

2.1. INTRODUCTION

In this chapter, three main literature blocks will be reviewed which are hydropower, climate change and climate modelling. The relevant literature related to the hydropower success stories in the world are presented and the main components for hydropower for a hydropower scheme are outlined. Furthermore, different hydrological models used to model the catchment runoff will be presented.

2.2. BACKGROUND OF WEST AFRICA

Figure 2.1: Background of West Africa
 (Source: Google Map)

The West African region of Africa lies between latitudes 4°N and 28°N and longitudes 15°E and 16°W (see fig Figure 2.1). West Africa has 16 countries Benin, Cape Verde, Gambia, Ghana, Guinea, Guinea-Bissau, Ivory Coast, Liberia, Mali, Mauritania, Niger, Nigeria, Senegal, Sierra Leone, Togo and Burkina Faso (FAO, 1985). The countries which are of particular interest in this research are Ghana, Burkina Faso, Ivory Coast and Mali because the study area spans across these

four countries and the discharge point of the catchment is located in Bole Bamboi in Northern Ghana (FAO, 1985). West Africa has 6 agro climatic zones which are humid mostly along the coast, sub humid covering the greater part of Ghana, sub humid covering Northern Ghana and Northern Nigeria and arid, semi-arid and lastly hyper arid.

2.3. CLIMATE CHANGE IN WEST AFRICA

West Africa is one of the world's most vulnerable regions to climate change and variability. There is evidence that Africa temperature will increase by 3 °C or 4°C by the end of century (UNDP, 2019). West African temperatures are predicted to increase by 1.5 and 4 °C by mid-century (FCFA, 2019). A clear warming is trending over most West Africa countries including Ghana. Since 1950 average temperatures in West Africa have been rising with an increment of 1° recorded across major weather stations in the region. Nonetheless change in temperatures in the Sahel region is higher, approximately 1.5 and 2 °C. This warming is in agreement with the IPCC report of 2013. Padgham (2015) reported that the whole West Africa has recorded a warming between 0.3 and 1 °C in the last decade and this is also in agreement with the research done by Sylla et al., 2016). Global models predicts an increase in temperature over West Africa coupled with a decrease in rainfall and high frequency of weather extremes (floods, droughts) and extension of dry season (Sedogo et al., 2015). Delay in the onset of rain season and dry spells during rainy season is also predicted (Sedogo et al, 2015). However, there is a lot of uncertainty in all these projections. Climate models do not agree on whether rainfall will decrease or increase and many models shows significant trend in both directions (FCFA, 2019). Rainfall variability in West Africa has been linked to increase in carbon dioxide concentration, change in sea surface temperatures and pollution of the northern hemisphere (FCFA, 2019). When sea surface temperatures in the Northern Tropical Atlantic decreases and temperatures in the south Atlantic increases slightly West Africa tends to be drier particularly the Sahel region (FCFA, 2019). In spite of all this, there is still argument on whether this is due to nature or human activity or both. Heat wave days are envisaged to increase automatically by mid – century especially in Sahel region (FCFA, 2019) .

Fig 2.2 below shows the projected temperature and precipitation changes in the region as a result of climate change. From the figure 2.2 below the West Africa region is projected to have temperature increase which range from 1.5 to 4 ℃ whilst precipitation is projected to decrease by 200mm to 500mm. This decrease in precipitation may have a negative impact on hydropower potential of the region.
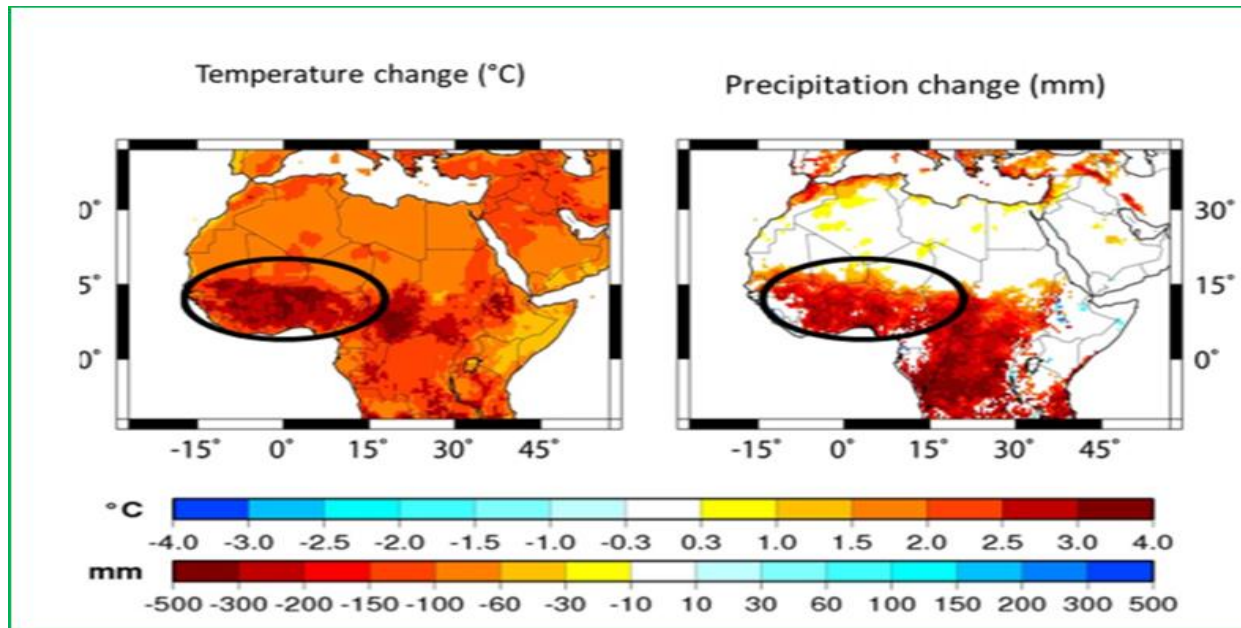
Figure 2.2: Predicted Temperature and Precipitation change

 (Source : Sedogo et al., 2015)

2.4. CLIMATE MODELLING

Climate models use calculable methods to mimic the interactions of the important drivers of climate change which includes atmosphere, oceans and land surface. They can be used to study the dynamics of the climate system to climate change projection (ULC, 2008) .

Schematic representation of the development and use of a climate model

Figure 2.3 shows the development and use of a climate model. Models are developed from physical and biological principles and they have forcing parameter and boundary conditions. Results of models are projections see figure 2.3.
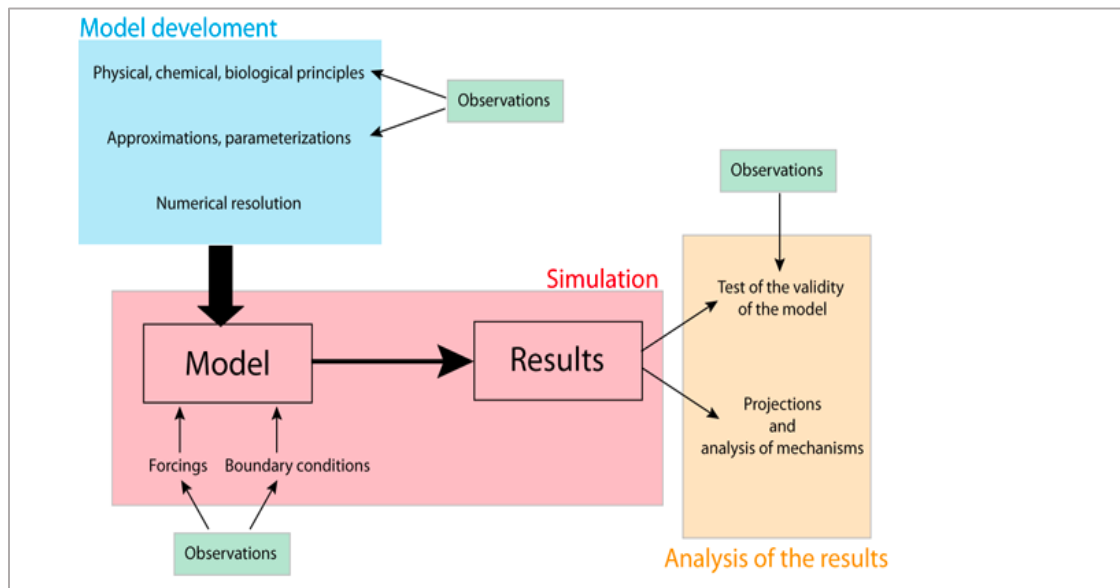
Figure 2.3 : Schematic representation of the development and use of climate model

(Source: UCL, 2008)

2.5. IPCC REPORT

Global warming is expected to increase the temperatures by 1.5 °C compared to pre-industrial levels. The major contributors to this increase in temperature are known to be human activities through industry. Human activities are judged to have contributed to around 0.8°C to 1.2°C of the global temperature increase (Masson-Delmotte et al., 2018). A warming by 1.5°C is expected to occur between 2030 and 2052 if current rates of increase persists (IPCC , 2018). Increase in temperatures has been felt already in some parts of the world mainly in the inland. However, the rate of warming is slower in oceanic. Current warming from GHG emissions from pre-industrial period up to present day will continue to change the climate system for centuries to come, however there is a small chance that anthropogenic emissions alone are likely to cause a 1.5°C global temperature increase (IPCC,2018). Climate change will pose many dangers to humans, animals and the planet but the magnitude of damage depends on the intensity and rate of warming, level of development, geographical location and susceptibility. Climate related risk depend also on the peak and duration of warming. If the warming exceeds 1.5°C and if the same temperature is maintained for a long period the danger that will happen will be long lasting or unchangeable. However climate adaptation and mitigation will reduce the detrimental effects of climate related risks (IPCC, 2018).

Hydrological cycle

Water cycle is also called the hydrological cycle. Fig 2.4 shows the hydrological cycle. Water in rivers and lakes evaporates by the process of evaporation. The evaporated water turns into vapour and it condenses by the process of condensation and then it will fall as rainfall. Rain water the moment it falls into the ground some will infiltrate; the rate of infiltration depends on the moisture content of the soil. Part of the water evaporates and the remaining water will flow as runoff or discharge in rivers. The part that flows as runoff is the one that can be utilised in hydropower generation in runoff river systems.

First instances

$Q = P - E - \Delta S$

Where

Q is Discharge, P is Precipitation, E is Evaporation, and ΔS is change in soil moisture

After long period

Moisture is assumed to be constant, therefore $Q = P - E$

Runoff coefficient

$\alpha = Q/P$

Understanding the hydrological cycle is important in the analysis of run off (discharge), run off is of particular importance to this study because it affects hydropower generation.
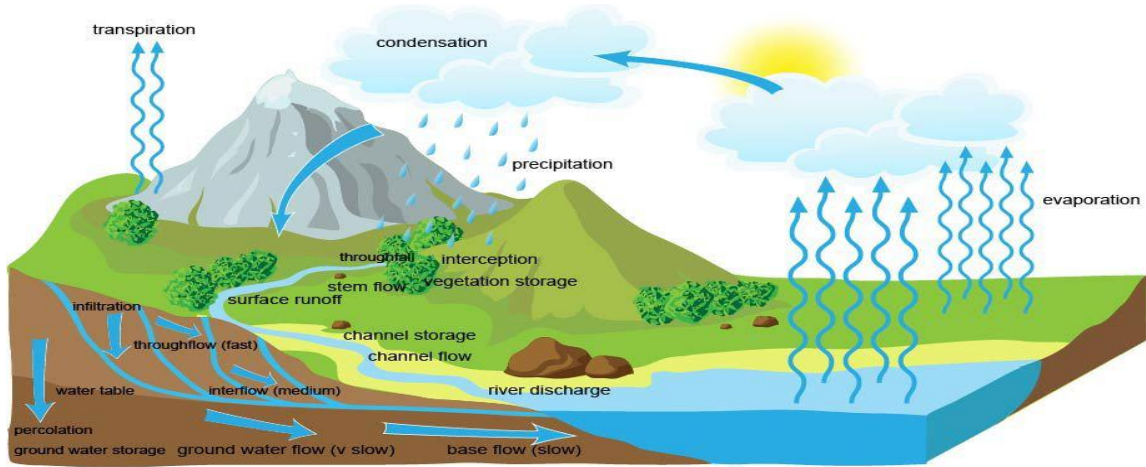
Figure 2.4 : Hydrological cycle

2.6. CLIMATE CHANGE AND HYDROPOWER

Climate change impacts on hydropower is caused by changes in runoff. Runoff depends on precipitation, temperature, evapotranspiration and to a lesser extent on soil moisture which comes as a result of climate variability.

Figure 2.5 shows climate change effects on hydropower.
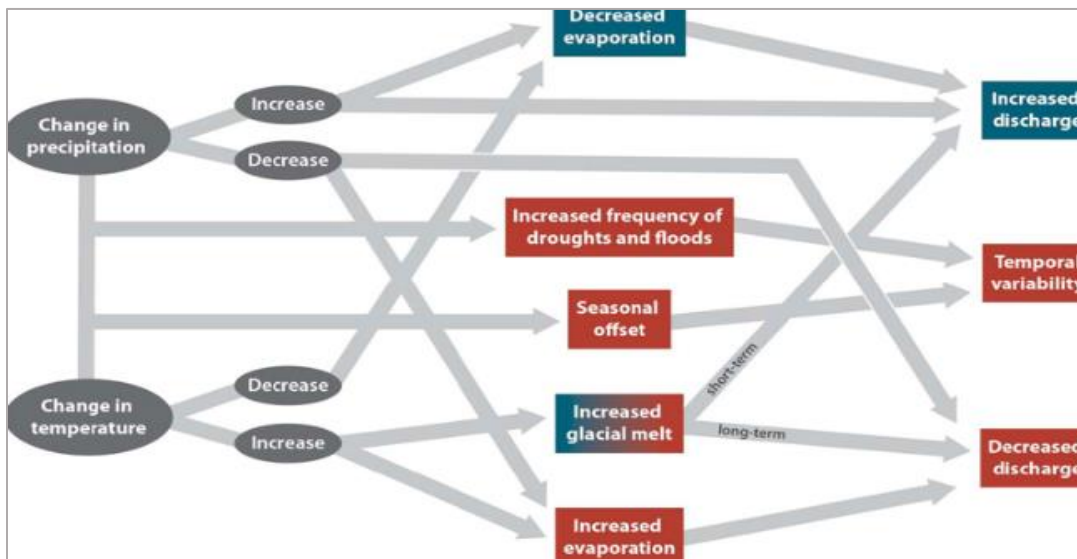
Figure 2.5 : Flow chart of climate change effects on water resources

(Source : Climate Change and Hydropower, 2014)

Red colour indicates negative effects that climate change will have on hydropower whereas blue indicates the potential positive impacts climate change will have on hydropower. Increase in temperature increases evaporation and cause the glacial to melt which increases discharge in the short term period, however in the long term it will cause a decrease in the discharge which affects hydropower generation. On the other hand, a decrease in temperature decreases evaporation which increase discharge.

Effects of climate change on the Energy sectors

Climate change has significant effects on the energy sector:

- On the supply side, climate change will lower energy production from hydropower plants as a result of reduced discharge in rivers (Harrison et al, 2014). Thermal generating stations requires river water for cooling. stations may therefore suffer operational disturbances due to reduced river flows.

- On the demand side climate change will increase the cooling demands in summer due to increased air temperatures and on the positive side it will lower heating demands in winter due to increased air temperatures.

- Other renewable energy technologies may also be affected by climate change such as wind and solar, wind will be affected due to wind pattern changes while solar will be affected by cloud cover (Harrison et al , 2014).

- It also results in scheduled projects being postponed or cancelled completely.

- It will cause many countries to shift to fossil fuels for energy due to depleting renewable energy resources which will further accelerate the climate change.

- Hampers energy development in a country.

- Decreases the sustainability of hydropower plants which results in an increase in the price of electricity**.**

River Basin Response to Climate Change

Figure 2.6 shows the river basin response to climate change with, with a degree temperature increase there is a small decrease in runoff and precipitation, however when the temperature rise doubles there is a sharp decrease in runoff and precipitation this could be as a result of an increase in evapotranspiration. This brings to this conclusion temperature increase reduces the flow duration in rivers there by hindering hydropower generation.
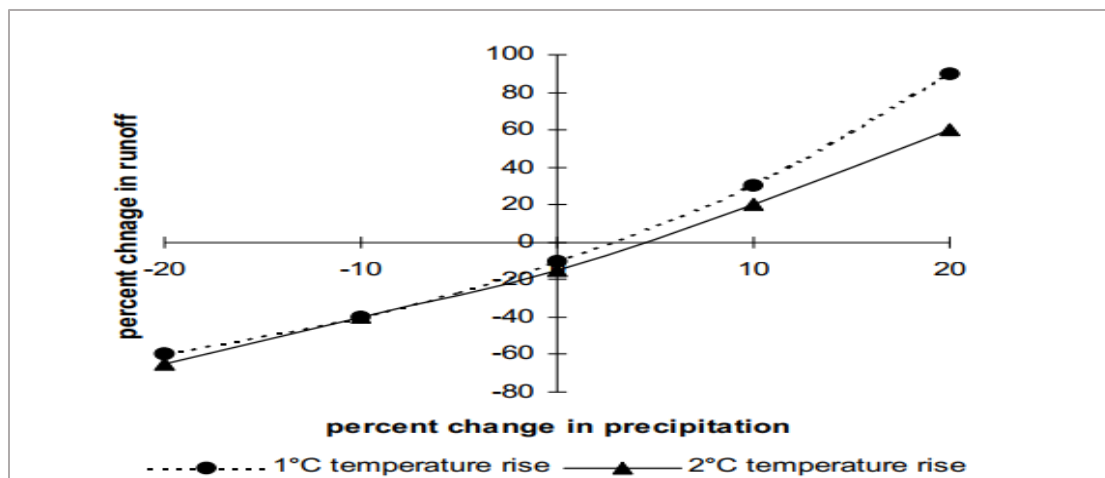
Figure 2.6: River Basin Response to Climate Change (Source :Harrison et al., 2014)

2.7. HYDROPOWER

2.7.1.   Hydropower studies

- **Reconnaissance studies** – they are done to find the potential and to estimate the energy available in streams.
- **Feasibility studies** – they are done to determine the feasibility of a project; they use flow duration data to determine the available discharge and to make possible capacity sizing of the plant.
- **Definite plan or design studies** – these studies are made before the implementation of the final design and the project. They require the flow duration curve for a long period and power duration curves (TEMIZ, 2013) .

2.7.2.   Potential of hydropower resources

Hydropower resource potential are categorised into 3 categories which are theoretical, technical and economic (Canyon Hydro, 2013).

- **Theoretical potential** is the sum of the energy potential available at a place including losses.
- **Technical potential** is the part of theoretical potential which can be utilized with the current technology regardless of economic and other considerations.
- **Economic potential** is the part of the technical potential which can be generated as economic, it takes into consideration the price of alternative energy sources**.**

16

- **Exploitable hydropower** is the part of the economic potential which can be harnessed considering the environment and other special restrictions**.**

NB: This study will look at the technical and economic potential of hydropower potential in West Africa**.**

- ✓ On technical potential it will look at how climate change will impact the amount of energy that can be produced from the catchment considering design discharge.
- ✓ On economic potential it will look at how climate change will impact the hydropower development cost and payback period because exploitable hydropower power is the part of economic potential hydropower which can be harnessed considering the environment and other special restrictions.

2.8. HYDROPOWER CLASSIFICATION

Hydro power systems are classified according to different criteria's which are as follows:

1. Installed capacity
2. Operational mode
3. Operating conditions (type of load)
4. According to head

 Installed capacity

Hydropower schemes can be classified as large, small, mini, micro and pico hydropower station (Canyon Hydro, 2013). These names depend on the installed capacity and also according to countries or region.

Mini hydropower 100 kW to 1 MW

Micro hydropower 10 kW to 100 kW

Pico hydropower less than 10 kW

Large hydro they are greater than 1MW

Types of load (operating conditions)

Hydropower plants are classified according to the type of load

- **Base load**

They carry operation continuously delivering constant power and they provide the power demand at the base of the load curve. Run of river type and storage type can provide base load power. This study will look at run of river hydropower and a design which is available for 80% of the time will be considered in order to generate electricity every time.

- **Peak load**

These type of plants only come in operation when there is high demand, they only supply peak power at peak times, e.g. pumped storage type plant.

- **Head**

Head is an important parameter in hydropower schemes and it is directly proportional to power output. The higher the head the higher the higher the power output.

Head description

Table 2.1 Head description

Description	Head
Low	H<10
Medium	10<H>100
High	H>100

Source: (Penche, 2004)

2.8.1. Operational mode

Last but not least, hydropower stations are also classified according to operational mode:

1. Storage type

2. Run of river type

3. Pumped storage.

- **Storage type**

The most common type of hydroelectric power plant used around the world is the storage type hydropower scheme they also referred to as reservoir and impounded plants and they are mainly used in large scale schemes. They use a dam to store river water in a reservoir and act as base load power plant to supply constant energy throughout the year. Water is stored in the dam when there is high flow mainly in rain seasons and this storage water will be used during low flow seasons (See Figure 2.7). The main advantage of hydro facilities with storage capability is their ability to respond to peak load requirements (WEC, 2016). Figure 2.7: Shows the storage hydropower plant
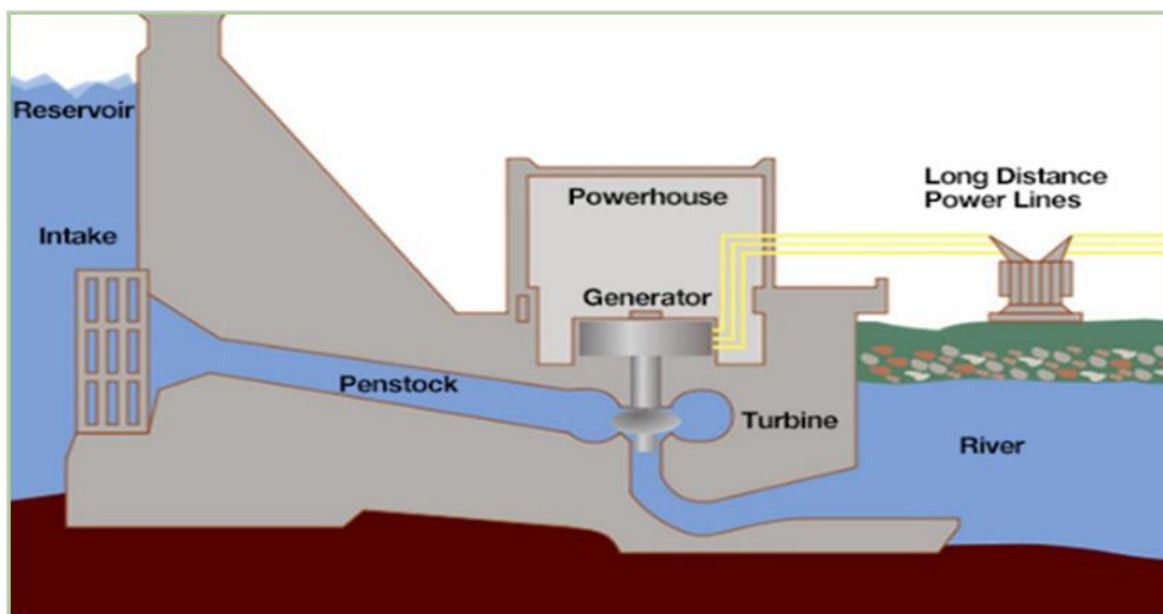
Figure 2.7 : Storage Hydropower plant (Source: Kharagpur, 2012)

- **Run of river type**

Fig 2.7 shows the run of river type this type of they do not have a big dam or big reservoir to store water they divert water from the main river by means of a canal or weir and given to the transmission canal. Run-of-river projects may have a small dam or reservoir for temporal water storage. Run-of-river hydro plants are known for continuously supplying electricity throughout the year, however they are also affected by seasons and climate change. In rain season they supply a lot of electricity and in dry seasons the capacity reduces. Run of river are generally installed to provide base load power to the electrical grid because of reliability (WEC, 2016).
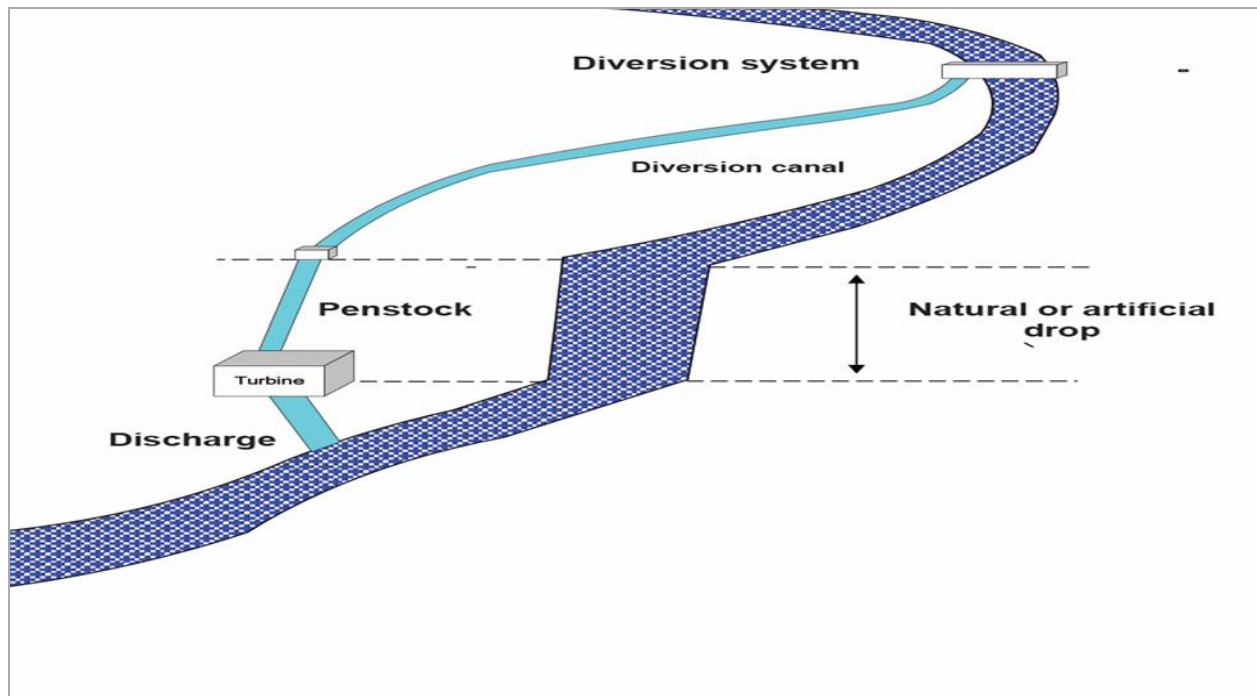
Figure 2.8 : Run of river scheme

(Source **:** Penche, 2004)

This research will evaluate hydropower potential based on run of river approach in Black Volta river.

Pumped storage

Pumped storage power plants they are generally installed to provide peak load supply see Figure 2.9 . Water is cycled between a lower and upper reservoir by pumps, to produce electricity so the name pumped storage. Surplus energy from the system is used at times of low demand. Electricity is produced by releasing water from the upper reservoir to the lower reservoir through turbines. Some pumped-storage projects have natural inflow to the upper reservoir which will augment the generation available. Pumped-storage hydropower is a zero sum electricity producer. Its value is in the provision of energy storage, enabling peak demand to be met, assuring a guaranteed supply when in combination with other. One advantage of pumped storage hydropower is it can be combined with another renewable energy and operates perfectly because pump-storage installations can provide back-up reserve which is immediately dispatchable during periods when the other variable power sources are unavailable (Penche, 2004).
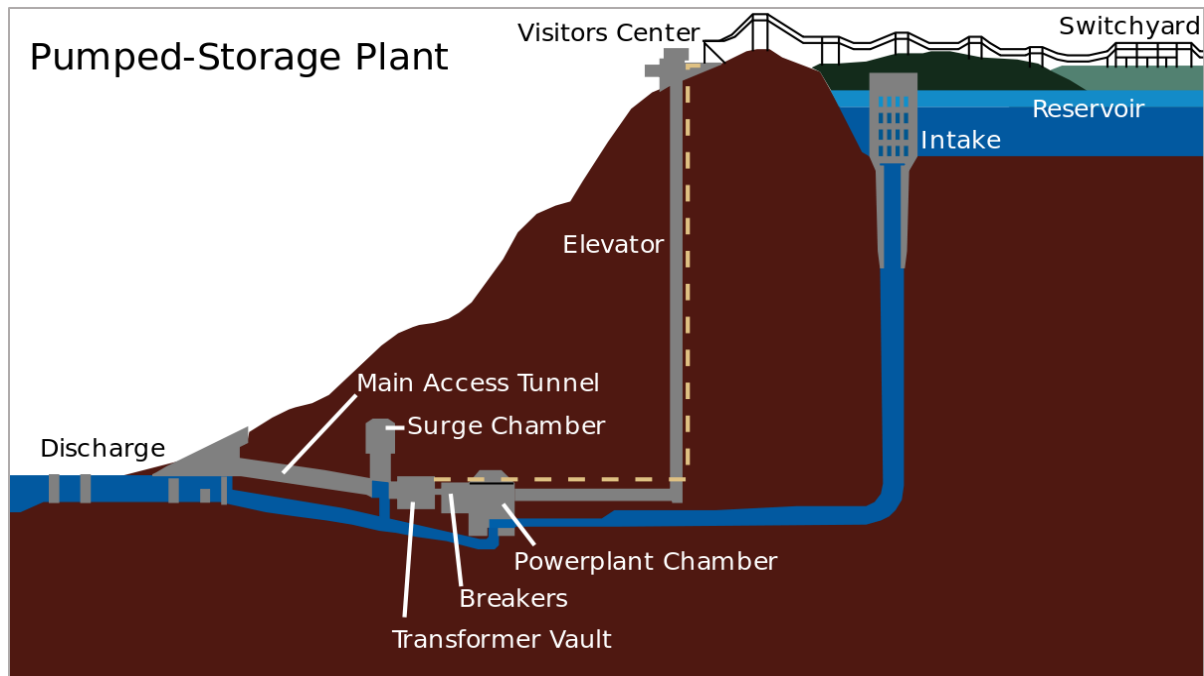
Figure 2.9 :Pumped storage hydro power plant

(Source**:** ANDRTZ, 2017)

2.9. TURBINES

Hydraulic turbines are machines that develop torque from the dynamic pressure action of water and convert the torque to produce electricity in a generator. Turbines have blades, buckets, runner, spirals and they rotate about an axis by the action of water to produce electricity. The rotating part of the turbine is called runner (Hamududu & Killingtveit, 2012).

There are two categories of turbines:

- Reaction
- Impulse

2.10. REACTION TURBINE

It uses the combination of the pressure energy and kinetic energy of water to produce electricity. The reaction is contributed by pressure drop throughout the runner. There is a change of velocity direction from inlet to outlet which results in a pressure drop through the runner. Reaction turbines can be further divided into several types, of which the principal two are the Francis propeller and the Kaplan turbines (Otuagoma, 2016).

Reaction turbines include:

Kaplan

It is a reaction turbine, so the reaction force of leaving water is used to turn the runner of the kaplan turbine, As the water flows through the twisted blades a lift force is generated in the opposite direction of the leaving water and that lift force causes the blades to rotate there by generating power.

Turgo turbine

The turbine is designed such that the jet of water strikes the buckets at an angle to the face of the runner and water passes over the buckets in the axial direction before being discharged at the opposite side (Renewables first, 2018).

Cross Flow

Cross flow turbines have lower efficiency than the modern turbines. They are designed for large water flow and lower head. They operate at low speeds and they are mostly constructed as two different turbines, different capacity as well sharing the same shaft. The turbine wheels will have the same diameter but of course the length will not be the same in order to handle different volumes (Penche, 2004)

2.11. IMPULSE TURBINE

2.11.1. Impulse Turbines include:

Potential energy of water flowing from the fore bay is converted into jets of water which strikes the single or bowl-shaped buckets of the runner. There is no pressure drop through the runner and it operates in nearly atmospheric pressure.

Pelton

This type of turbine is suitable for high heads with low flow rate and it is one of the most efficient turbines). Energy change occurs in the nozzles where by fluid energy is converted to kinetic energy and they will be a corresponding pressure drop in the nozzles They consist of multi bucket – shaped bucket which have jets which are just directed tangential to the turbine producing impulsive force (ANDRTZ, 2017).

2.12. TURBINE SELECTION

The choice of a turbine for a particular site depends on the available head and discharge. Other factors such as power to be developed and the required speed should also be considered. The following factors have the bearing on the selection of the right type of hydraulic turbine (Penche, 2004):

- Rotational Speed
- Specific Speed
- Maximum Efficiency

Rotational speed

Generators are directly coupled to turbines to reduce the transmission losses. Generators operate at synchronous speed. Generators generate power at constant voltage, speed and constant frequency. The synchronous speed of the generator is given by:

$N=60*f/p$

Equation 2.1

N speed rpm; *f*- frequency of the generator (usually 50hz or 60 hz), *p*- number of pair of poles of the generator and *p* are constants thus *N* is constant.

Turbine Specific speed

Is the speed at which turbine is running to produce 1kw power through a head of 1m. Turbines operate with a specific speed; specific speed characterises the shape number of the turbine and it is one of the main criteria's of matching a turbine with its particular speed.

Table 2.2 : Turbine specific speeds Runner	Specific Speed Ns (rpm)		
	Slow	Medium	Fast
Pelton	4-15	16-30	31-70
Francis	60-130	151-250	251-400
Kaplan	300-400	451-700	701-1100

Source :(TEMIZ, 2013)

$$N_s = \frac{N \sqrt{P}}{h^{5/4}}$$

$$N_s = \frac{1750}{h^{1/2}} \quad for \quad 18 \; < \; h \; < \; 300 \quad m$$

$$N_s = \frac{1475}{h^{1/3}} \quad for \quad h \; < \; 18 \quad m$$

<div align="right">Equation 2.2</div>

Turbines with identical geometric proportions have the same specific speed regardless of size. All turbines with the same specific speed also have an optimum efficiency. However, it is most common to select a high specific speed runner as it more economical.

Head flow ranges of turbine

Chart in Figure 2.10 is used to select the turbine based on power output, head and discharge. In this study after evaluating the power potential of the catchment, the turbine will be selected based on the head of the given area, discharge and the power output.
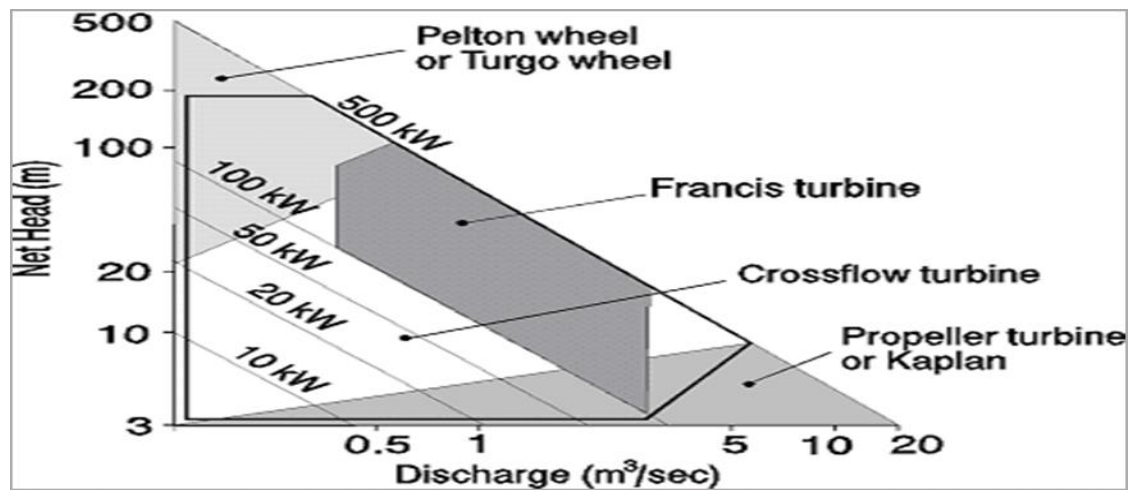
Figure 2.10 : Head flow ranges (Source : ANDRTZ, 2017)

2.13. EVALUATION OF HYDROPOWER POTENTIAL

Data used for this calculation are the head, various component efficiencies, a flow duration curve representative of the flow over the year. Flow duration curve is a plot that shows the percentage of time that flow in a stream is likely to equal or exceed some specified value. Design discharge is obtained from the flow duration curve. Head is obtained from contour maps, remote sensing maps and topography maps.

<u>Power output</u>

$$P0 = \rho g Q H \eta \qquad\qquad\qquad\qquad \text{Equation 2.3}$$

Where:

Po: the power out (Watt)

ρ: density (kg/m^3=1000)

g: gravity (m/s^2= 9.8)

H: water level above the turbine

2.14. HYDROLOGICAL MODELS

Physically based model

They are also called mechanistic model it is a mathematically illustration of the real world. They include physical processes and they use state variables which are functions of both time and space.

Conceptual model

Lumped conceptual models are models which have a good description of the hydrological system The advantages of the lumped conceptual models are the simplicity and limited requirements of input data. A conceptual model HBV light model will be added in this research.

Distributed models

This type is more complex and takes into account the spatial variability of both physical characteristics and meteorological conditions. Distributed models are partitioned into hydrological units and each process is computed independently in each of the units (Donald et al. 1995). Implementing these models is time consuming and the requirements of data and parameters are large. Distributed models are therefore restricted to use in certain areas.

2.15. HBV-LIGHT

Hydrologiska ByransVatten (HBV-light) is a dynamic mass-balance model, which is run with a daily time-step, including other parameters within the catchment coupled to the water balance. It was developed in 1976 by Bergströmis. It is a conceptual model used to model the catchment runoff. It simulates basin discharge using meteorological data as inputs such as temperature, rainfall and evaporation. It is made up of different routines and it simulates catchment discharge on a daily time step time depending on precipitation, monthly potential evaporation and air temperature (Seibert & Vis, 2012). Precipitation is simulated as snow if T is less than threshold

temperature (TT) and precipitation is simulated as rainfall if temperature is more than the threshold temperature. Precipitation that is below TT is multiplied by Snow correction factor SFCF [-] (Seibert, 2005). HBV light model uses warm up period and it is applied in this research to model the Bamboi catchment runoff. Snow routine will not be applied in this research because West Africa does not snow.

2.16. HBV STRUCTURE

Input data for HBV

Basin height and area, precipitation, potential evaporation, pan evaporation, mm/d , min and max temperature, average temperature(°C) , cloudiness (%), average outflows(m3/s) (Riverso, 2010)

Table 2.3 :HBV light input data

Routine	Input data	Output data
Snow	Precipitation	Snow pack
Routine	Temperature	Snow –melt
Soil routine	Pot	Act
	Evaporation	Evaporation
	precipitation	ground water
	Snow melt	Recharge
Response function	Groundwater recharge	Run off to stream
	Pot / evaporation	Ground water level
	Run off to stream	
	Ground water recharge	
Routing routine	Runoff to stream	Run off at the outlet

Source: (Seibert & Vis, 2012)

Figure 2.11 Shows the HBV light windows.
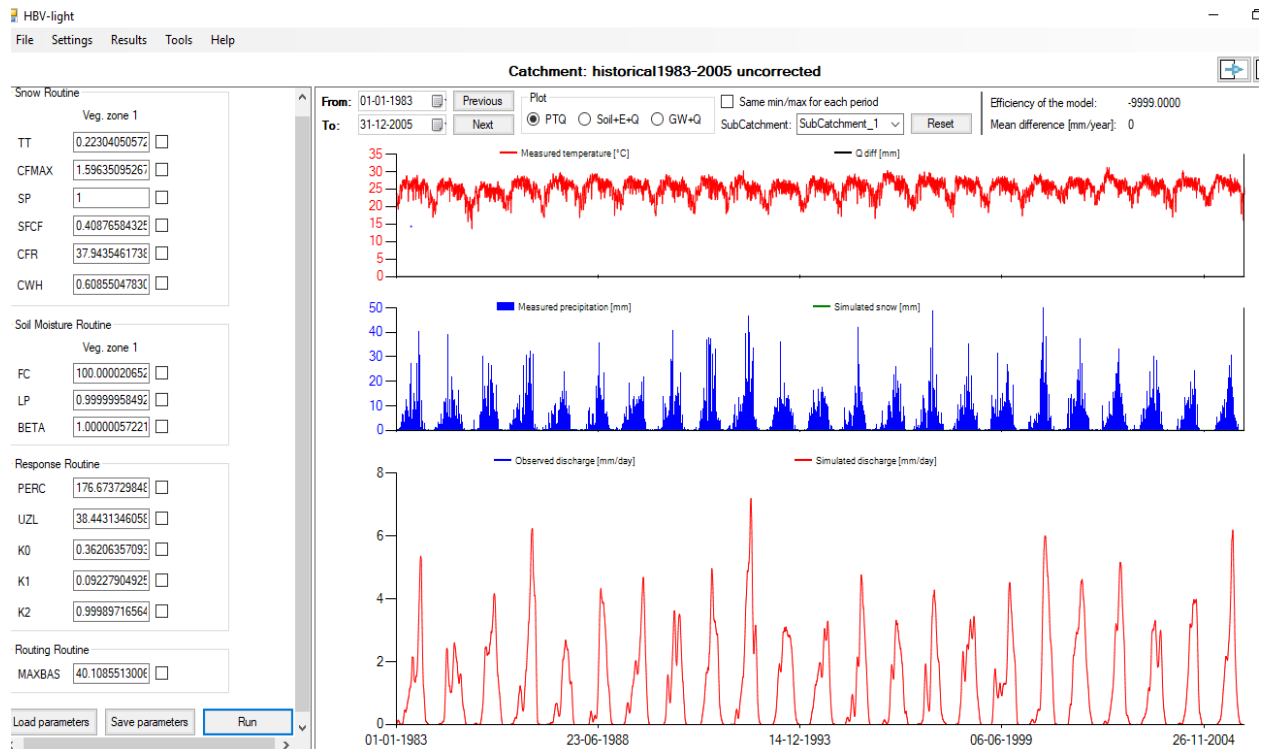
Figure 2.11: HBV light windows

2.17. CLIMATE IMPACT ASSESSMENT

The third objective of this research will be fulfilled by carrying out climate impact assessment. Climate impact assessment seeks to characterize, diagnose, and project risks or impacts of environmental change on people, communities, economic activities, infrastructure, ecosystems, or valued natural resources. In this research global climate data is downscaled by regional climate models. The corrected data is fed into a hydrological model and the output will be changes in runoff etc and these changes in run off will be used for assessment.
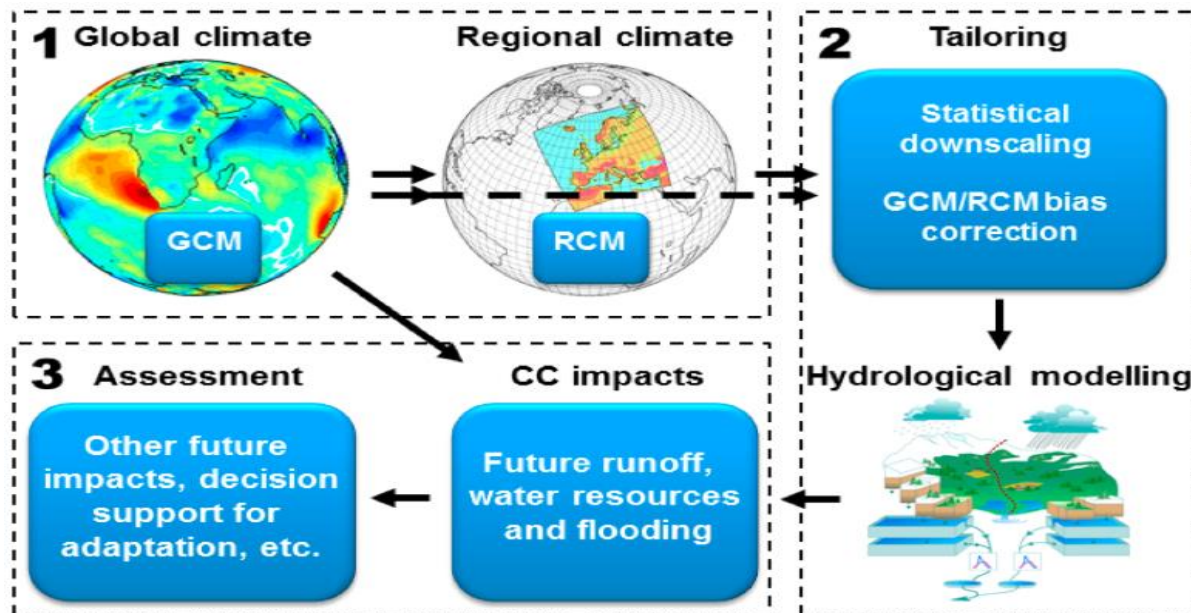
Figure 2.13 : Climate Impact Assessment process

(Source: Jonas et al, 2016)

 Due to the limited resolution of GCM 110 km of Global Circulation models, Regional Circulation models (RCMs) have gained ground over last years due to the fact that GCMs does not allow the resolution of topographic variation, coastlines, land use and mesoscale convection. High computational power is allowing to run RCMs at a higher resolution of even less than 12km and they give a more representation of the GCMs and the area. The WASCAL ensemble used in this research is a combination of three GCMs (Global circulation models with one RCM (Regional Circulation model) for the green house gas scenario concentration pathway RCP 4.5 (Representative concentration pathway).

Characteristics of the WRF simulations can be summarized as follows the WASCAL climate ensemble shows a cold bias WRF-E ~ 2–4 ◦C for greater part of the year. WRF-G exhibits characteristics of being consistently colder than, WRF-M is warmer than WRF –E, however among the three GCMs WRF-M agrees with the observed temperatures best .In fore casting the future WASCAL WRF runs ensemble climate scenarios predict increasing temperatures by 2.5–3 ◦C until the end of the century with respect to climate change which is in agreement with other global and regional climate (Sylla et al, 2003). Among these WRF-H predicts a much high climate change signal 4 ◦C while WRF-G predicts the lowest climate change signal of weakest (< 2 ◦C). For precipitation the WASCAL WRF runs forecasts a clearly wetter future for Guinea coast up to 300

mm/ year and up to 200 mm in the Soudano region and small increased amounts of precipitation in the Sahel region which is in agreement with other majority of the CMIP5 models.

2.18. BIAS CORRECTION

Outputs of GCMs and RCMs have been used for climate impact assessment both at global and local scale (Maraun, 2016). However, climate studies rarely use outputs of GCMs, RCMs or hydrological modelling outputs directly because this data has systematic error / biases as a result of low resolution, physics and thermodynamic processes, numerical schemes and climate knowledge. Errors in simulations relative to historical observed data are large therefore it is a prerequisite to bias correct raw climate data output in order to produce climate projections that are good.

$$\hat{x}_{m,p}(t) = F_{o,h}^{-1}\{F_{m,h}[x_{m,p}(t)]\}\,,$$
Equation 2.2

M = modelled data

O = observed data

H= historical period

T= time period
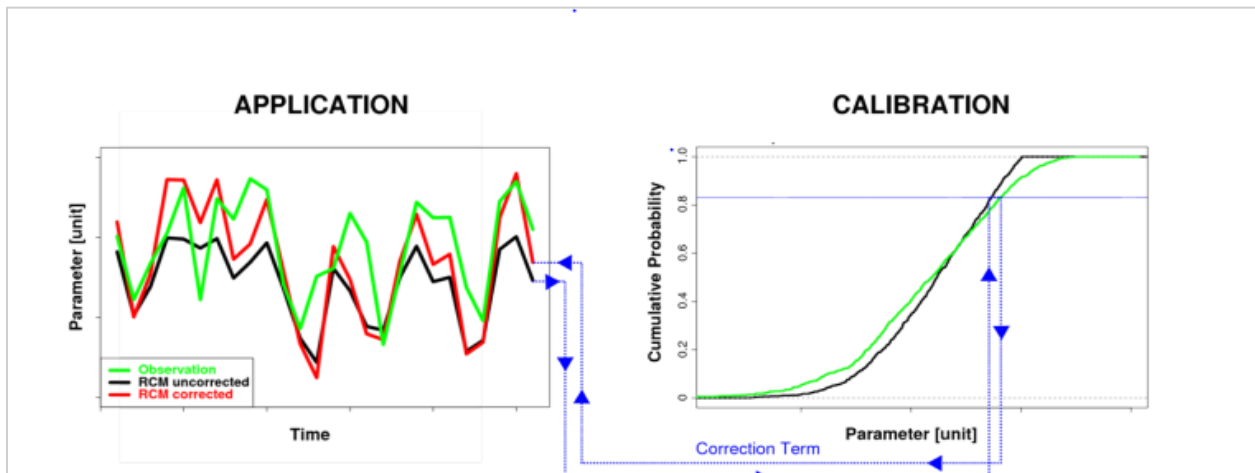
Figure 2.14: Bias correction

(Source :Maraun, 2016)

2.19. RCPS REPRESENTATION CONCENTRATION PATH WAY

A **Representative Concentration Pathway** (**RCP**) is a green house concentration adopted by the IPCC in 2014 to project different climate futures. Four pathways have been selected and all of them are considered possible depending on how much green houses are emitted in the years to come. Radiative forcing is the extra heat that earth retains as a result of additional greenhouses measured in watts/m² (Thomson et al., 2011).

RCP 8.5 - in this scenario CO_2 concentration are projected to continue to rise and there are few curbing of emissions with emissions reaching a high level of 940 ppm by 2100 and this is referred to as the most dangerous scenario (Coulibaly et al ., 2018).

RCP 6.0 - it is a stabilization scenario with lower emissions achieved after implementation of a series of mitigation measures. Carbon dioxide concentration measures rising less rapidly than RCP8.5. Total emissions reaching 660 ppm by 2100 and stabilizes shortly afterwards. The total radiative forcing is stabilized shortly after 2100 (Thomson et al., 2011).

RCP4.5 – it is a stabilizing scenario in which the total radiative forcing CO_2 concentrations are slightly above those of RCP 6.0 until after mid-century, but emissions peak earlier (around 2040), and the CO_2 concentration reaches 540 ppm by 2100 and stabilize shortly afterwards.

RCP 2.6 - is an ambitious mitigation scenario in which emissions peak around 2020 and rapidly decline. Carbon dioxide reaches 440 ppm by 2040 and slowly declines to 420 ppm by end of century 2100. This scenario requires participation from all stake holders and application of technologies that can remove carbon dioxide from the atmosphere. Its radiative forcing level first reaches a value around 3.1 W/m2 mid-century, returning to 2.6 W/m2 by 2100 (Thomson et al., 2011) .

Table 2.4 : RCPS

Name	Radiative forcing	C02-equiv (ppm)	Temp Anomaly ^{0}C	Pathway
RCP 2.6	3Wm^2 before 2100, declining-to 2.6Wm^2 by 2100	490	1.5	Peak & decline
RCP 4.5	4.5 Wm^2 post 2100	650	2.4	Stabilisation without overshoot
RCP 6.0	6.0 Wm^2 post 2100	850	3.0	Stabilisation without overshoot
RCP 8.5	8.5Wm^2 in 2100	1370	4.9	Rising

Source :(Thomson et al., 2011)

Scenario RCP 4.5 is the one applied for this research.

CHAPTER THREE: STUDY AREA

3.1. INTRODUCTION

This chapter outlines the study area of the catchment, it describes its location, population, land use, climate, socioeconomic activities and drainage relief.

3.2. LOCATION OF THE AREA
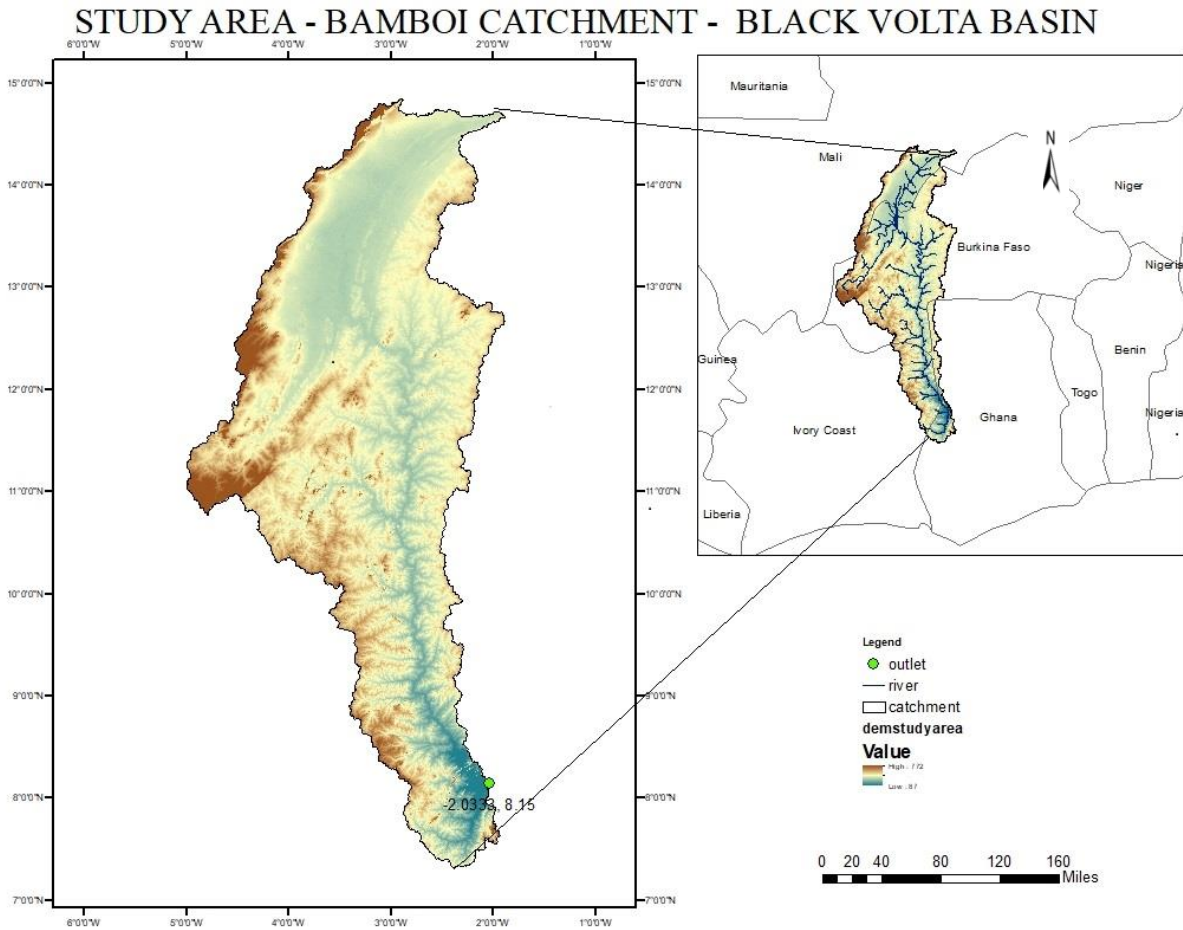
Figure 3.1: Location of the study area

The study was carried out in the Bamboi catchment (Figure 3.1) covering a total area of 134 200 km^2 (using the station number 153 1100 of the Global Runoff Data Center as outlet and the SRTM-90m as Digital Elevation Model). The Bamboi catchment is located in the Black Volta Basin. The outlet has a latitude of 8. 15, longitude of -2.0333 and an altitude of 93m. The Black Volta basin lies in the main Volta basin with a latitude of 7 ^{o} 00'00" N and 14°30'00" N and Longitude

5°30'00" W and 1° 30'00" The Black Volta river basin is shared among Mali, Burkina Faso, Ghana, Ivory coast and Togo (Obahoundje , 2015) . The Black Volta river has a length of 1325km and the total drainage of the Black Volta river is 154,900 km^2. Bamboi is mainly located in the South western part of Burkina Faso and North western part of Ghana, however it also passes through southern Mali and Northern Ivory coast. Black Volta is the main river in the Black Volta basin, it originates as Mouhoun river in Burkina Faso and become Black Volta in Ghana. Lery Dam in Burkina Faso controls the flowrate of Black Volta river partly. Flow rate of Black Volta is huge in the upper parts of the mainstream and it drops in the valleys. Flow rate increases at Bamboi due to several reasons which are increase in precipitation and due to its location downstream (UNEP-GEF Volta Project, 2013). Mean annual runoff of Black Volta river in Ghana is eight times than its source in Burkina Faso. The Volta basin is divided into four basins the White Volta , Red Volta and Black Volta.

Fig 3.2 Volta Basin

3.3. CLIMATE

The mean annual temperature in the basin ranges from 27 to 30 °C (Atulley, 2013) . Temperatures can rise as high as 44 °C and can be as low as 15°C (at night). March and April are the hottest months in the basin whereas the coolest month is August. The basin experiences unimodal rainfall (in the north) and bimodal rainfall (in the south) as a result of ITCZ (Inter Tropical Convergence Zone). The agro-climatic zones in the catchment range from sub humid in Ghana to semi-arid in northern Burkina Faso (UNEP-GEF Volta Project, 2013).

3.4. SOIL

There are 12 major soil types in the Volta basin. Most of the soil in the Volta basin are from the weathered of mid Palaeozoic parent materials. Luvisols are found in almost all the part of the basin except in the northern part where regesols and aeronosols are dominant. The northern part of the basin is where Burkina Faso and Mali are located. The regenosols found in the North are formed from the unconsolidated materials and are coarse- textured making them prone to soil erosion and they are highly permeable and have low holding capacity making them sensitive to drought. In the south part of the basin, there are lithosols after luvisols they are light textured, well drained and they are mainly found in Ghana. They have low organic content and fertility compared to those found in much humid conditions. These Lithosols in Ghana have surface sealing effects under rainfall resulting in increased runoff (UNEP-GEF Volta Project, 2013) .

3.5. EVAPORATION`

Evapotranspiration in the basin ranges from 1176 to 2400 mm per annum. Evapotranspiration is high in this region and it is estimated that around 80% of the rainfall in the Volta basin is lost through evapotranspiration. Evapotranspiration also depend on the soil properties and it ranges to around 10 mm in rain season and 2 mm in the dry season. Evaporation increases from south to north, meaning there is high evapotranspiration in Mali and Burkina Faso as compared to Ghana and Ivory coast. Humidity is high in rain season ranging to around 90% and low in dry season ranging to around 10% in Burkina Faso, while in Ghana it increases ranges from 30% to 80% (UNEP-GEF Volta Project, 2013).

3.6. VEGETATION

The catchment is shared across four countries Burkina Faso, Ghana, Mali and Ivory coast and the type of vegetation is mainly Sudan savannah and Guinea Savannah. In the southern part of the

catchment the area is covered by forests which is in Ghana, Southern Burkina and Ivory Coast while in Northern Burkina Faso and Mali the area is desert so there is little or no vegetation. The major land use in the area includes irrigation and agriculture, currently irrigation consumes 100 hectares of the land. Fig 3.2 shows the vegetation cover along the Black Volta catchment.
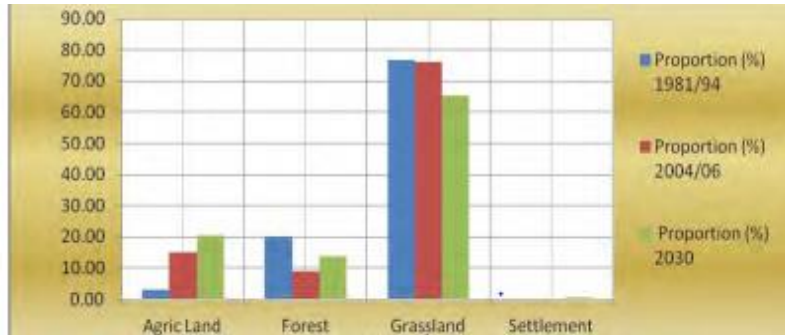
Figure 3.3 :Vegetation cover in the basin

Source **:** (ALL WATERS CONSULT AND LIMITED, 2012)

3.7.AGRICULTURE

Agriculture is the main economic activity in the Volta basin and it requires space and water. Each country in the Volta basin wishes to expand its agricultural production in order to feed its population and increase its gross domestic product (Obahoundje , 2015). Agriculture is small scale and it depends mainly on rainfall and there are few irrigation schemes in the region such as the ones at Boromo, Bui, Bamboi etc. Crops which are grown in the basin includes the following sorghum, millet, maize, cowpea, yam, cassava, cotton groundnuts, tamarin and round nuts. Although agriculture contributes to the economy of Volta basin countries, it has several impacts on the land which are land degradation, washing of top soil, erosion and pollution (UNEP-GEF Volta Project, 2013).

3.8. POPULATION DISTRIBUTION IN THE BLACK VOLTA BASIN

Population is distributed along the main river in the Black Volta basin. Burkina Faso and Mali population is mainly concentrated along the main river basin as compared to other fellow Volta countries this could be explained by the fact that these countries are Sahel countries therefore people prefer staying near rivers for water. The population density is 175 persons per km^2 in Burkina Faso which is Sahel region whilst in Ivory Coast the population is around 3 persons per/ km2 (non-Sahel region). The population of Black Volta basin stood at 4.5 million in 2000 and is

expected to double by 2025 (8 million). FIGURE 3. shows the population distribution along Black Volta.

Population distribution in Black Volta
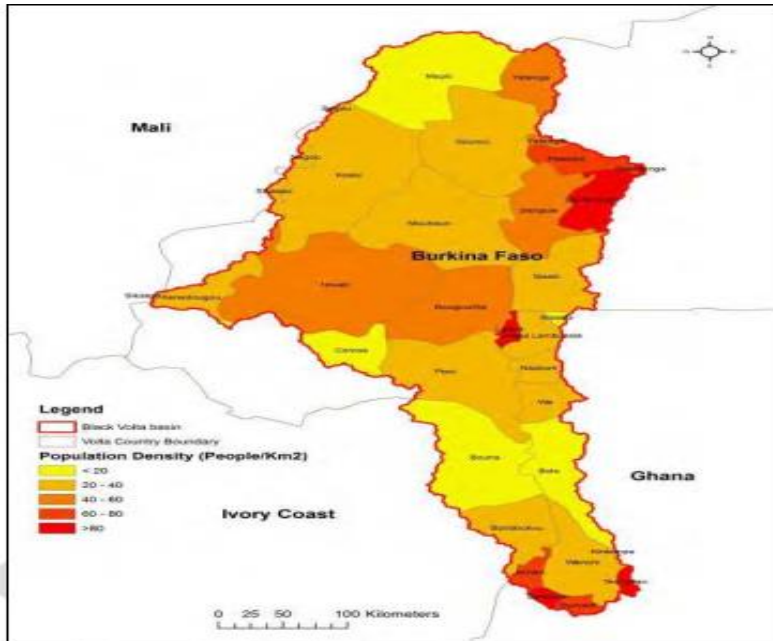
Figure 3.4 :Population distribution Black Volta

Source : (Allwaters consult & Limited, 2012)

3.9. ECONOMIC ACTIVITIES IN THE BASIN

Fishing

The basin is suitable for fishing and countries like Burkina Faso in the basin have increased their fish production due to construction of new dams in the area. Fish is a source of protein the basin and is affordable to most residents. In Ghana fishing is carried in the main Volta river and Tilapia and Cat fish are the most common fish in the region. In land fishing in the tributaries of the main Black Volta basin is mainly undertaken by non-native Malians and Ghanaians.

Livestock

Livestock is important in the basin and it is projected to increase in the coming years. It is one of the main sources of income in rural areas. Livestock is also an economic activity in the basin and it comes third after gold and cotton. Livestock is used for food, labour and export. Donkeys are mainly sold to Algeria, Niger and Burkina Faso for labour whilst cattle, sheep etc. are sold to Ghana and Nigeria for meat.

Water use and demand in Black Volta

Water is used for different purposes in the Black Volta basin some of which include fishing, livestock, domestic purposes, agriculture and mining. There are several organisations within the basin which are responsible for supplying portable water. Hydropower is the major water consumer in Ghana where as in Burkina Faso irrigation, livestock and domestic consumption consumes a large share of water. Generally, irrigation consumes much of the water in the Volta basin than any another activity in the basin and it is projected that by 2020 irrigation will increase its water consumption to about 82%. Domestic water supply is anticipated to increase from 360 million cubic meters in 2000 to 1,058 million cubic meters in 2025 consumption.
(Allwaters consult & Limited, 2012) . Drinking water is the second consumer of water in the Volta basin constituting around 23% of the total water consumption.

Table 3.1 :Water uses in Black Volta basin

Country	Agriculture	Hydropower	Fishing	Mining	Tourism	Livestock production	Industrial	Domestic
Burkina Faso	X	X	X	X	X	X	X	X
Ghana	X	X	X	X	X	X	X	X
Mali	X		X			X	X	X
Ivory coast	X		X	X	X	X	X	X

(Source : UNEP-GEF Volta Project, 2013)

3.10. ENERGY AND HYDROPOWER

People in the Volta basin rely much on burning biomass and charcoal as a source of energy. Hydropower is the main source of electricity in the basin, Ghana draws much of its energy from hydropower. Akasombo, Kpong and Bui hydropower stations on the Volta river supply electricity to the population of Ghana. The Kompienga dam and the Bagre dam of Burkina Faso supplies 14 MW and 16 MW of electricity respectively to the population of Burkina Faso. According to the studies carried out by the Volta River Authority the main Volta sub basins have total of 905MW of unexploited hydropower resources (UNEP-GEF Volta Project, 2013) . The Bamboi catchment spans across four above mentioned countries in the Black Volta basin therefore a brief description of the energy scenarios of these four countries will be done below.

3.11. GHANA

Ghana is a West African country with 5.5500° N, 0.2000° W. It has a total land area of 238.540 km² and it has a population of 28,33 million as of 2017. Ghana's electricity has been dominated by hydropower, for a long time because of its three large hydropower dams, Akasombo, Bui and Kpong. Hydropower provides the cheapest source of electricity however due to the discovery of petroleum, Ghana started fossil fuel power generation to meet the rapidly growing demand for electricity. The installed generation capacity for Ghana is 4398.5 MW. 50 percent of the installed capacity is from hydropower while the rest is from fossil fueled plants. The Akasombo and Kpon hydropower is owned by Volta River Authority (VRA) while Bui hydropower is owned by Bui Power Authority. The Akasombo dam was constructed in 1961 to 1965 and it has a capacity of 1,020 megawatts (MW). Ghana highly depended more on hydropower for electricity generation in the past which made its electricity generation to lower in 2006 because of decreased water levels in the Akasombo Dam. The Access of electricity in Ghana is currently at 85 % which is way better than most Volta countries. Two northern regions in Ghana forming the core of the Volta Basin have accessibility rates far below than in the southern regions. Bamboi catchment outlet is in the northern region, installation of a hydro power-station at Bamboi station will improve the electrification rate in the northern region (UNEP-GEF Volta Project, 2013). Hydropower plays a significant role in energy mix of Ghana, see   Figure 3. showing the energy mix in Ghana. Hydropower constitutes 44 % in the energy mix of Ghana while thermal constitutes 54% and the remaining renewables constitutes the remaining 2%.
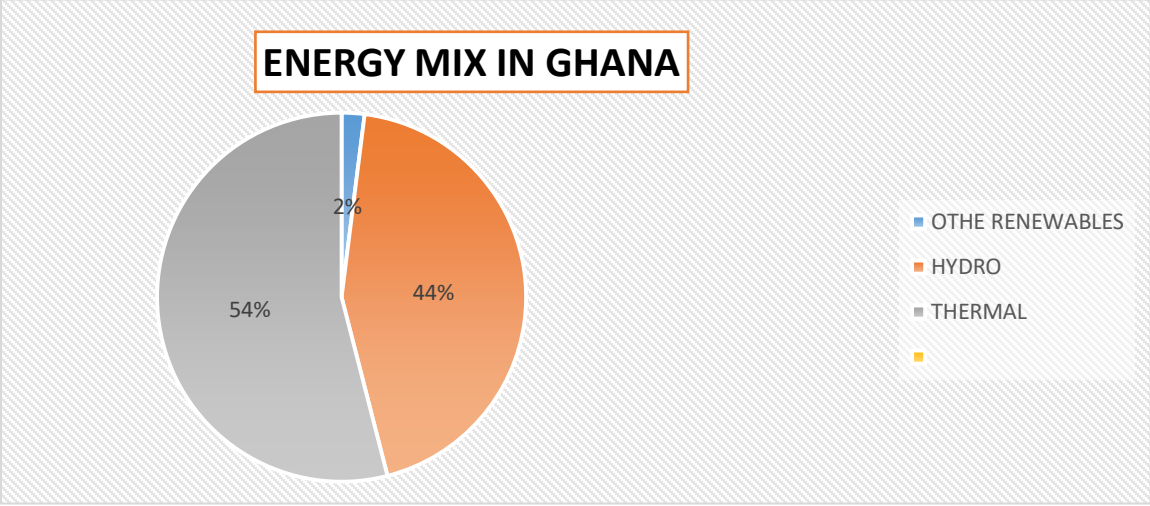
Figure 3.5: Energy mix in Ghana

(Source : Energy for growth hub, 2019)

3.12. BURKINA FASO

Burkina Faso is a country located in West Africa formerly known as Upper Volta and has a population of around 19.193 million people as of 2017 (Energypedia, 2019) . It is located 12.3333° N, 1.6667° W. The current electricity access rate in Burkina Faso is 19.16% and of this 60% of the population is in the urban while 3% is in the rural areas. 80 % of the power production from Burkina Faso is mainly from thermal generators and less than 15% is from hydropower. The current energy consumption is dominated by biomass at over 80% while petroleum and hydropower together were less than 16%. The majority of population still relies heavily on fuel wood and charcoal as a source of energy. SONABEL the national utility of Burkina Faso depends mainly on subsidies from the Government to cover its electricity production cost since tariffs cannot cover. The Government of Burkina Faso has a vision of reaching 95% electricity access to its population where by 50% will be in rural areas and universal access to clean cooking solution 65% in rural areas by 2030. In view of this they also want to increase the renewable energy in the electric mix by 50% by 2030 excluding biomass. It is high time for Burkina Faso to invest more in renewable energy electricity production given the fact most rivers originate from Burkina Faso such as Mouhoun river.

Utility of Burkina Faso

Burkina Faso has one of the most expensive electricity in the region around $ 0.22 - 0.25/kwh.

Energy access in Burkina Faso
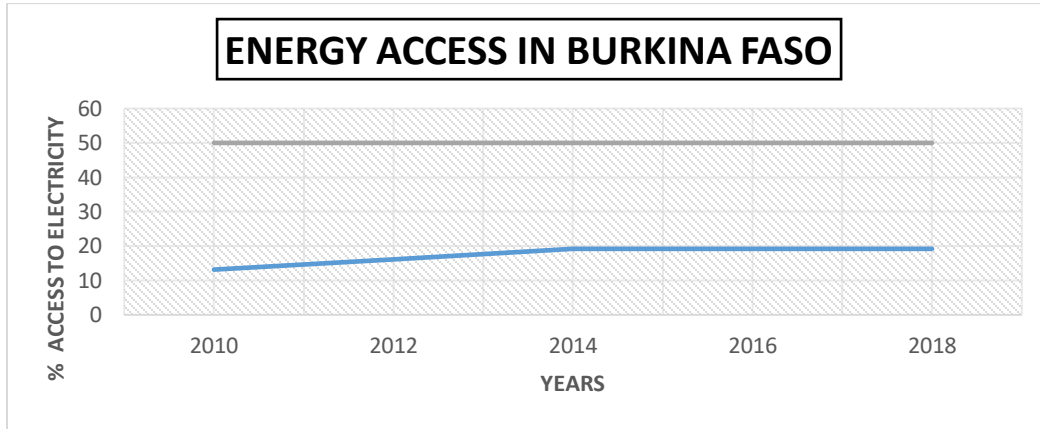
Figure 3.6 : Energy access in Burkina Faso

Figure 3. shows that the access to energy in Burkina Faso is very low it is far barely reaching the 50% mark) meaning more energy projects should be implemented to counter for the gap.

Energy mix in Burkina Faso
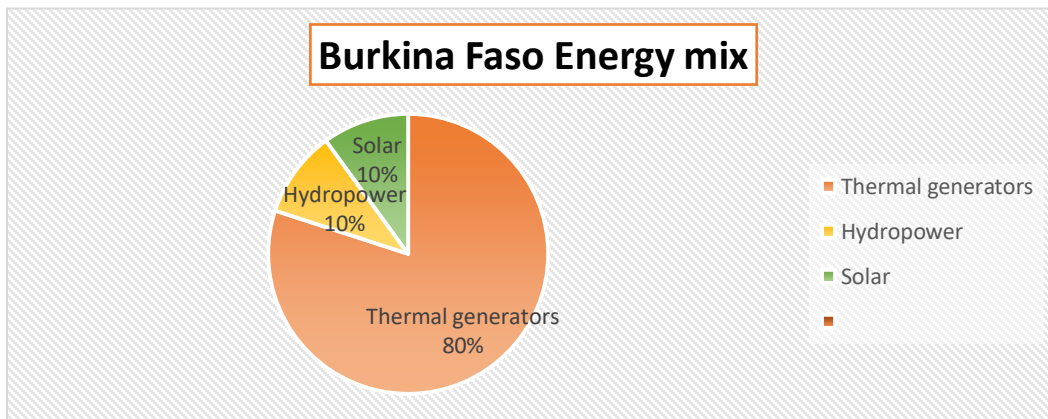
Figure 3.2 Energy mix of Burkina Faso

Source : (Power Africa, 2018)

Barriers to hydropower development in Burkina Faso

- Climatic conditions
- Institutional frame work related to water is more focused on water supply rather than hydropower.
- Few perennial rivers leaving most potential sites economically unviable (UNIDO, 2016)

3.13. IVORY COAST

Ivory Coast also known as Côte d'Ivoire electricity access has reached 92% of the population in urban areas while in the rural areas is still limited to 38% (IRENA, 2019). However, the overall electricity access rate is around 62% which is one of the highest rates in the region. Biomass still remains a primary energy source in Ivory Coast providing around 70 % of the energy in the country. Ivory Coast has significant potential for hydropower and it relied on it in the past but however with the discovery of more and more oil and gas the country is shifting its focus to thermal power generation.

3.14. MALI

Mali has less than 35.1 % of the population with access to electricity and its only major source of hydropower potential is along the Niger river. The population rely solely on biomass.

Existing and planned hydropower dams in the Black Volta basin

Table 3.2: Planned Hydropower Projects along the river

Name	Sub basin	Country	State	Capacity MW
Samendeni	Black Volta	Burkina Faso	Planned	2.4
Noumbiel	Black Volta	Burkina Faso	Planned	48
Koubil	Black Volta	Ghana	Planned	68
Ntereso	Black Volta	Ghana	Planned	64
Jambito	Black Volta	Ghana	Planned	55
Lanka	Black Volta	Ghana	Planned	95
Bon	Black Volta	Burkina Faso	Planned	7.8
Bontioli	Black Volta	Burkina Faso	Planned	5.1
Bonvale	Black Volta	Burkina Faso	Planned	0.3

Gongoorou	Black Volta	Burkina Faso	Planned	5

Source :(UNEP-GEF Volta Project, 2013)

3.15. CONCLUSION

Hydropower produces cheap electricity because of less operating costs. The demand for energy among the Black Volta states has increased tremendously over the past years but the generation capacity has remained the same resulting in high demand for electricity consequently leading to high levels of load shedding in the basin. In regard of this the Black Volta states must invest in hydropower. However, the sustainability of hydropower in future is at stack because of climate change. Policies should be put into place to ascertain that every hydropower planned projects must undergo climate impact assessment first in order to avoid surprises and wasting resources on an unsustainable project. Climate impact assessment is also important in order to look for ways to counter the climate change impacts (IRENA, 2019).

CHAPTER FOUR: HYDROLOGICAL MODELLING

4.1. INTRODUCTION

This chapter covers all activities and procedures followed in hydrologic modelling which includes data collection, data preparation, calibration and validation. This chapter basically answers the first objective "To set up the conceptual hydrological simulation model HBV for Bamboi catchment. The HBV light is setup to model the runoff of the Bamboi catchment. The achieved results for the calibration and validation process will determine whether the model can be used for climate impact assessment or not. This chapter will present the hydrological modelling process and the results will be outlined at the end of the chapter.

4.2. METHODOLOGY OF THE HYDROLOGICAL MODELLING

Hydrological modelling was carried out to model the Bamboi catchment run off. Catchment delineation is the first step in Hydrological modelling in order to set boundaries of the case study. Data was collected from meteorological stations inside the boundaries of the catchment. After data collection the HBV light model is set up (calibration and validation). The results of the calibration and validation process will determine the efficiency of the model to model the catchment runoff. Detailed information of the hydrological modelling process is detailed below. Figure 4.1 describes the steps followed in hydrologic modelling from data collection up to model validation.

Catchment delineation

Data collection and processing

Model set up

Model Calibration

Model validation
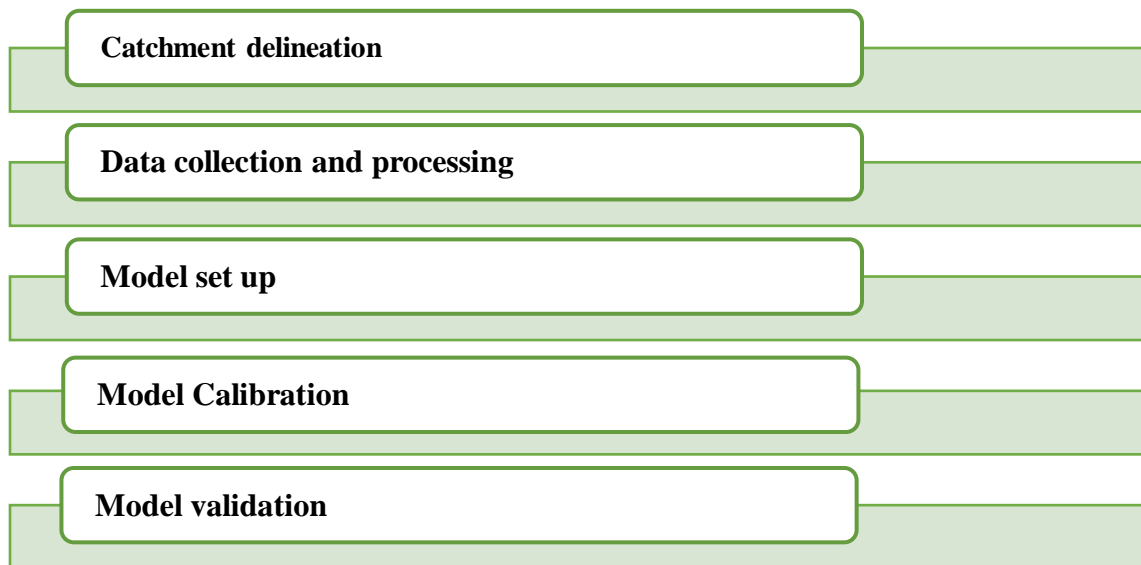
Figure 4.1: Methodology of Hydrological Modelling

4.3. CATCHMENT DELINEATION

4.3.1. Digital elevation model data

The DEM data for this study area Black Volta basin was downloaded from (://asterweb.jpl.nasa.gov/gdem.asp) and it had 90km resolution. The DEM data store topographic information inform of grid cells. The DEM data was used for watershed delineation which includes stream definition, outlets and inlets definition.

4.3.2. Catchment delineation

The catchment was delineated using hydrology tool set from the spatial analysist tool in Arch GIS version 9.2 and STRM 90, The shape file of Black Volta basin downloaded from the country borders shape file was collected. DEMs contains pits, ponds that should be removed before being used in hydrological modelling. Pits are points where would accumulate drainage patterns are being extracted. Pits are errors in the DEM and they must be removed.

Steps to delineate the catchment

1. Creating shape files
2. Contour digitalization
3. Preparation of DEM
4. Filling of the DEM
5. The DEM data is the input surface raster for the Filling process
   - Navigate Toolboxes > system toolboxes> spatial analyst tool> hydrology> fill
6. Flow direction
   - The flow direction tool was done to determine the direction of the flow from each cell
   - The input is the output of the fill process
   - Navigate Toolboxes > system toolboxes> spatial analyst tool> hydrology> flow

4.4. HBV LIGHT MODEL

HBV light model is made up of different routines and it simulates catchment discharge on a daily time step depending on precipitation, monthly potential evaporation and air temperature. Precipitation is simulated as snow if T is less than threshold temperature (TT) and precipitation is

44

simulated as rainfall if temperature is more than threshold temperature 5 (TT). Precipitation that is below TT is multiplied by Snow correction factor SFCF [-].

The water balance equation,

$$P - E - Q = \frac{d}{dt}\left[SP + SM + TZ + UZ + LZ + lakes\right]$$

Equation 4.1

Where:

P is precipitation, E is evapotranspiration, Q is runoff, SP is snow pack, SM is soil moisture, TZ is storage in soil top zone (introduced in HBV-light), UZ is upper groundwater zone, LZ is lower groundwater zone

Lay-out of the HBV equations

(Seibert, 2005)

Snow melt with degree day method

$$melt = CFMAX(T(t) - TT)$$

Equation 4.2

Refreezing

When the temperature falls below TT water freezes again

$$refreezing = CFR \; CFMAX(TT - T(t))$$

Equation 4.3

Rainfall and snowmelt (P) are separated into water filling the soil box and groundwater recharge depending on the relation between water content of the soil box (SM [mm]) and its largest value (FC [mm] Siebert 2005).

$$\frac{recharge}{P(t)} = \left(\frac{SM(t)}{FC}\right)^{BETA}$$

Equation 4.4

Actual evaporation from the soil box = potential evaporation provided SSOIL / PFC is above PL on the contrary linear reduction is used when SM / FC is below this value PL. Ground water recharge is added to the upper ground water box SUZ mm. PERC (maximum percolation rate from upper to the bottom reservoir (SLZ mm).

$$E_{act} = E_{pot} \ \min\left(\frac{SM(t)}{FC \cdot LP}, \ 1\right)$$

Equation 4.5

Runoff from the groundwater boxes is computed as the sum of two or three linear outflow equations depending on whether .SUZ is above a threshold value, UZL [mm] When SUZ is above the threshold value UZL mm runoff from groundwater boxes is calculated as the addition of 2 or 3 linear equations (Seibert, 2005).

$$Q_{GW}(t) = K_2 * SLZ + K_1 * SUZ + K_0 * \max(SUZ - SLZ, 0)$$

Equation 4.6

Runoff is finally converted by a triangular weighting function defined by MAXBAS to give the simulated runoff [mm d-1].

$$Q_{sim}(t) = \sum_{i=1}^{MAXBAS} c(i)\, Q_{GW}(t-i+1)$$

$$\text{where } c(i) = \int_{i-1}^{i} \frac{2}{MAXBAS} - \left| u - \frac{MAXBAS}{2} \right| \frac{4}{MAXBAS^2}\, du$$

Equation 4.5

$$P(h) = P_o \left(1 + \frac{PCALT\,(h - h_o)}{10000} \right)$$

$$T(h) = T_o - \frac{TCALT\,(h - h_o)}{100}$$

Equation 4.9

The long-term mean of the potential evaporation, Epot, M for a certain day of the year can be corrected to its value at day t, Epot(t), by using the deviations of the temperature, T(t), from its long-term mean, TM, and a correction factor, CET [°C-1] .

$$E_{pot}(t) = \left(1 + C_{ET}\left(T(t) - T_M \right) \right) E_{pot,\,M}$$

$$\text{but } 0 \le E_{pot}(t) \le 2\, E_{pot,\,M}$$

Equation 4.6

4.5. METEOROLOGICAL AND HYDROLOGICAL STATIONS

The Bamboi catchment has two types of stations meteorological stations located in the basin which are synoptic stations which only measure rainfall, temperature; wind speed, radiation and relative humidity and their hydrological stations which measures discharge.

Meteorological and Hydrological stations in the study area catchment.
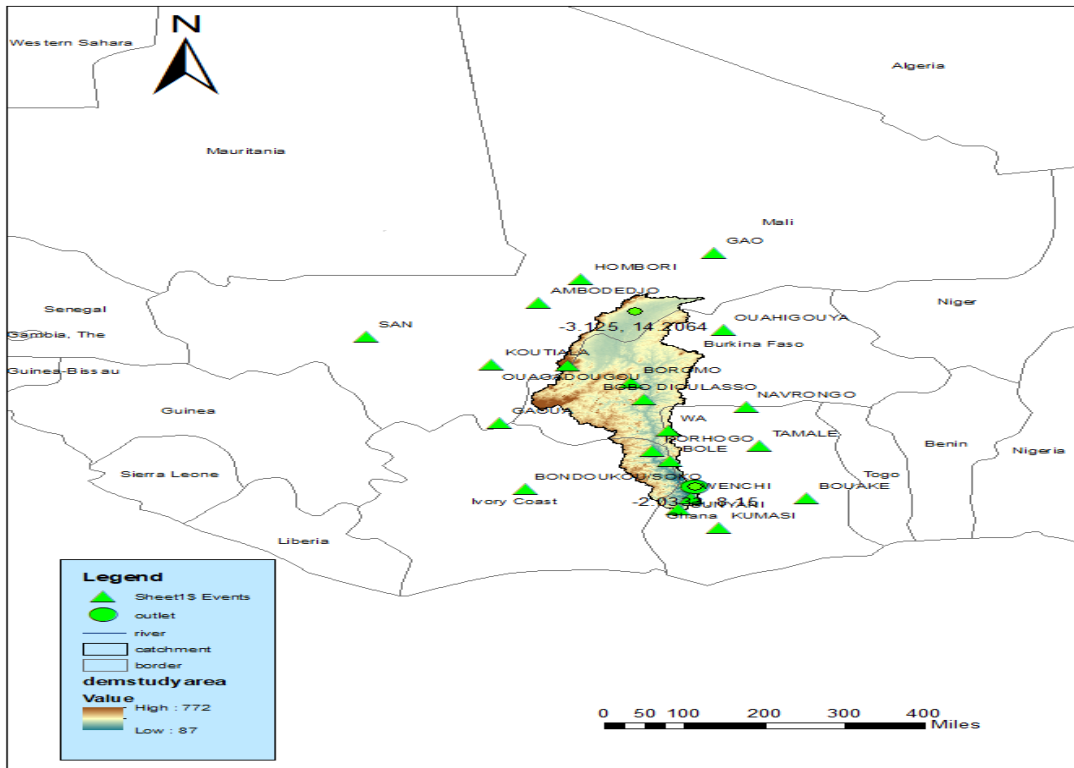
Figure 4.2: Location of Hydrological and Meteorological stations in the Black Volta basin

4.6. INPUT DATA FOR HBV LIGHT MODEL

Climate data

Climate data is an important driver of hydrologic models, however it is difficult to acquire in developing countries for several reasons, including sparse, damaged or non-existent rain gauge stations (Poméon et al., 2017). Furthermore, data from the existing rain gauge stations often have inaccurate or large data gaps. The climate data for this research was first downloaded from the NNDC Climate data online with the following link:

(https://www7.ncdc.noaa.gov/CDO/cdoselect.cmd?datasetabbv=GSOD); However, the data had large gaps, for a complete time series there was no single year with 100% complete data or even up to 60% which led the researcher to look for other ways of acquiring data with few or no gaps at all. The data which was eventually used is from the CFSR (Climate Forecast System Reanalysis) coupled atmosphere-ocean-land system from this link (link https://globalweather.tamu.edu/). The

48

data requested had a time series of 35 years from Jan 1979 to July 2014. The data was almost complete it had very few gaps, the only gaps were for a period of 10 days in 1986. The CFSR is developed at NOAA –NCEP and it provides several climate variables which are precipitation, wind speed, relative humidity, solar radiation and temperature. The CFSR Inco-operates various data sources from surface observations, radiosondes and from satellite instruments. However, there is debate on the eligibility of these data sets. According to the study carried out by Poméon et al. (2017) on evaluating the performance of remotely sensed and reanalyzed precipitation data over West Africa using HBV light the results showed that most data sets managed to predict the observed steam flow data which make this data sets reliable (Poméon et al., 2017).

Precipitation data

For a satisfactory calibration and validation of modelling using HBV light, ten years data was used to increase the accuracy of the model. Precipitation data was collected from 6 meteorological stations which lies within the basin (see table 4.1 above). The precipitation data was requested from the CFSR (Climate Forecast System Reanalysis) coupled atmosphere-ocean-land system. The time series of the data was for a period which ranged from 1979 Jan 1 to 2014 July 31.

Air temperature

Maximum and minimum temperature data were collected from 6 meteorological stations within the catchment requested from the CFSR (Climate Forecast System Reanalysis) coupled atmosphere- ocean-land system. The mean air temperature for each day was used as input to the HBV model and the time series was for a period of 35 years.

4.7. HYDROLOGICAL DATA

4.7.1. Discharge data

Historical discharge data of Bamboi catchment of Black Volta river was requested from the GRDC station number 153 1100 (Bamboi gauge station). Mean daily discharge data obtained from the station is for a period of 32 years from January 1975 to February 2007. The data was obtained in m^3/s and in that file all the missing data were replaced with -999.9.

4.8. CLIMATE DATA PROCESSING

Data used to carry out this research was obtained from CFSR (Climate Forecast System Reanalysis) coupled atmosphere-ocean-land system. Data was exported to excel sheet and was

arranged into different columns. The date column was arranged in this format Year, Month, Day. The data recorded was in calendar date order. Data from six different stations were added together and the average of the stations data was used. One of the challenges encountered during data cleaning was the date column had different dates format 01/ 01/ 1979 and 1/ 01/1979 which made them not be read as date in excel. To rectify the problem all entries in the date column were corrected to this particular format (1/01/1979). After arranging the data in specific columns the data was checked for inconsistence and outliers were removed or replaced with the correct figures (nearest station, long term mean monthly value.). All climate data in different units was converted into the precipitation in mm per day, temperature in degrees Celsius, wind speed in m per day, humidity in percentage and solar radiation in W/m².

Checking for missing data

A pivot table (MS-Excel) was used to analyse, visualise and to check for the missing data. It was used to generate a simple count of the data available in a year.

Pivot table
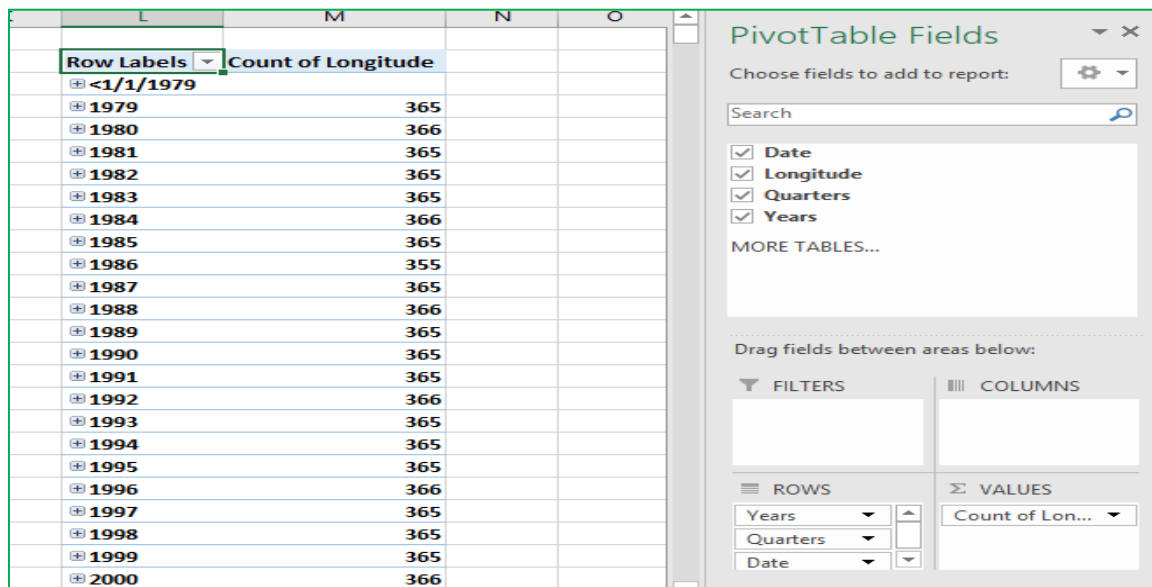
Figure 4.3 : Screen shot pivot table in excel windows

Calculation of the missing data

The percentage of missing data per year should be calculated by using this formula

Let percentage of missing data be **x**

50

let the available data in a year be **n**

Equation 4.7

$$x = \left(\frac{(365-n)}{365} \right) * 100$$

NB: all climate data has the same time series and the same number of missing data because it was acquired from the same source.

Table 4.1 : Percentage of missing climate data for time series (1979 – 2014)

Year	Number-of-available data	Percentage-of available data
1979	365	100%
1980	366	100%
1981	365	100%
1982	365	100%
1983	365	100%
1984	366	100%
1985	365	100%
1986	355	97%
1987	365	100%
1988	366	100%
1989	365	100%
1990	365	100%
1991	365	100%
1992	366	100%
1993	365	100%
1994	365	100%
1995	365	100%
1996	366	100%
1997	365	100%
1998	365	100%
1999	365	100%
2000	366	100%
2001	365	100%

2002	365	100%
2003	365	100%
2004	366	100%
2005	365	100%
2006	365	100%
2007	365	100%
2008	366	100%
2009	365	100%
2010	365	100%
2011	365	100%
2012	366	100%
2013	365	100%
2014	212	58.8%

From the table above only two years has missing data for climate data which is 1986 and 2014.

Discharge data

Discharge data collected from GRDC site. The data has a lot of gaps and they were replaced with -999.9.

Table 4.2: Percentage of missing discharge data for time series (1979 – 2007)

Year	Available data	% of Available data
1979	0	0%
1980	60	16%
1981	0	0%
1982	53	14%
1983	0	0%
1984	153	42%
1985	0	0%
1986	0	0%
1987	0	0%
1988	0	0%
1989	208	57%
1990	152	42%

1991	231	63%
1992	365	100%
1993	181	50%
1994	0	0%
1995	315	86%
1996	30	8%
1997	0	0%
1998	0	0%
1999	259	71%
2000	366	100%
2001	365	100%
2002	213	58%
2003	339	93%
2004	331	91%
2005	365	100%
2006	365	100%
2007	'59	16%

From the above table most discharge data was missing this posed problem in getting good model efficiency during calibration and validation steps because of frequent gaps. Only 5 years out 28 years had 100% available data.

4.9. DATA GAP FILLING

- **Precipitation**

Precipitation data was obtained from six stations and the data time series was not simultaneous, it had 10 days missing data for the year 1986.

Three methods were considered to fill the missing data which are:

- Ignore the missing data
- Treat the missing value as zero
- Interpolate the missing data by using data from other stations

Ignoring the missing data could not be applied because HBV light model cannot run data with gaps. In this case all the missing precipitation data was treated as zero.

- **Temperature**

There is a gap of 10 days of temperature missing from the available data. The mean monthly average data was used to fill the gaps of the missing data of that particular month**.**

- **Relative humidity, wind and solar radiation**

Relative humidity, wind and solar radiation had **t**en missing days and it was filled by using data from a nearby meteorological station using correlation.

- **Discharge data**

Discharge data was not simultaneous and there were a lot of gaps. Out of a time series of 28 years from 1979 to 2007 only 5 years had complete data sets (see discharge table 4.2 above). This missing discharge data was replaced by inserting 999.9 on each missing data

4.10. ETO CALCULATOR

ETo is a key factor in hydrological modelling and climatology studies. In this research daily weather data from six different stations within the catchment employed during the time series (1979 – 2014) were used to calculate the ETo. ETo data was calculated from the climate data of temperature, wind, relative humidity and solar radiation using ETo calculator. The output ETo was then used as input to the HBV light model. ETo data is a prerequisite to prepare an Evap text file that is used to run HBV light model. Figure shows the ETo calculator window.
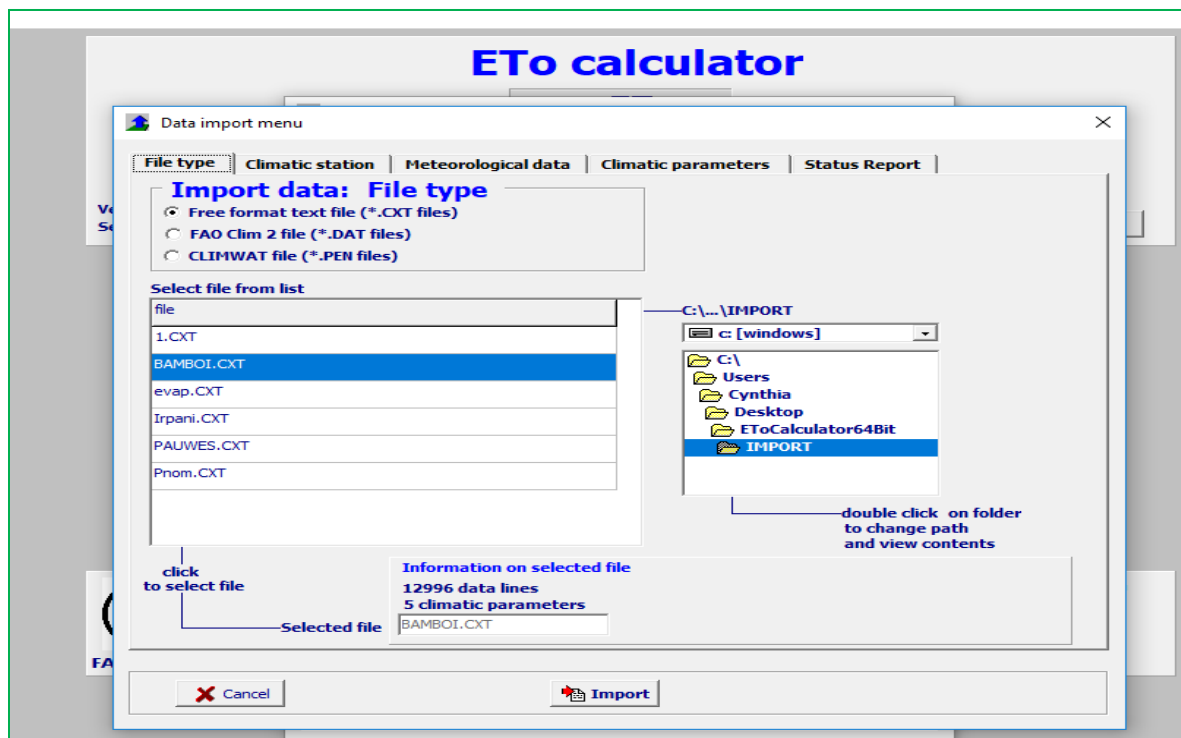
Figure 4.4 : Screen shot from ETo windows

4.11. HBV LIGHT MODELLING

Creation of ptq file

Ptq.txt: create ptq file – a file which contains precipitation, temperature and discharge. First the excel file should be converted into ASCII file, then set the columns in the sequences of year, month, day, precipitation, mean temperature and discharge. The data recorded must be in calendar date order. After processing the step data analysis, the resulting indices series are stored in sub-directory indices in csv format.

Creation of Evap file

Evap.txt- create Evap file – a file which contains ETo values. First the excel file should be converted into ASCII file, then set the columns in the sequences of year, month, day and a column of Eto. The Data recorded must be in calendar date order. After processing the step data analysis, the resulting indices series are stored in sub-directory indices in csv format.

Model setup

The first step in hydrologic modelling is to create the ptq file and evap file. The time series of the given data is divided into three parts, the warm up period, the calibration period and the validation step.

Warm up period

HBV light uses warm up period to allow state variables evolve from standard initial values to their appropriate values according to climatic conditions and parameter values. The warm up period is done to allow all parameters to normalise . Warm up period used in calibration step was from 1979 to 2001 and the warm up period used in the validation step was from 1979 to 2004.

4.11.1. Calibration

Model calibration is the process of calculating the best model parameter set by comparing the simulated data with the observed data under similar conditions. The calibration period was chosen for periods with few missing discharge data. Time series with large number of missing data was used as the warm up period. The estimated best parameter set will then be used as inputs to the model in climate impact assessment (Moriasi et al., 2007). In this research calibration was carried out using discharge data available from the GRDC for Bamboi station, the discharge data ranged from 01 Jan 1979 to 2007 Feb 28. The data from 1979 Jan to 2001 Jan was used as the warming period. The data from 01 Jan 2001 to 01 Jan 2004 was then used for calibration. Calibration was done by GAP optimisation to acquire the model parameters that will the best possible agreement between observed and simulated discharge of the catchment. GAP simulation technique was done by decreasing the lower limits values and increasing the upper limits values. The number of model runs were increased from 10 000 runs to 75 000 runs. The best parameter setting was found at 50 000 runs. 50 000 Monte Carlo simulations runs were done to identify the best parameter set. The calibration process was repeated iteratively until the best parameter set was achieved. The best parameter set is the set of values that give best model efficiency.

4.11.2. Validation

Model validation is a process of proving that a given model can make accurate simulations, it is done by running the model using the best parameter set obtained during the calibration phase. During the validation process warm up period was taken from 01 Jan 1979 to 01 Jan 2004 and the validation period ranged from 2004 Jan 1 to 2007 Feb 28. Model Validation represents the model's

ability to answer the present and future and to simulate the observed discharge. Validation step was done using the best parameter set obtained from the calibration period (Moriasi et al., 2007).

4.12. SPI (STANDARDIZED PRECIPITATION INDEX)

SPI is a drought analysis tool which is used to monitor water resources in a region. The input is only precipitation. SPI requires 30 years of continuous data. In this research data for 34 years was used to run the Drinc software in order to calculate SPI for Bamboi catchment.

Classification of dryness/wetness based on the SPI

SPI values	Class
>2	extremely wet
1.5 to 1.99	very wet
1.0 to 1.49	moderately wet
-0.99 to 0.99	near normal
-1 to −1.49	moderately dry
-1.5 to-1.99	severely dry
< -2	extremely dry

Figure 4.5 :SPI index range

Figure 4.5 SPI Index range used to interpret the results of SPI, it assesses periods which had drought and the periods which were extremely wet. SPI index is also used to justify choice of selection of the period of running the model (calibration and validation). Choice of calibration and validation years should be years with SPI values of near normal range in order to give exact representation of the catchment.

4.13. PARAMETERISATION OF THE HBV LIGHT MODEL

Process parameters in the HBV-light model are not physically measurable thus they must be calibrated. There is no reputable method to estimate model parameters, calibration method is used to determine the best parameter by varying gap optimization parameters by selecting the minimum and maximum value of each parameter. The best parameters that gives the best model efficiency will then be loaded in the next step of climate impact assessment

4.14. MODEL EVALUATION

Different techniques are used to assess the fit of the simulated runoff to the observed runoff which are accumulated difference, statistical criteria and visual inspections of plots with Qsim and Q Obs. The criteria for model evaluation used in this research was done by several criterias, the first criteria was by visual inspection by observing the peaks and the similarity of the simulated and observed graphs. The second criteria was by considering performance, Nash-Sutcliffe efficiency (NSE), coefficient of determination (R^2) and KGE. Nash-Sutcliffe efficiency (NSE) is the model efficiency.

4.14.1. NSE (Nash-Sutcliffe efficiency)

$$NSE = 1 - \frac{\sum_{t=1}^{T}(Q'_o - Q'_m)^2}{\sum_{t=1}^{T}(Q'_o - \bar{O}_o)^2}$$

Equation 4.8

Generally, NSE is very good when NSE ranges from to 0.75 to 1, good when between 0.65 to 0.75, satisfactory when between 0.5 to 0.65 and unsatisfactory when it below 0.5. This is how the calibration and validation process were evaluated (Bhattarai et al., 2018).

4.14.2. R^2 and r

Pearson correlation coefficient R^2 and coefficient of determination they describe the relationship between simulated and observed data. The correlation ranges from -1 to 1, the higher the values the higher the collinearity between the two. If r =0 there is no perfect relationship at all. If r = 1 or -1 it's a perfect positive or perfect negative (Moriasi et al., 2007).

$$R^2 = \left(\frac{\sum_{i=1}^{N}(Q_{oi} - \bar{O}_o)(Q_{mi} - \bar{Q}_m)}{\sqrt{\sum_{i=1}^{N}(Q_{oi} - \bar{O}_o)^2 \sum_{i=1}^{N}(Q_{mi} - \bar{Q}_m)^2}} \right)^2$$

Equation 4.9

4.14.3. Kling Gupta efficiency

$$KGE = 1 - \sqrt{(r-1)^2 + (\beta - 1)^2 + (\gamma - 1)^2}$$

General performance ratings for recommended statistics parameters

0.75 <NSE<=1	Very good
0.65 <NSE<=0.75	Good
0.5 <NSE<=0.65	Satisfactory
NSE<=0.5	Unsatisfactory

4.15. RESULTS

Figure 4.6 SPI (standardized precipitation index) shows the results of the SPI index of

SPI index for Bamboi catchment.
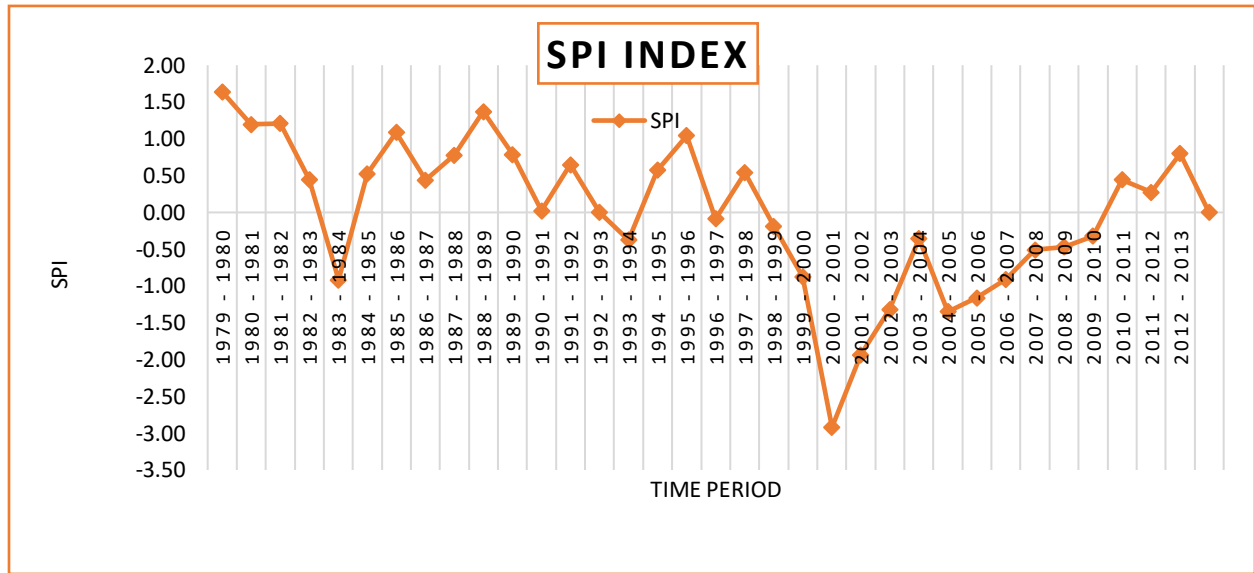
Figure 4.6 : SPI index results

The Standardized Precipitation Index of the catchment for the period 2001-2007 (see Figure 4.6 of the SPI index for Bamboi catchment), indicates that calibration and validation periods include a couple of dry -moderately to extreme- years (2001-2002). However, the rest of the calibration-validation period is rather normal therefore represents the long term normal climate of the catchment.

4.15.1. Results of best parameters of GAP optimization

Table 4.3 shows the gap optimization best parameter set obtained during the calibration and validation phase. This best optimisation parameter set will be used for climate impact assessment phase.

Table 4.3: Results of best parameter sets of Gap optimization in HBV light modelling

Parameter	Initial gauge		Best parameter values
	Lower value	Upper value	Best parameter
TT	-2	1	0.49988977888
CFMAX	0	4	3.71669012705
SP	0	1	1
SFCF	0	1	7.40547917774
CFR	0	1	7.91358771133
CWH	0	1	9.3983037728
Soil moisture routine			
FC	1	2000	123.356178052
LP	0	1	0.99999428837
BETA	1	30	1.0042775346
Response routine			
PERC	0	50	0.01087754346
UZL	0	150	0.07494044537
K0	0	0.99999	0.99899603491
K1	0	0.99999	0.70166626583
K2	0	0.99999	0.01877919273
Routing Routine			
MAXBAS	1	30	40.4828532428
P CALT	1	30	
T CALT	0	30	

4.15.2. Calibration

The model statistical quality measures achieve during the calibration are shown in

Table 4.4 : Goodness of fit for the Calibration and Validation period , while simulated and observed discharge for the same period are shown in Figure 4.7. The quality measures achieved during calibration equal 0.66, 0.66 and 0.73 for $R2$, NSE and KGE respectively, indicating a

satisfactory to good agreement between observed and simulated discharges. Making the model efficiency able to simulate the catchment discharge. The visual inspection of the hydrograph shows a broad agreement between simulated and observed discharge. However, several discrepancies can be observed. Notably, (i) some peaks are not well reproduced in 2001 and 2002, (ii) peaks are underestimated in 2001 and 2002, and (iii) peaks are overestimated in 2003. Using reanalysis climate data can reasonably have explained these discrepancies. In general, model achieved efficiencies up to 0.73 and the simulation of the annual pattern of the discharge fits to the observation indicating its ability to reproduce the hydrological regime of the catchment.

Table 4.4 : Goodness of fit for the Calibration and Validation period

Process	*R^2*	*NSE*	*KGE*
Calibration	0.66	0.66	0.73
Validation	0.59	0.57	0.75

Observed and Simulated discharges for the calibration period
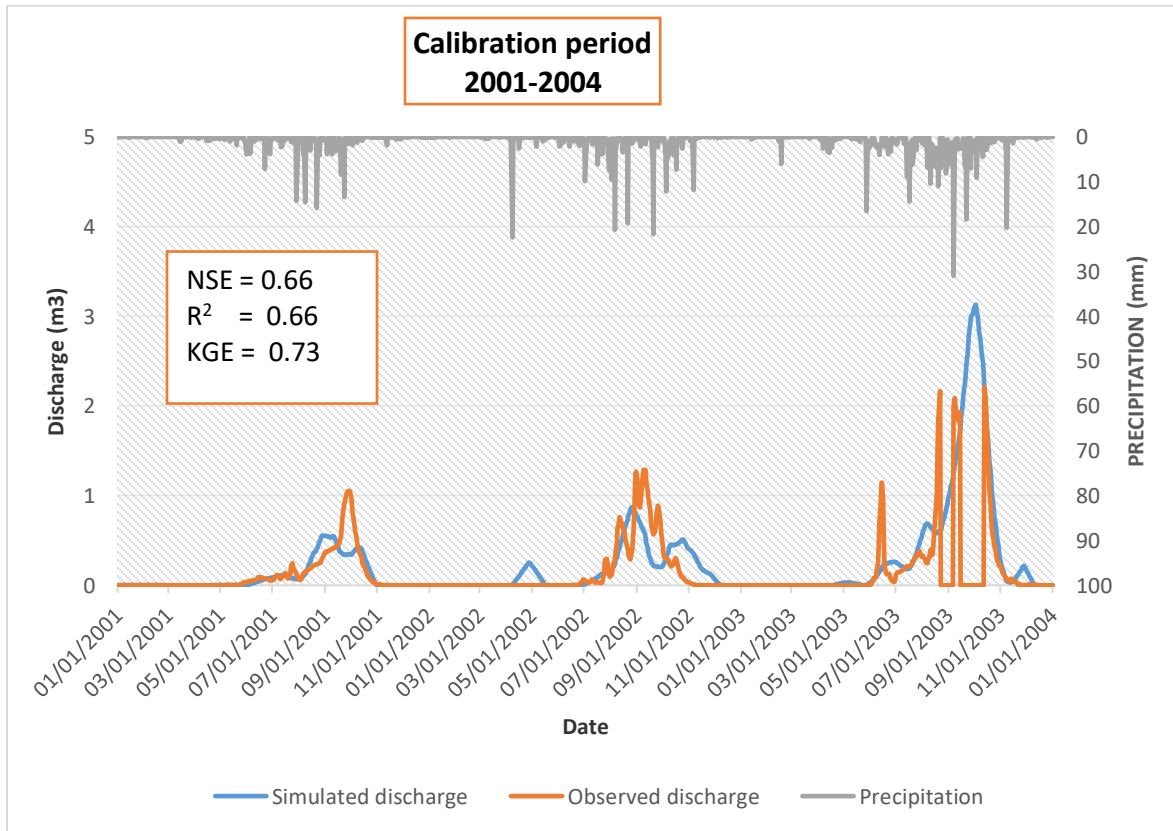
Figure 4.7 Observed and Simulated discharges for the calibration period

4.15.3. Validation

The model efficiency during the validation step is shown in Table 4.4. A validation efficiency of 0.56 was obtained compared to calibration efficiency of 0.66. The reason for the decrease is frequent missing discharge data. The validation was done during the period of 3 years from 2004 to 2007. Figure 4.8 shows observed and simulated discharges for Bamboi catchment for the validation period. Similarly, to the calibration period, underestimated peaks are noticed for years 2004 and 2005. Unlike for the calibration phase, discharge overestimation is not observed for the validation period. The statistical measures and hydrographs of the calibration phase are confirmed by this validation phase and are within acceptable range indicating the ability of the model to reliably simulate catchment hydrological behavior.
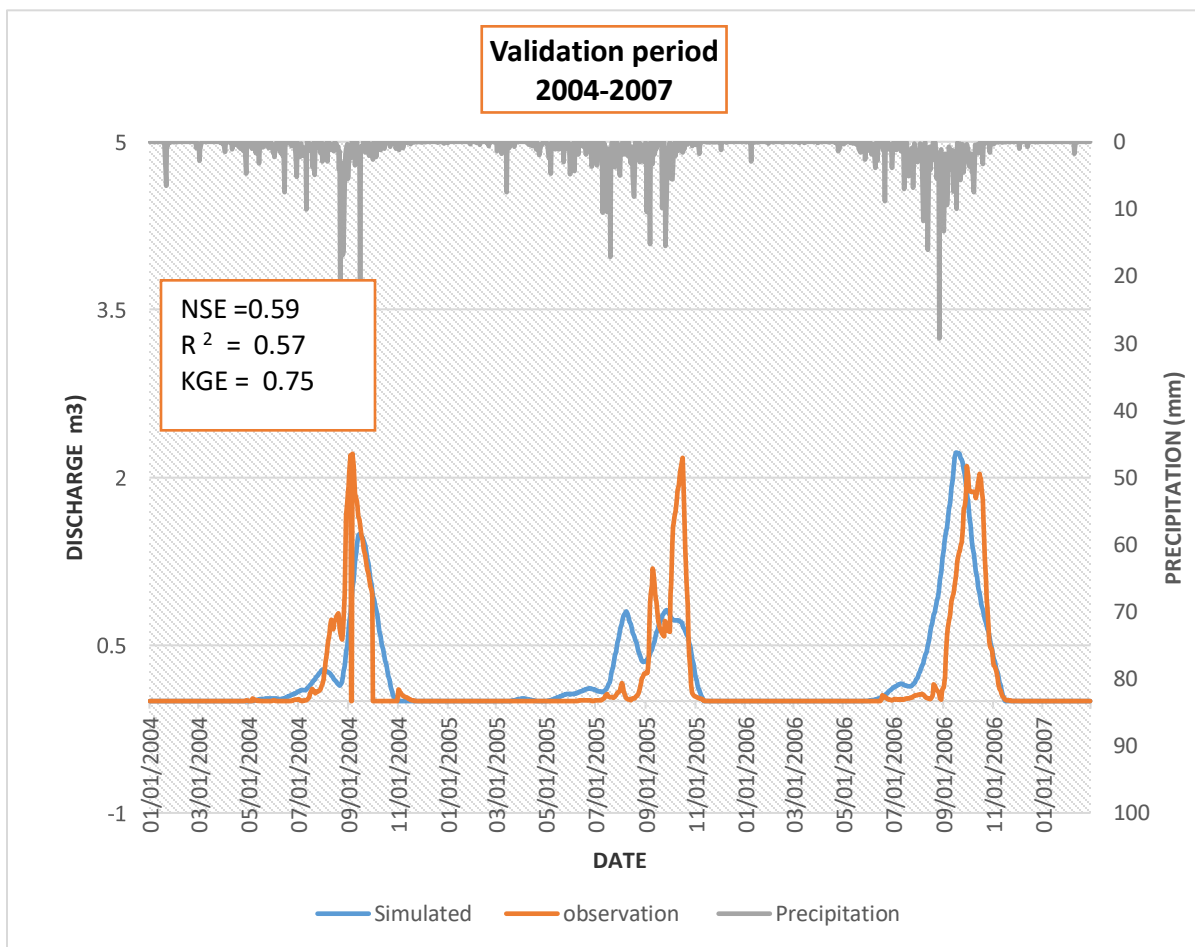
Figure 4.8 Observed vs Simulated flow during the validation period

4.16. CONCLUSION

Achieved model statistical quality measures are fair to good for the calibration and validation periods, indicating a good agreement between simulated and observed discharges for the Bamboi catchments. HBV - light model has been proved to be very effective to simulate discharge of Bamboi catchment. The model was calibrated for the period 2001- 2004 and validated for the period 2004 -2007 with satisfactory results producing values NSE coefficient of 0.66 during calibration and 0.56 during validation. The value of coefficient of determination R^2 during the calibration is 0.66 and 0.59 during validation. All the aforesaid shows that the model is effective in simulating the observed discharge which makes it suitable to carry out climate impact assessment.

CHAPTER FIVE: CLIMATE IMPACT ON THE HYDROLOGY OF THE CATCHMENT

5.1. INTRODUCTION

This chapter addresses the impact of climate change on the hydrological regime of the Bamboi catchment. It basically answers the second specific objective of the study, i.e. "To assess the impact of future climate change on the hydrological regime of the catchment through scenario (RCP4.5) application comparing a reference period (1983-2005) to two future periods 2020-2049 and 2070-2099". The assessment is done through the application of climate simulation products to the validated hydrological model. Two climate simulation datasets are used: (i) a WASCAL high resolution simulation dataset for west Africa and (ii) a CORDEX dataset, both datasets are developed under RCP4.5 scenario.

5.1. DATA SOURCES

Due to the limited resolution of Global Circulation models-GCMs (about 110 km), Regional Circulation models (RCMs) have gained ground over last years. Indeed, the resolution of GCMs does not allow reproducing topographic variation, coastlines, land use and mesoscale convection etc. High computational power is allowing to run RCMs at high resolution of even less than 12km and they give a more representation of the GCMs and the area. The climate simulations products developed by WASCAL (RCP4.5) WRF- G (GFDLESM2M) as well as the CORDEX climate product with the same concentration pathway RCP 4.5 were applied in this study to assess climate change impact on the hydrological regime of the catchment.

5.2. WASCAL CLIMATE PRODUCT

The first GCM – RCM high resolution climate product for the greenhouse gas scenario concentration pathway RCP 4.5 (Representative concentration pathway) developed by WASCAL at 12 km resolution using WRF was used in this research. RCP 4.5 was chosen specifically because of limited computational resources and is based on the fact that the difference between RCP 4.5 and RCP 8.5 became significant after 2040 and that the RCP4.5 is a reasonable scenario according to COP 21 agreement (Heinzeller et al, 2018). High resolution data provide a more accurate portrayal of the topographic features and coastline which improves the reliability of the simulations. WASCAL climate product has three GCMs downscaled using the Weather Research and Forecasting Model (WRF). It is an ensemble of WRF–E with GCMs driven runs WRF-M,

WRF-G and WRF-H. Only WRF- G (GFDLESM2M) was used in this research. The simulation covers the period 1980- 2005 as the historical period or reference period and the two future periods 2020 – 2050 and 2070 – 2100. The data for WASCAL high climate resolution can be downloaded from CERA long term archive of Germany climate computing center with subset available at the PANGAEA Data Publisher for Earth & Environmental Science portal. The link below for downloading:(https://doi.pangaea.de/10.1594/PANGAEA.880512). Data provided is in compressed net CDF4 CF -1.6 compliant format. WASCAL Data is produced at high temporal resolution 3-hourly, 6- hourly summed to daily or monthly time series and 25 pressure. As for the current study, the applied dataset was readily available at the WASCAL Competence Center.

5.3. CO-ORDINATED REGIONAL CLIMATE DOWNSCALING EXPERIMENT (CORDEX)
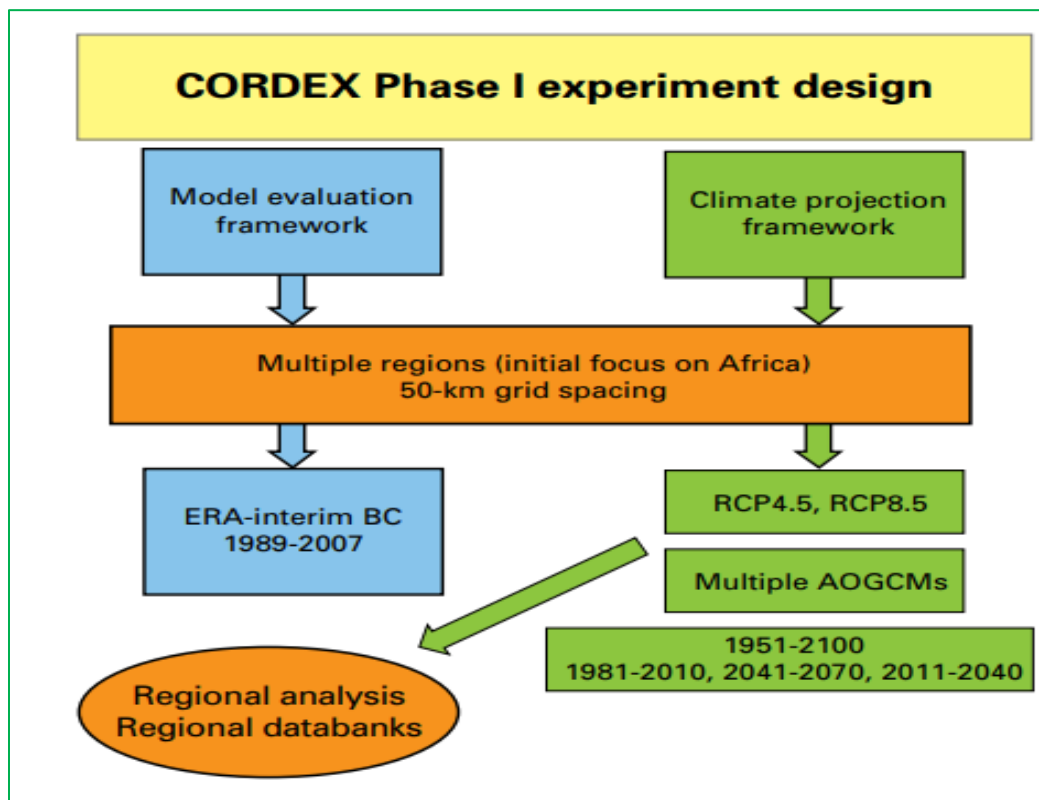
Figure 5.1 : Experiment design source: (Giorgi et al, 2009)

The second climate dataset used was obtained from the regional climate model REMO developed in the framework of CORDEX-Africa project and available on a 0.44° spatial grid. The use of a CORDEX climate dataset in this research is based on data availability and the reliability of climate

models over West Africa. Furthermore, REMO has been successfully used in quite a number of climate studies in Africa. MPI – ESM is the global model and REMO is the regional model which is downscaling the GCM. REMO simulations are driven by MPI-ESM –LR with RCP 4.5 concentration pathway. The simulation covers the period 1980- 2005 as the historical period or reference period and the two future periods 2020 – 2050 and 2070 – 2100. The purpose of the CORDEX high regional climate simulations for climate change is to provide high regional climate simulations at regional and local level. CORDEX data can be downloaded from the CORDEX domain Max Planck Institute of Meteorology website. As for the current study, a dataset readily available at the WASCAL Competence Center was used. Each data sets have historical runs and projections based on scenario RCP 4.5. REMO is a three-dimensional, hydrostatic atmospheric circulation model which solves the discretized primitive equations of atmospheric motion (Mbaye et al, 2015).

Table 5.1: REMO characteristics

Institute	Max Planck Institute of Meteorology , Germany
Main driving Model	MPI-ESM
Projection	Rotated spherical grid
Resolution	0.44 deg
Vertical coordinates	Hybrid

Source : (Mbaye et al, 2015)

5.4. DOWNSCALING

Downscaling is a technique of transferring information from a limited resolution GCMs to a finer scale higher resolution (RCM) over a limited area with initial and boundary conditions taken from a driving GCM using a forcing model. In this research two GCMs are downscaled using the Weather Research and Forecasting Model (WRF) for the WASCAL product and REMO for the CORDEX product to estimate the impact of climate change in the region and to reduce the degree of un certainness. RCMs are more reliable than GCMs and they are better represented at regional level.

Table 5.2 : RCM –GCM Products and the corresponding label used in the study

Framework	Institute	GCM/ESM	Name	RCM	Experiment
CORDEX	Max-Plank institute (MPI)	MPI-ESM	MPI-ESM REMO	REMO	Hist./Proj
WASCAL	WASCAL	GFDL ESM2M	GFDL-ESM2M	WRFV3.5.1	Hist./Proj

The two selected GCMs are based on different calendar dates. MPI-ESM-MR model and ERA interim use Gregorian calendar GFDL-ESM2M use a 360-day calendar (30 days X 12) and (365 days no leap year).

5.5. METHODOLOGY OF CLIMATE IMPACT ASSESMENT

A statistical bias correction using the Empirical Quantile mapping was applied to the climate data sets. Both corrected and non-corrected data were used as inputs to the HBV light hydrological model to simulate the catchment runoff. The suitability of HBV light to simulate the hydrology of the Bamboi catchment was confirmed in Chapter 4 of the current study. Details of the model set up is available in that Chapter. Minimum values of 0.57 for Nash Sutcliffe Efficiency, 0.73 for Kling-Gupta Efficiency and 0.59 for R^2 were achieved during the calibration and validation using observed discharge. Three periods (i) 1983-2005 (reference), (ii) 2020-2049, and (iii) 2070-2099 are compared. The expected climate change is expressed as the relative difference between simulated hydrological variables under reference period 1983 -2005 and the two future periods (mid-century 2020-2049 and end of century 2070 -2099). The climate change signals between different periods will be compared and impact on the hydrology of the catchment analysed. Hhistorical and projected discharges data obtained from the current chapter will be key inputs to the hydroelectricity generation approach as addressed in the next chapter.

Figure 5.2 below describes the methodology used to carry out climate impact assessment of Bamboi catchment. It explains the methods, techniques and appropriate tools used to achieve the desired results**.**
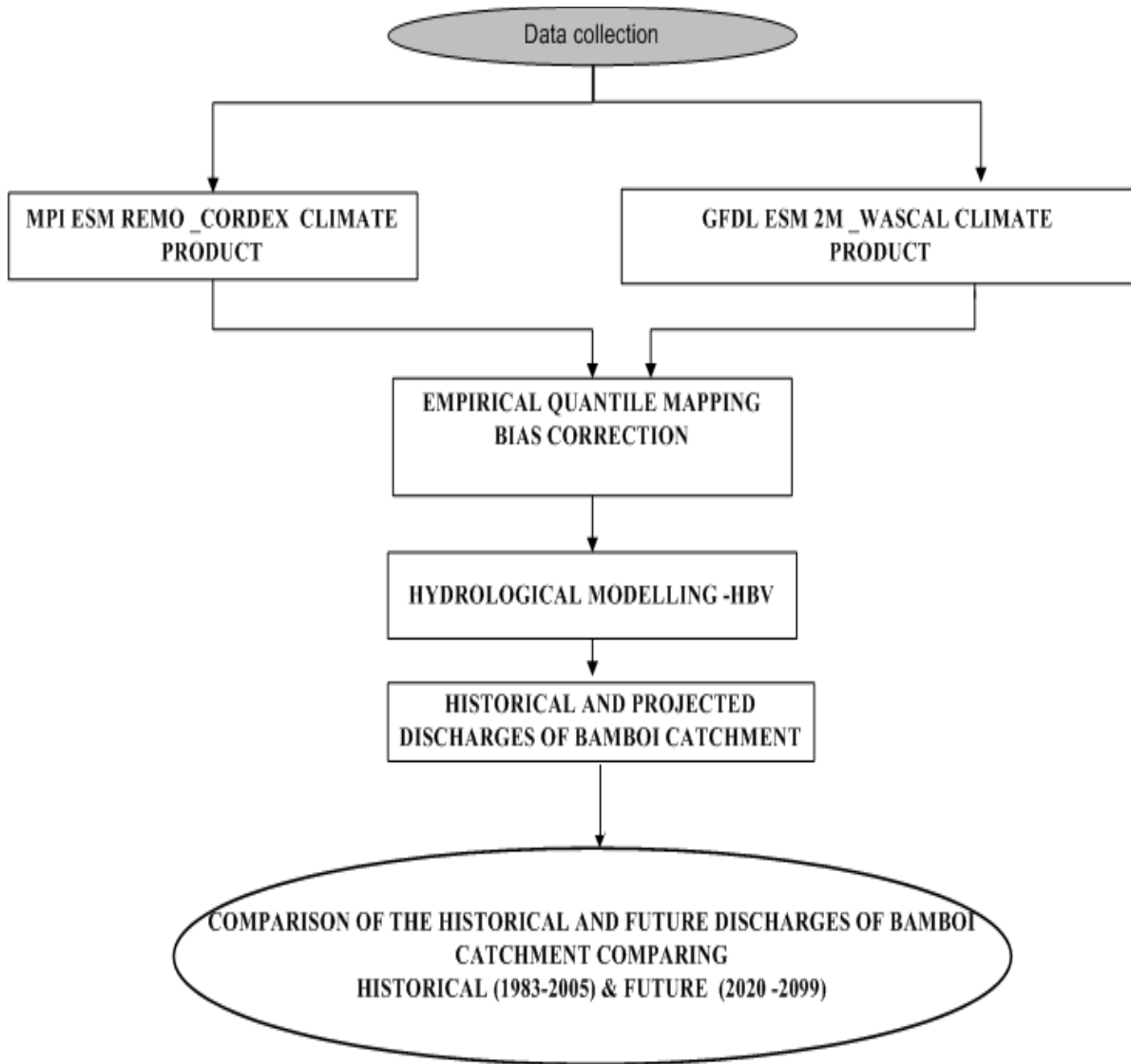
Figure 5.2 : Methodology of climate impact assessment

5.6.DATA ASSESSMENT

Comparison of historical observed and historical simulated

A comparison of the historical simulated and historical observed data sets is done to assess how much the historical simulation data deviates from the observed data set. Decision will then be made whether to directly use RCM outputs or to carry out bias correction in order to correct the data. Deviation between historical simulated and observed data was analyzed. This difference is assessed by plotting for each member of the climate models ensemble, historical observed and historical simulated data for each climate variable.

Historical observed vs historical simulated climate data of Bamboi catchment

From the comparison of simulated and observed temperature, precipitation and wind graphs (figure 3.5 fig 5.4 and fig 5.5) important differences can be noticed. Indeed, the simulated precipitation, wind and temperature are all overestimated with respect to the observed data. Thus, it is advisable bias correcting the data before using them as input for hydrological modelling. However, as bias correction can alter climate change signal, in the current study both bias corrected and non-bias corrected data are applied and presented.

Observed precipitation vs simulated precipitation
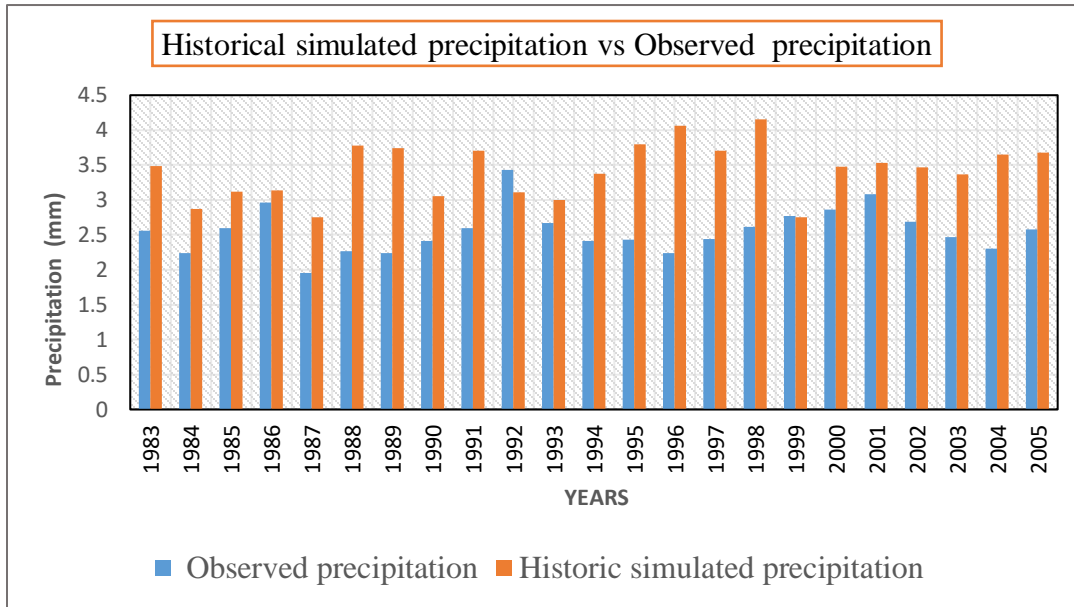
Figure 5.3: Historical simulated and observed precipitation

5.6.1.   Historical simulated temperature vs observed temperature of Bamboi catchment
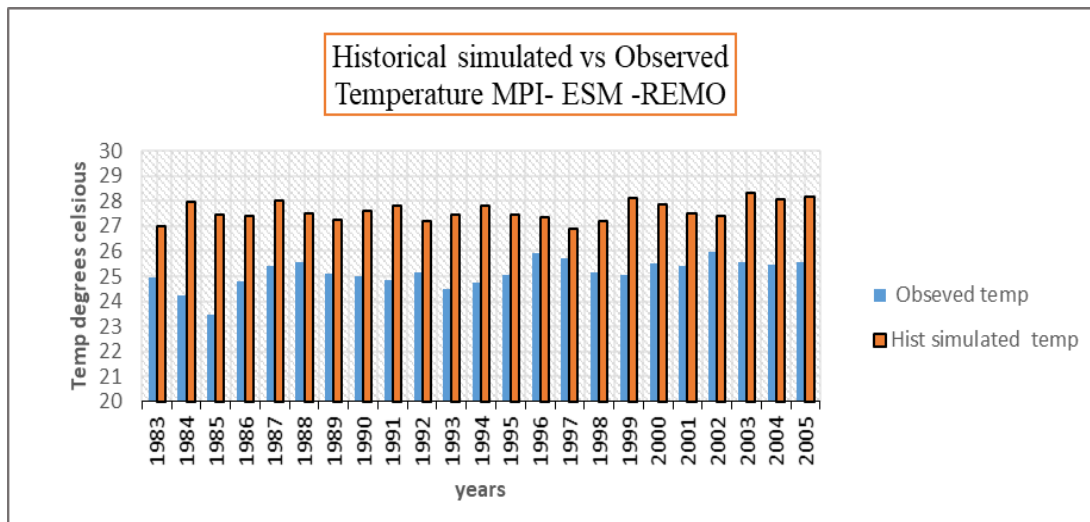
Figure 5.4 : Historical simulated and Observed temperature

5.6.2. Observed wind speed vs corrected and uncorrected wind speed

Observed wind speed vs corrected and uncorrected wind speed

(Legend: Obs Windspeed, Sim Wind uncorrected, Sim wind bias corrected)
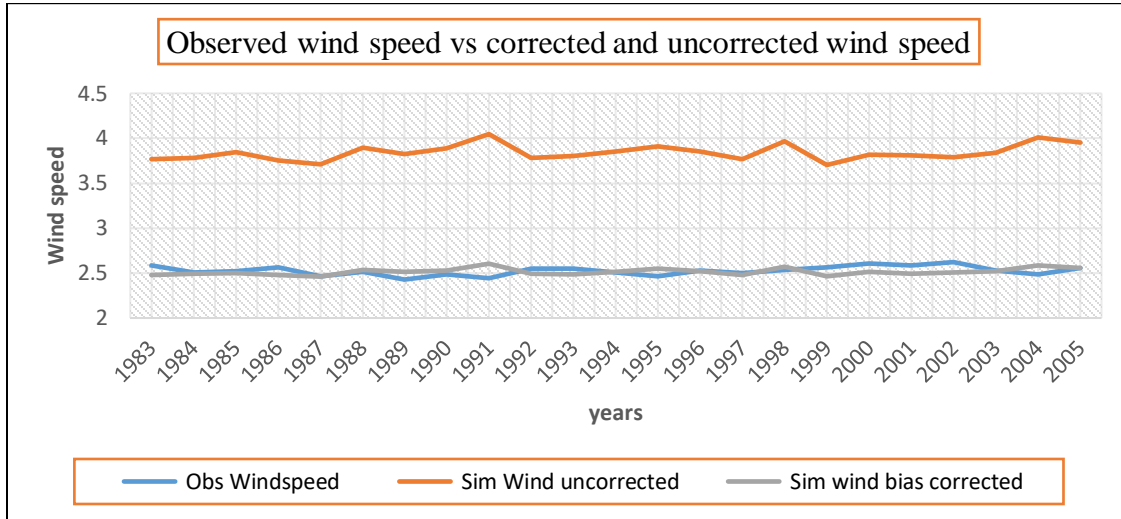
Figure 5.5 : Historical Simulated and Observed data

5.7. DATA PROCESSING

Climate data sets used in this research are observed daily temperature, wind speed, humidity, precipitation and solar radiation for two GCM RCM models. Data was grouped into three groups historical data 1983- 2005 and two future period near future (2020- 2049) and far future (2070-2099). Bias correction was applied to the historical and future projected data sets to reduce the RCM outputs errors. Eto and ptq files created from the historical and future reference were used as input data in the HBV light model. CORDEX humidity data was available as specific humidity and it was converted to relative humidity by applying Equation 5.1.

Equation .5.1

$$RH = 100\frac{w}{w_s} \approx 0.263pq\left[\exp\left(\frac{17.67(T - T_0)}{T - 29.65}\right)\right]^{-1}.$$

P = pressure in Pascal

q = specific humidity or the mass mixing ratio of water vapor to total air (dimensionless)

T = temperature (K)

T0= reference temperature (typically 273.16 K) (K

5.8. BIAS CORRECTION

There is an important difference between historical observed data and the simulated data (1983 -2005). The bias correction method corrects the projected raw data using the differences between the mean and variability between observed and simulated climate results in order to get correct and reliable data (Jie Chen et al , 2013). Bias correction methods are capable of reducing errors in RCM output (Maraun, 2016). A statistical bias correction (empirical quantile mapping) was applied to the two GCMs– RCMs datasets. Temperature, humidity, precipitation and wind speed were all bias corrected. For each data set, transfer functions (TFs) were derived over the period of 1983 to 2005. Quantile mapping establishes transfer function between observations and simulations at same spatial scale in the bias correction process. Afterwards the transfer functions were applied to the projected climate scenarios (period 2020 to 2049) and (2070 - 2099). The calibration period starts 1/1/1983 and ends 31/12/2005. R script for bias correction was created and it was run in R studio for the bias correction. R Studio is an integrated development environment for R that allows a user to run R in a more user-friendly environment providing a console, a scripting window, a graphics window, an R workspace and other.
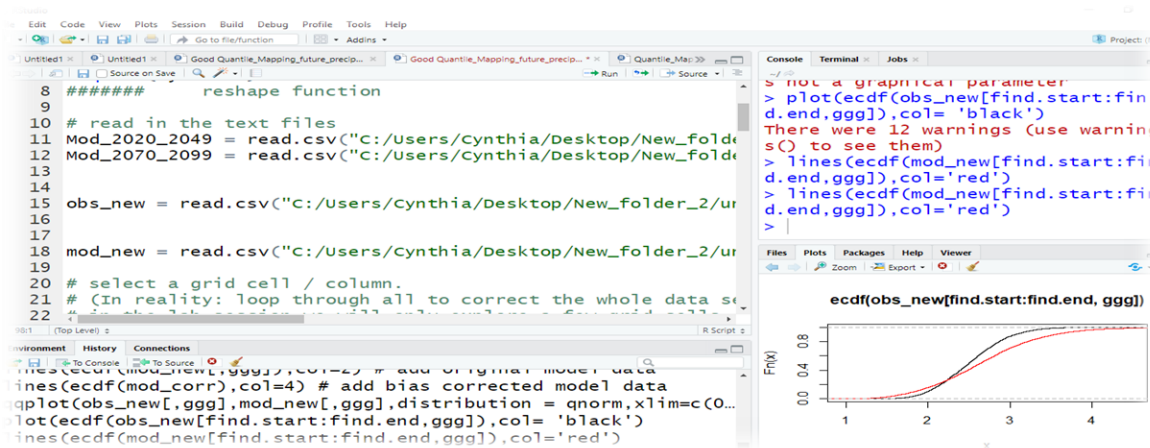
Figure 5.6 : R windows page

5.9. HYDROLOGICAL MODELLING

GCMs - RCM based (historical runs and projections) were used as climate input for the HBV light model. The best parameters sets obtained during calibration and validation phases in the previous chapter were used as the model set parameters for climate impact assessment. The HBV light

model was run with both bias corrected and non-bias corrected climate inputs for the ensemble. The expected climate change for an GCM- RCM is the difference between the simulated hydrological model under the reference period (1983- 2005) and the two future periods (2020-2049 and 2070-2100). The input files are ptq file and evap file. Each data set consists of historical runs and projections based on emission scenarios RCP 4.5.

RESULTS 1

5.10. CLIMATE DATA EVALUATION AND CORRECTION

The comparison between WASCAL (GFDLESM2M-WRF) and CORDEX (MPI –ESM REMO) historical datasets and observations for climate data such as temperature, wind humidity and precipitation is done for the reference period of 1983–2005 for average monthly values. Observed data is plotted against the bias (corrected and uncorrected) for a cross comparison between RCMs–GCMs in order to assess the relative ability of each climate product to represent historical climate conditions in the catchment. Results of observed and bias corrected and uncorrected data was explored in the first section of the results.

1. Temperature

(a). Evaluation of temperature for GFDESM2M

Figure 5.7 shows a trend towards an overestimation of annual temperature for the GFDLESM2M-WRF WASCAL climate product throughout the reference period 1983- 2005. Figure (a) and (b) shows temperature data before and after bias correction respectively. Figure (c) Shows the temperature data before and after correction with respect to observed data.

(a.) Before correction   (b.)   After correction

(C.) Observed vs Simulated Temperature
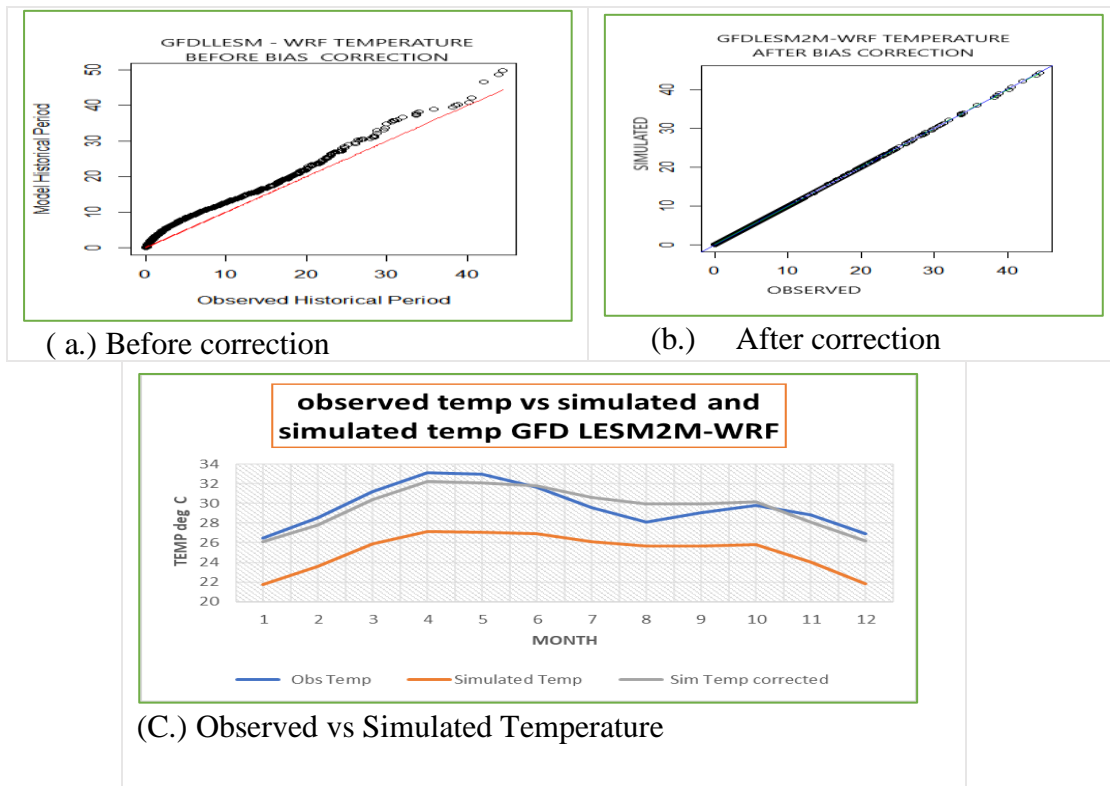
Figure 5.7 : Observed temperature data before and after correction for GFDLESM 2MWASCAL dataset.

An overestimation of temperature simulated by GFD LESM2M climate product is noticeable in fig C. The historical simulated temperature is higher than the observed temperature. A statistical bias correction (empirical quantile mapping) was applied to the data and data was transformed from *a* to *b* as shown by fig 5.7 .

Figure 5.7ig 5.7 (a) shows that the data had errors after bias correction, the line became a perfect line y =x meaning that historical observed data matches with the historical simulated. After bias correction the simulated corrected temperature curve (grey line) overlapped the historical observed graph (blue line).

(b). Evaluation of temperature for MPI –ESM REMO

MPI –ESM REMO CORDEX climate product

(a). Before correction
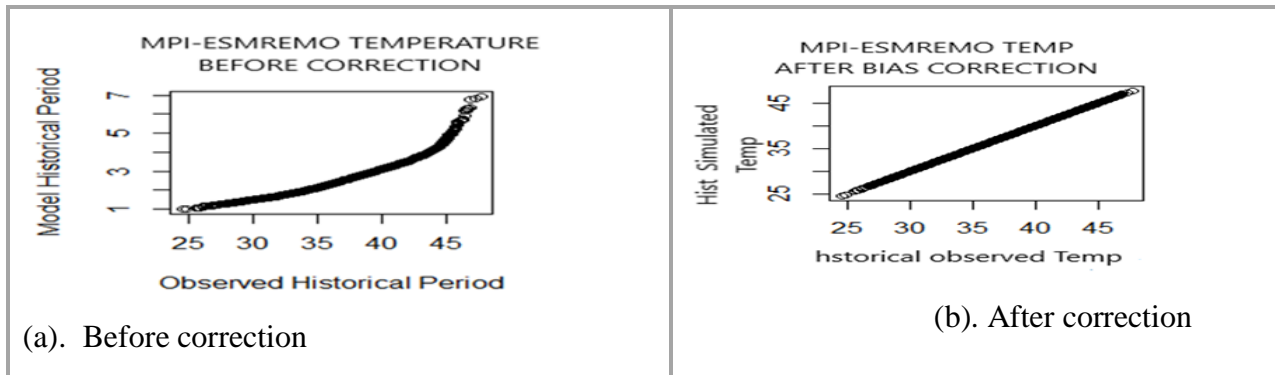
(b). After correction

(c.)
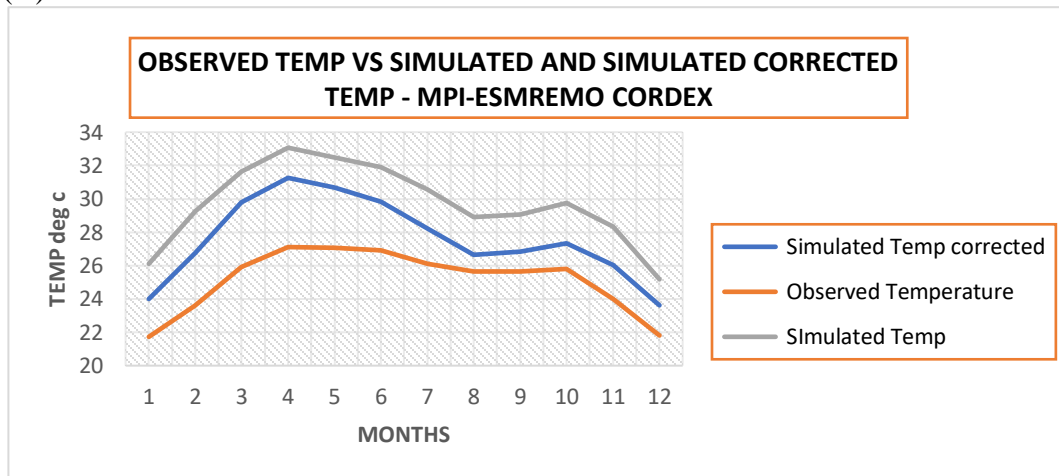
Figure 5.8 : Temperature data before and after bias correction for CORDEX climate dataset

An over estimation of temperature is also modeled by MPI- ESM REMO climate dataset. (Figure 5.8). The simulated temperature MPI –ESM REMO (CORDEX) product is higher than the historical observed for the reference period 1983 - 2005. As for the GFDESM2M dataset, after bias correction the observed data and simulated corrected data have matched.

2. Precipitation

(a). Evaluation of precipitation simulated by MPI –ESM REMO

Figure 5.9 (a) and (b) shows the cumulative distribution function of bias corrected and uncorrected corrected precipitation data for the MPI –ESM REMO model over 1983–2005. Figure 5.9 (c) shows observed precipitation vs simulated and simulated corrected precipitation.

(a.) Before correction   (b.) After correction
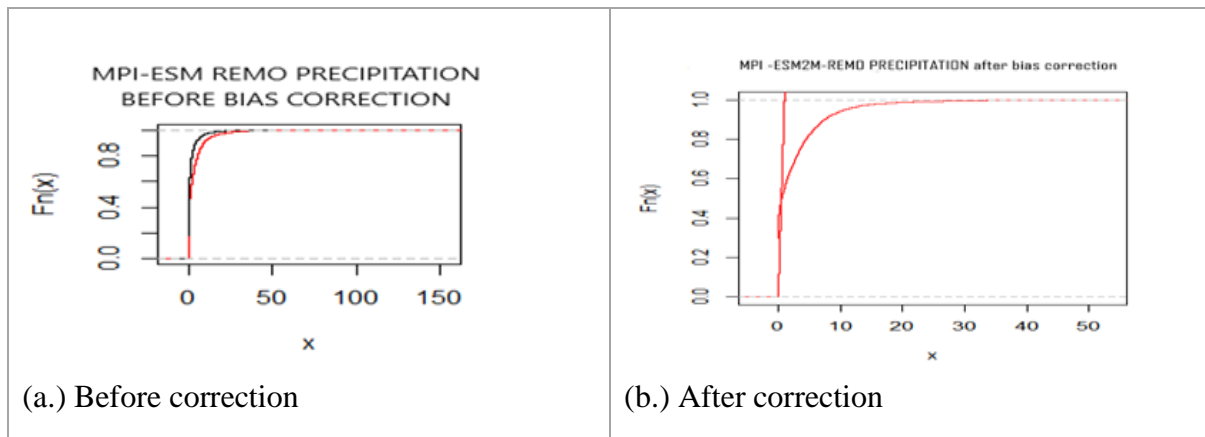
(c.)
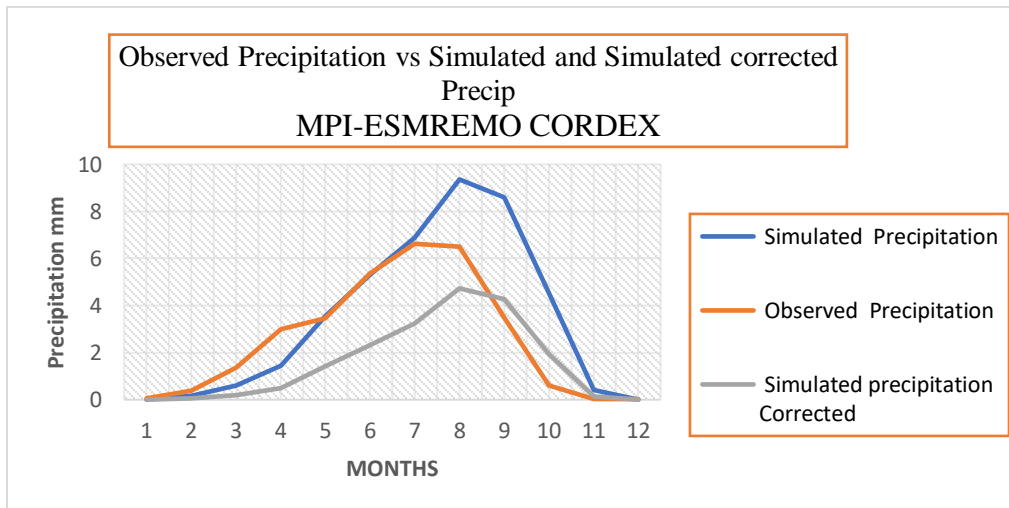
Figure 5.9 : Precipitation data before and after bias correction for CORDEX climate dataset

A systematic positive bias and large deviation from observed precipitation is exhibited by the MPI –ESM REMO model. This motivated the bias correction of precipitation. After correction, the positive bias was significantly reduced and an improvement is clearly visible. The quantile mapping bias correction method approach was well-able to bring the historical simulations close to the observed while maintaining the change signal between the present and the future.

(b). Evaluation of precipitation by GFDLESM2M-WRF

a.) Before correction
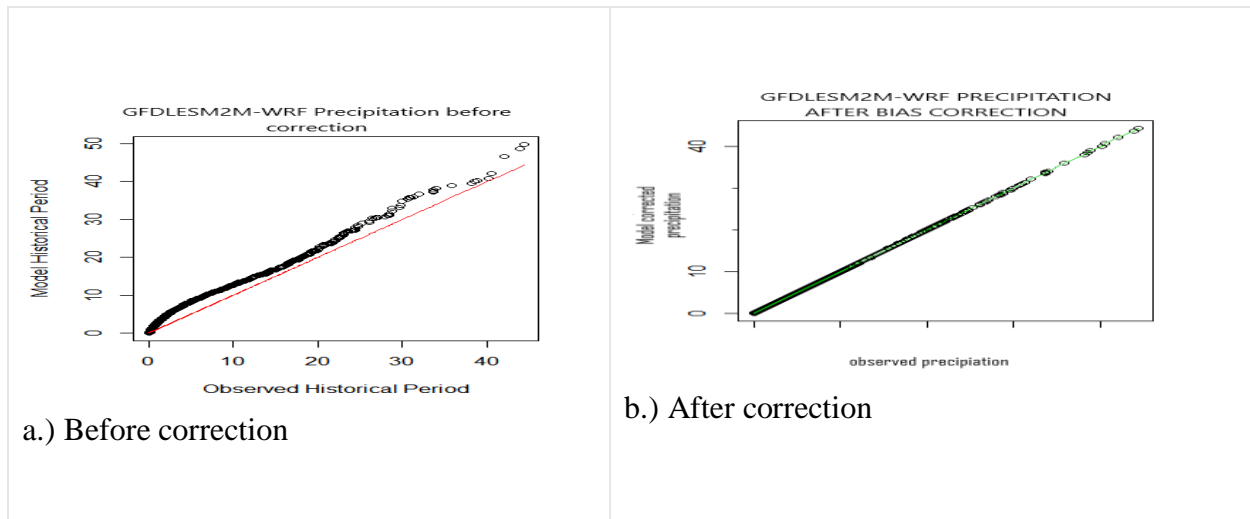
b.) After correction

(c.)
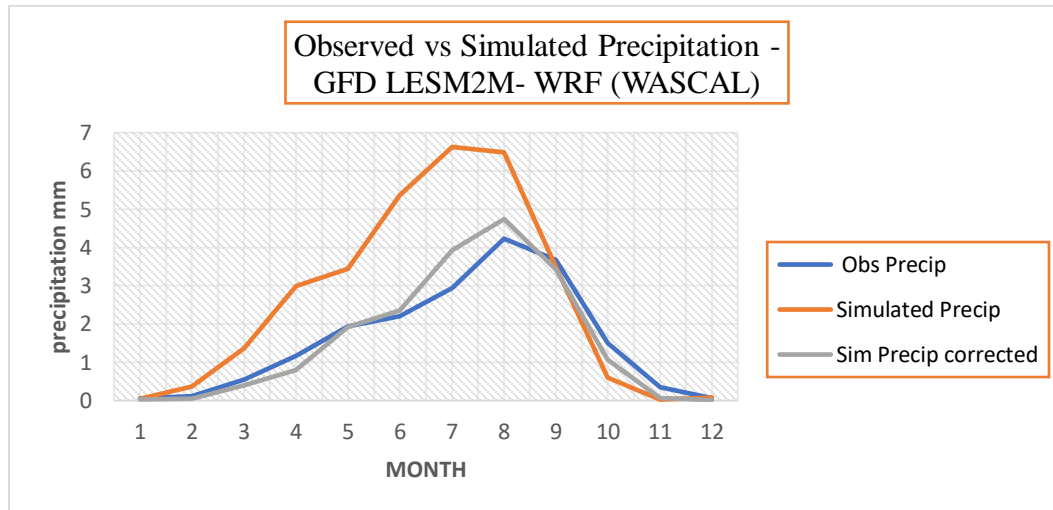
Figure 5.10 : Precipitation bias (corrected and not corrected) for GFDLESM2M-WRF compared to the observed data for the period of 1983–2005. Figure 5.10 (a) and (b) shows precipitation data before bias and after bias correction .

Figure 5.10 (c) shows observed precipitation vs un corrected simulated and simulated corrected precipitation for WASCAL climate dataset. Figure 5.10 shows that GFDLESM2M-WRF overestimates precipitation in relation to the observation precipitation. Simulations overestimate precipitation especially from April to August. After bias correction using quantile mapping the simulated precipitation curve overlaps the observed precipitation.

3. Humidity

(a). Evaluation of humidity simulated by GFD- LESM 2M-WRF

Figure 5.11 shows Humidity bias (corrected and not corrected) for the GFD- LESM 2M-WRF compared to the observed data for the period of 1983–2005. Figure 5.11 (a) and (b) show the cumulative distribution of humidity before and after bias correction of humidity data respectively and (c) shows humidity vs uncorrected simulated and simulated corrected humidity.

a) Uncorrected

b.) Uncorrected
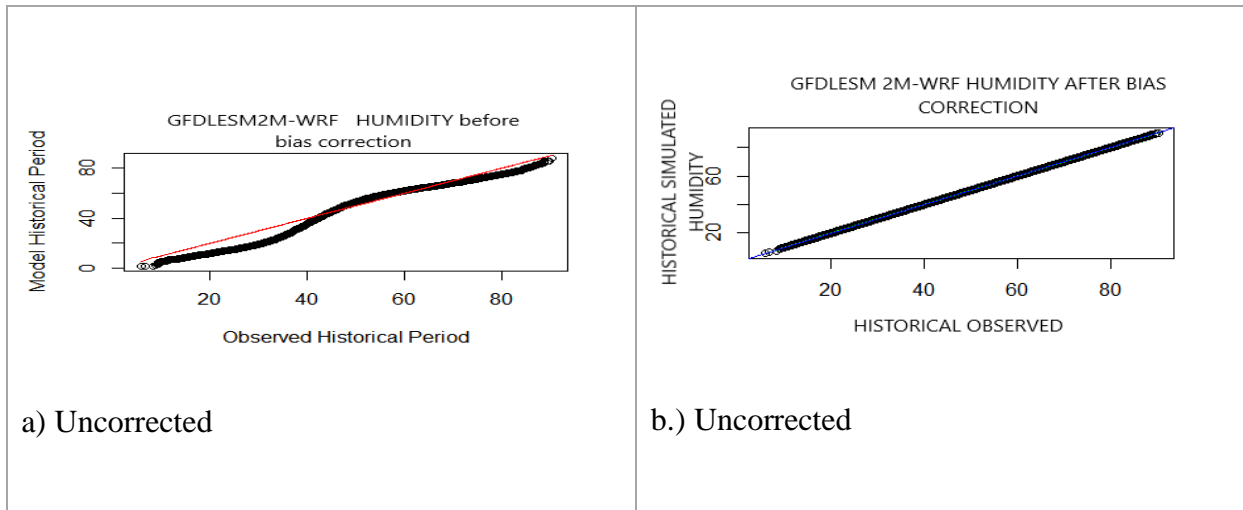
(c)
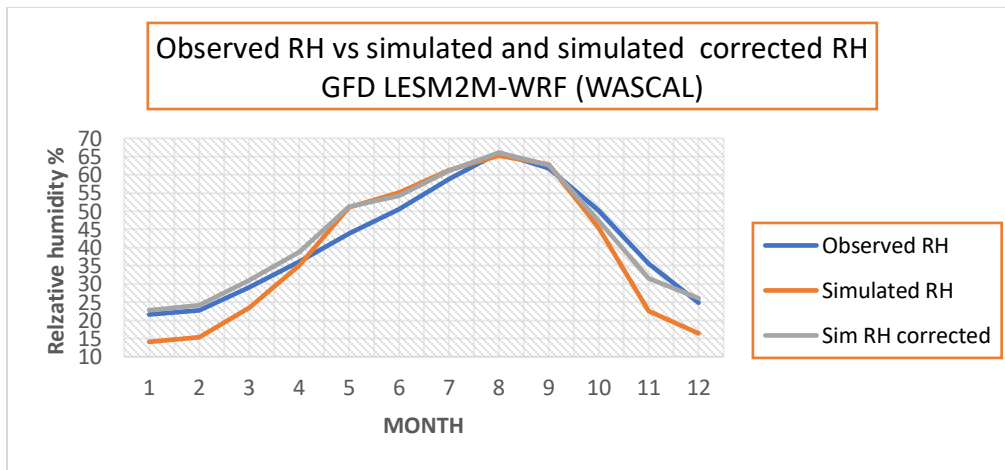
Figure 5.11: Relative humidity data before and after bias correction for WASCAL climate product

For the GFD LESM2M WASCAL climate product the simulated humidity reproduces the observed humidity although it underestimates the humidity for the first five months of the year After bias correction the corrected simulated humidity overlaps the observed humidity showing that negative biases have been removed.

(b). Evaluation of Humidity simulated by MPI –ESM REMO
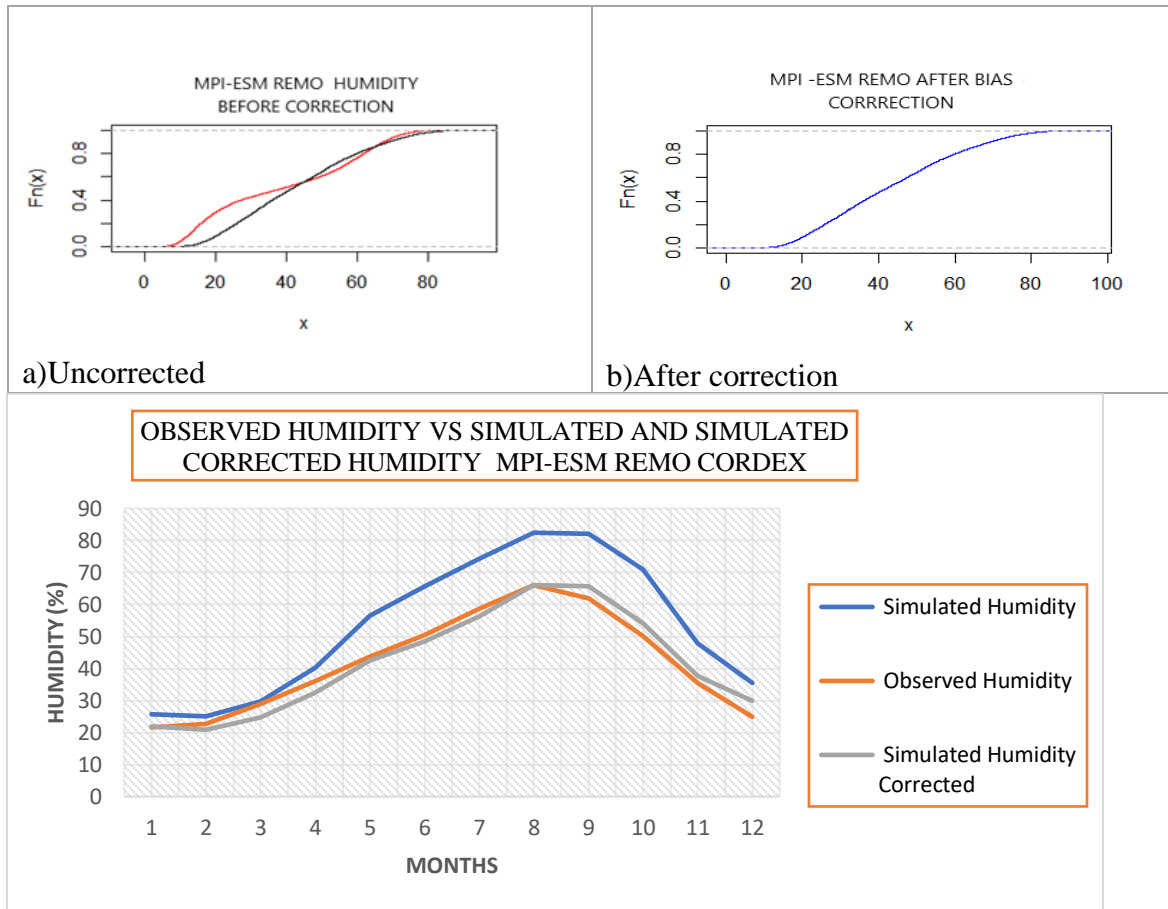
Figure 5.12 : Relative humidity data before and after bias correction for CORDEX climate product.

Uncorrected data was corrected using quantile mapping method. In Figure 5.11 and Figure 5.12 both graphs have the same pattern. The simulated humidity by GFDLESM2M –WRF WASCAL and MPI –ESM REMO- CORDEX are systematically higher than the historical observed for the same time period. After correction, positive biases were removed as shown in graph (b) of Figure 5.11 and Figure 5.12. The simulated corrected curve overlaps the historical observed for both figures showing that the biases have been removed.

4. Wind speed

(a) Evaluation of Wind speed simulated by GFD LESM2M-WRF

Figure 5.13 and Figure 5.14 below shows corrected and un corrected wind data for GFD LESM2M-WRF and MPI –ESM REMO- CORDEX, respectively over the period of 1983–2005.

a.) Uncorrected

b.)Bias corrected
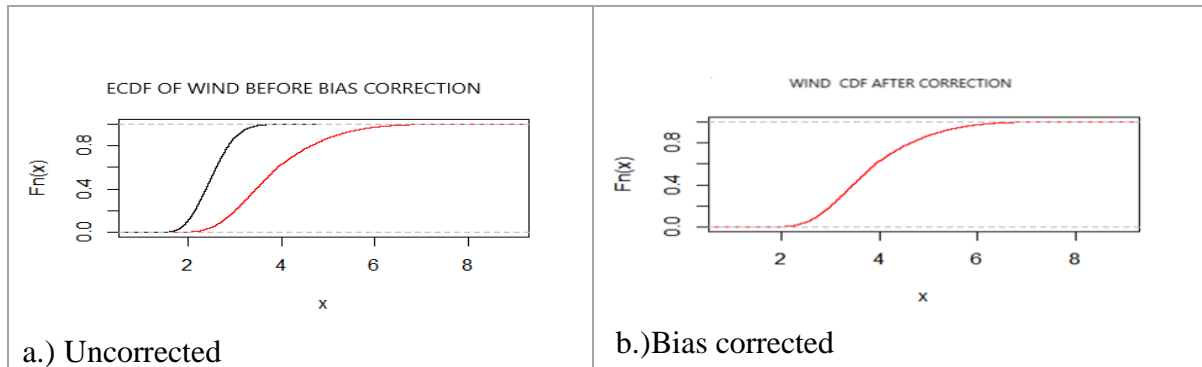
(C.)
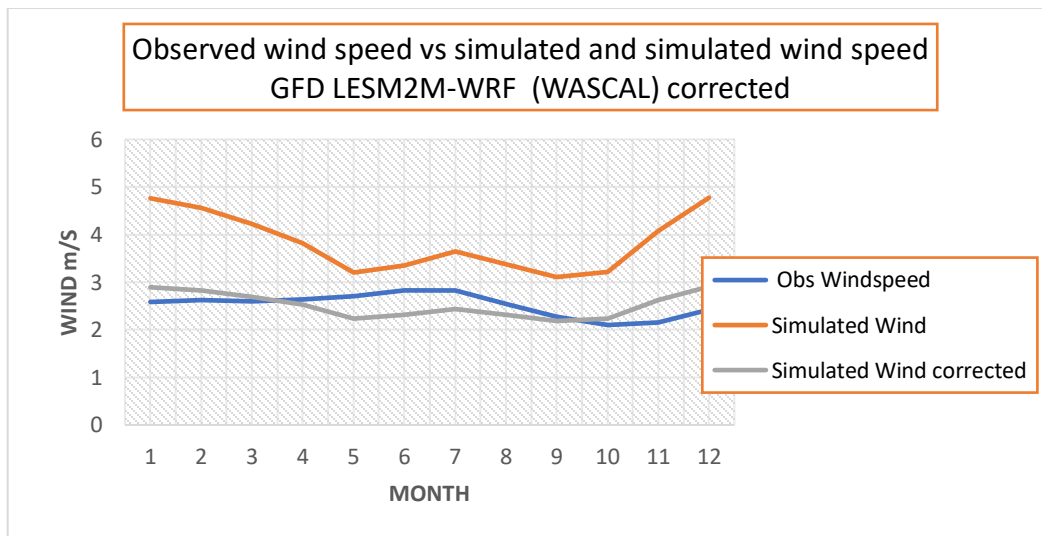
Figure 5.13: Observed wind speed vs Simulated wind speed for WASCAL climate dataset

OBSERVED WIND VS SIMULATED AND SIMULATED CORRECTED WIND MPI- ESMREMO
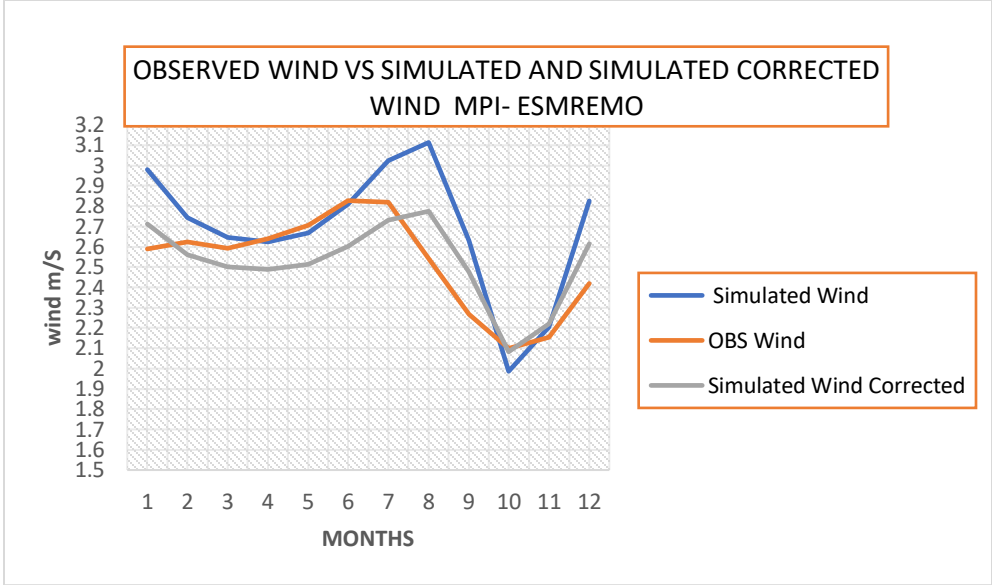
Figure 5.14 : Observed wind speed vs Simulated wind speed for CORDEX climate dataset.

The simulations by GFD LESM2M-WRF and MPI ESM REMO overestimate the observed wind speed. After bias correction, the simulated wind speed overlaps the observation. This implies that the biases present in the data in both models (see Figure 5.13 and Figure 5.14) were removed.

RESULTS 2

5.11. PROJECTED CHANGES.

5.11.1. Precipitation

Projected change in precipitation for MPI ESM REMO and GFD LESM2M-WRF for both bias corrected and uncorrected data for the period of 2020-2099 compared to the reference period (1983-2005) is presented in figure 5.15. From the graphs Figure 5.15 both climate products are agreeing that precipitation will increase in the mid-century 2020 -2049 before slightly decreasing in the late century 2070 -2099.
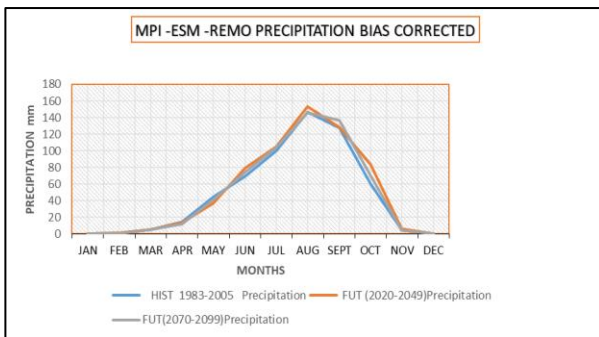
a .CORDEX bias corrected
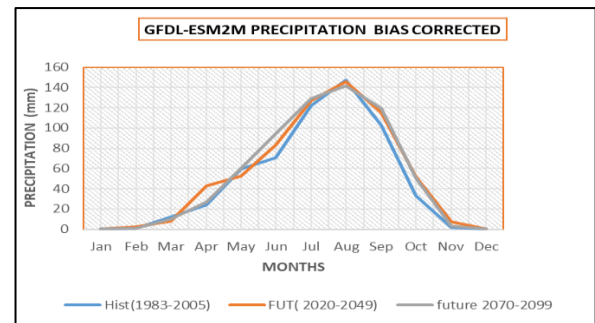
b. WASCAL bias corrected
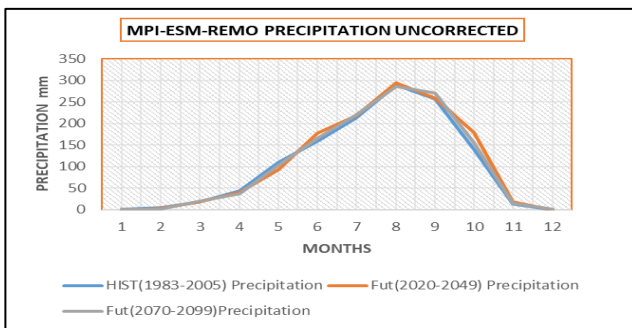
C. CORDEX non-bias corrected
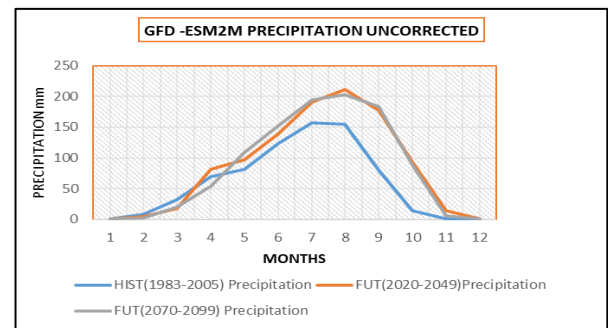
d. WASCAL non-bias corrected

Figure 5.15 : Climate change signal of precipitation between the reference period (1983 -2005) and two future periods (2020-2049) and (2070 -2099) of GFDLESM 2M WASCAL and MPI-ESM-REMO CORDEX (corrected and uncorrected data)

The monthly precipitation observed in the baseline period and projected under RCPs 4.5 for GFD LESM2M –WRF (WASCAL) and MPI –ESM REMO (CORDEX) corrected and uncorrected data showed an overall increase in average monthly precipitation in the wet season when compared to the values obtained in the dry season. Wet seasons will become wetter and dry seasons will become dryer.

Table 5.3: Projected precipitation change between the reference (1983–2005) and future periods (2020– 2049) and (2070 -2099) periods with bias corrected and non-bias corrected RCM–GCM based simulations.

Climate model	Reference (1983 -2005) Precipitation mm	Projected (2020-2049) Precipitation %	Projected (2070-2099) Precipitation %
Bias corrected			
GFD LESM2M –WRF WASCAL	574.4826087	+11	+10.9
MPI–ESM REMO CORDEX	575.4826	+6.6	+3.7
Mean of model ensemble	574.9826	8.8	+7.3
Non-Bias corrected			
GFD LESM2M –WRF	722.72	+42.3	+40.14
MPI–ESM REMO	1249.609	+3.7	+1.6
Mean of model ensemble	986.1645	+23	+20.87

For annual average precipitation change both climate products are predicting an increase in precipitation for the 2020 – 2049 period by 8 .8 % for corrected data, 23% for uncorrected data mean ensemble. A slight increase of precipitation in the end of century period (2070 – 2099) is projected by both products 7.3% for corrected data and 20.87% for uncorrected data as compared to the reference period (1983-2005) (Table 5.3). The annual mean precipitation for the baseline period is 574.4826 mm and the projected one is 612mm for the mid-century and 595.37mm for the end century for MPI –ESM REMO (CORDEX). For GFD LESM2M –WRF (WASCAL) the historic is 574.4826 while mid-century is 638.6 mm and for the end of century it is 637.24 mm.

Furthermore, both climate products showed that when precipitation data was not bias corrected the projected precipitation for the mid-century and late century by both climate products were too high. However, after bias correction, the agreement between RCM–GCM based precipitation and observation is considerably improved (Table 5.3). The overestimation of rainfall before correction is greatly reduced after bias correction.

5.11.2. Discharge

Projected change in Discharge for MPI ESM REMO and GFD LESM2M-WRF for both bias corrected and uncorrected data for the period of 2020-2099 compared to the reference period (1983-2005) is presented in figure 5.16.
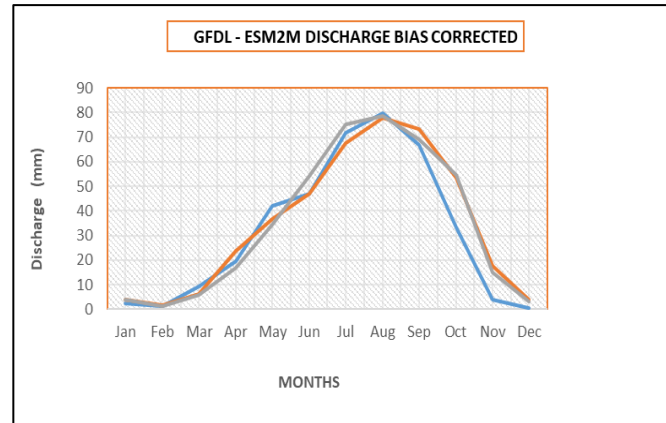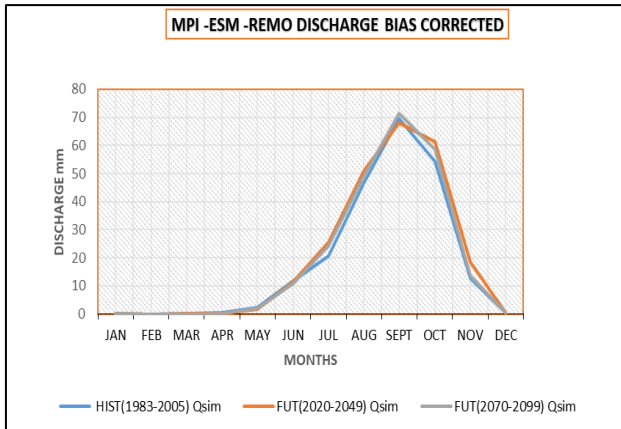
a. CORDEX bias corrected

b. WASCAL bias corrected
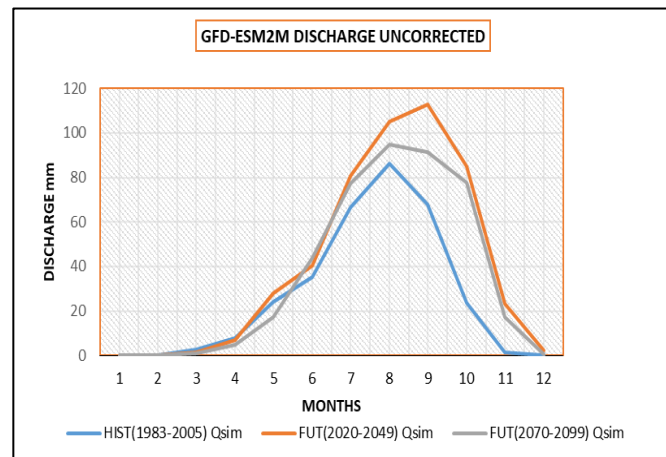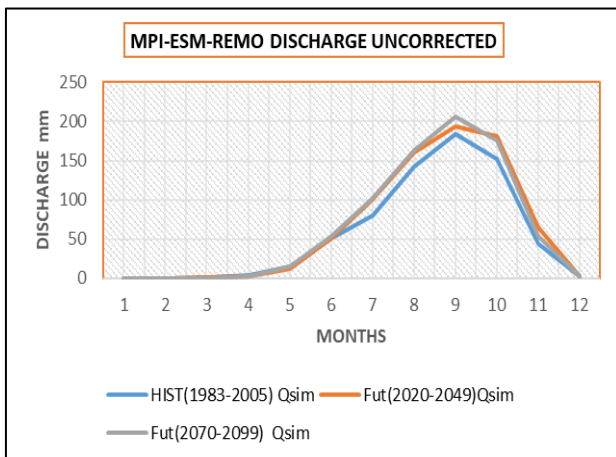
C. CORDEX non-bias corrected

d. WASCAL non-bias corrected

Figure 5.16 : Simulated discharges over the reference period (1983 -2005) and two future periods (2020-2049) and (2070 -2099) for GFD LESM 2M WASCAL and MPI ESM REMO CORDEX models (corrected and uncorrected data).

Discharge simulated with GFD LESM2M –WRF (WASCAL) and MPI –ESM REMO (CORDEX) (RCPs 4.5) historical runs (bias corrected and non-bias corrected) was compared to the reference discharge. This comparison showed that an increase in the annual discharge change is projected by both climate models. With bias corrected climate data, the following is projected (i) For the mid-century (2020-2049) GFD LESM2M –WRF (WASCAL) product predicts a 14.4 % increase in annual discharge, which is a consequence of relative increase in precipitation of around 11 %. However, for the end of century there is a slight decrease in discharge, as compared to mid-century (2020-2049). For the (2070-2099) period the predicted discharge decreased to 14.2 % as a result of precipitation decrease by 10.9%. For MPI –ESM REMO (CORDEX) climate dataset, in the mid-century there is a projected increase of discharge by 8.4 % which is a consequence of relative increase in precipitation of around 6.6 %. As predicted by the WASCAL dataset, the CORDEX dataset indicates the same behavior for the late century period (2070-2099), i.e. a slight decrease in discharge and precipitation, compared to mid-century (2020-2049). For the (2070-2099) period the predicted discharge decreased by 5.27 %, and precipitation by 3.65% (Table 5.4). All this brings to the conclusion that the simulated annual mean discharges (increased) in the same way that the projected precipitation did with both MPI –ESM REMO (CORDEX) and

GFD LESM2M –WRF (WASCAL) model. The discharge changes with non-bias corrected climate data are similar in trend (with however differences in magnitude) compared to the changes observed with bias corrected data, which is consistent with changes in the climate signal induced by the bias correction.

Table 5.4: Projected discharge change between the reference (1983–2005) and future periods (2020– 2049) and (2070 -2099) periods with bias corrected and non-bias corrected RCM–GCM based simulations.

Climate model	Reference (1983 -2005) discharge mm	Projected (2020-2049) discharge %	Projected (2070-2099) discharge %
Bias corrected			
GFD LESM2M –WRF	200.890087	+14.4	+14.2
MPI–ESM REMO	218.9933	+8.4	+5.27
Mean of the ensemble	209.94	+11.4	9.735
Non bias corrected			
GFD LESM2M –WRF	314.8618	+54.2	+35
MPI–ESM REMO	673.4019	+14.3	+15
Mean of the ensemble	494.13185	+34.25	+25

5.11.3. Temperature

Fig below shows temperature change for MPI ESM REMO and GFD LESM 2M-WRF for both bias corrected and uncorrected data.
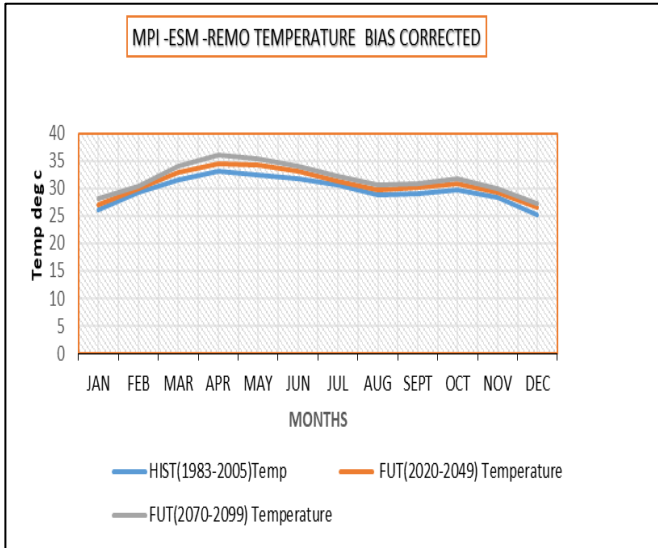
a. CORDEX bias corrected
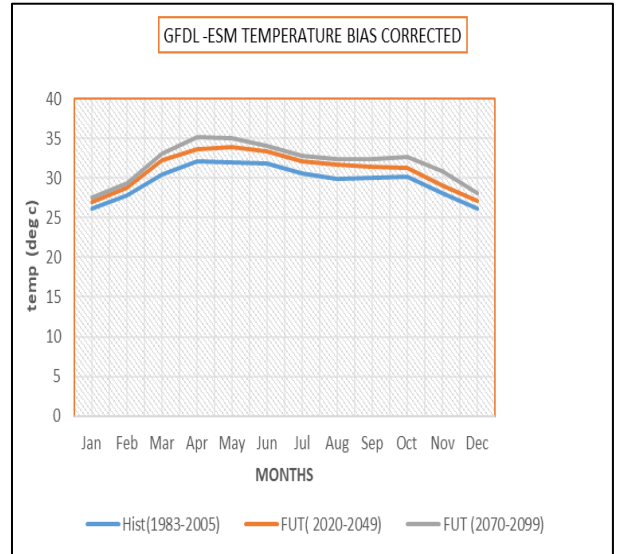
b. WASCAL bias corrected
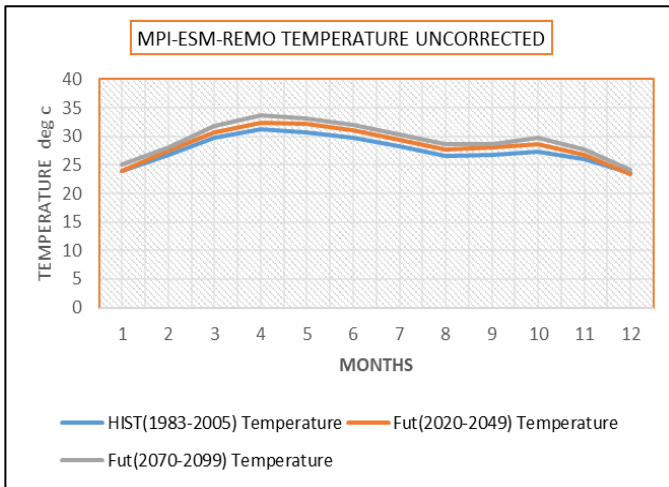
c. CORDEX non-bias corrected
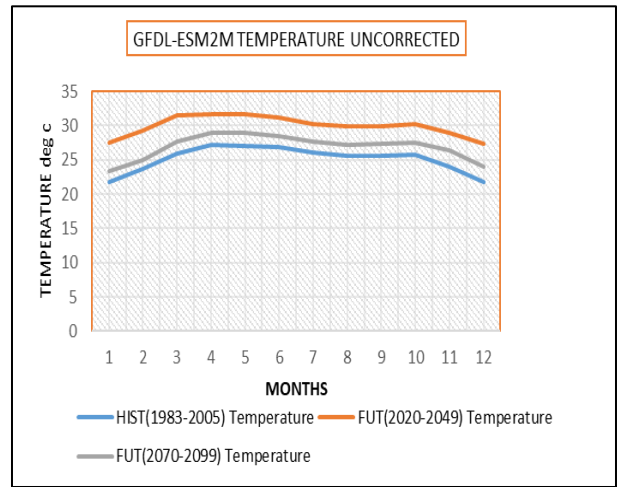
d. WASCAL non-bias corrected

Figure 5.17 :RCM–GCM based temperature simulations: (a) and (b) RCM temperature is bias corrected and (c) and (d) RCM temperature non-bias corrected.

Figure 5.17 presents the monthly average temperatures of the Bamboi catchment obtained from projected climate data according to GFD LESM2M –WRF (WASCAL) and MPI – ESM REMO (CORDEX) under RCPs 4.5. Both the corrected and uncorrected simulations predict a continuous increase in projected temperatures up to 2099 by 0.8 $^{\circ}$C to 2.8ºC when compared to the value observed during the baseline period (1983-2005), Thus, by horizon 2099, the average temperature in the catchment will be 35.17 ◦ C and 36. ◦ C in the hottest month of (April) and 32.8◦C and 32.3 ◦C in the coolest month (July) as predicted by GFD LESM2M –WRF (WASCAL) and MPI –ESM REMO (CORDEX), respectively. The temperature simulations are obviously improved after the bias correction as shown by the cumulative distribution function curves. These results are in line with the analysis of Mbaye et al. (2015), Yira et al. (2017), Coulibaly et al. (2018) Sylla et al. (2016) and IPCC (2016) report concerning the projected temperatures in West Africa .

5.11.4. AET (Actual Evapo-transpiration)

Figure below shows a plot of the AET curves for MPI ESM REMO and GFD LESM2M-WRF for both bias corrected and uncorrected data.
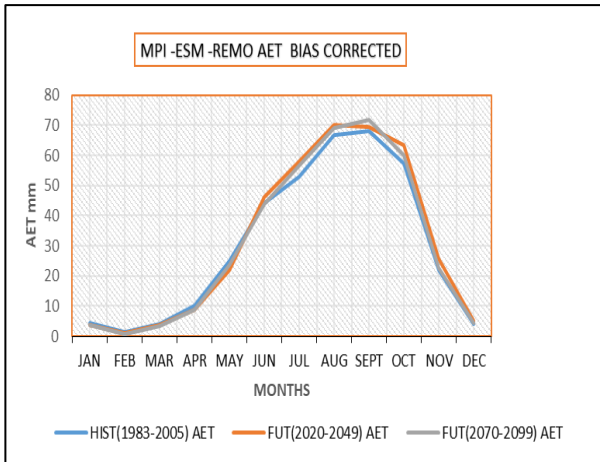
a.   CORDEX bias corrected
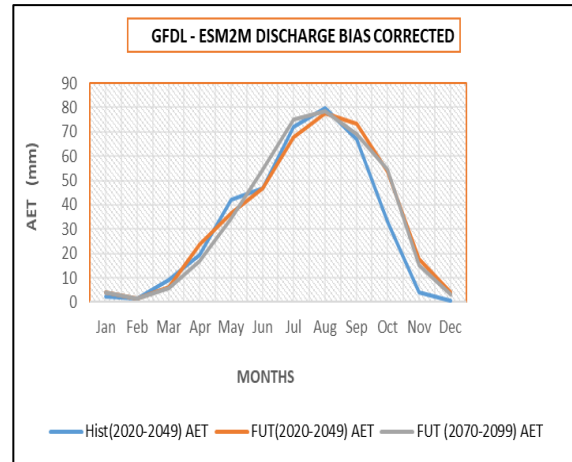
b .WASCAL bias corrected
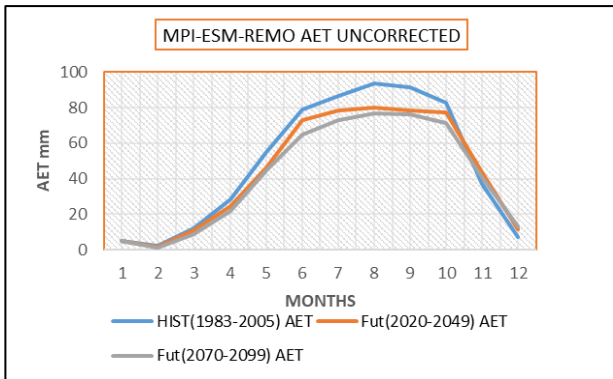
c .CORDEX non bias corrected
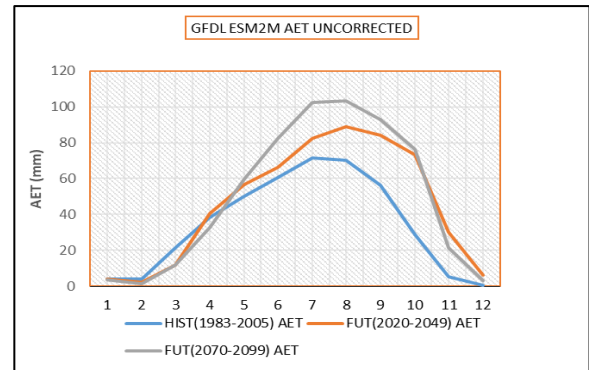
d .WASCAL non bias corrected

Figure 5.18: AET change between the reference period (1983 -2005) and two future periods (2020-2049) and (2070 -2099) of GFD LESM 2M WASCAL and MPI ESM REMO CORDEX (corrected and uncorrected data).

Actual evapotranspiration (AET) strongly depends on precipitation and temperature. The changes in AET are plotted in fig 5.18. Figure 5.18 shows that by the end of century (2070 – 2099), an increase of AET is likely to occur in the entire basin from 9.4% to 9.2 % for GFD LESM2M – WRF (WASCAL) and 2.3 % to 4.8% for MPI –ESM REMO (CORDEX) for bias corrected data as compared to the reference period . For both datasets using uncorrected and corrected values present the same signal of increase in general even though there are differences in magnitude. The magnitudes of change are more pronounced in the uncorrected simulations than in the bias corrected data.

5.11.5. PET -Potential evapotranspiration

Projected PET changes between the reference (1983–2005) and future periods (2020– 2049) and (2070 -2099) periods with bias corrected and non-bias corrected RCM–GCM based simulations are shown in Figure 5.19.
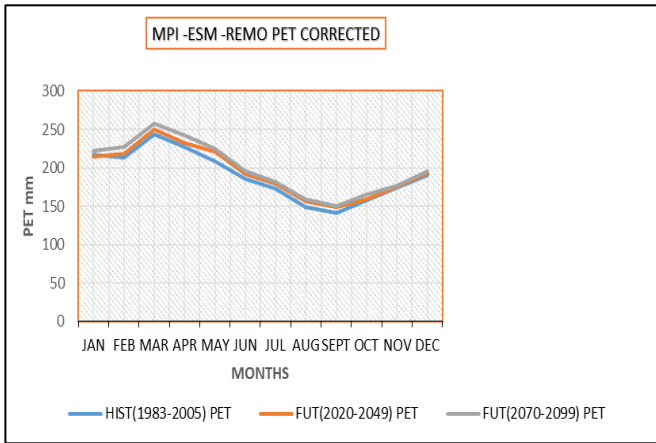
a. CORDEX bias corrected
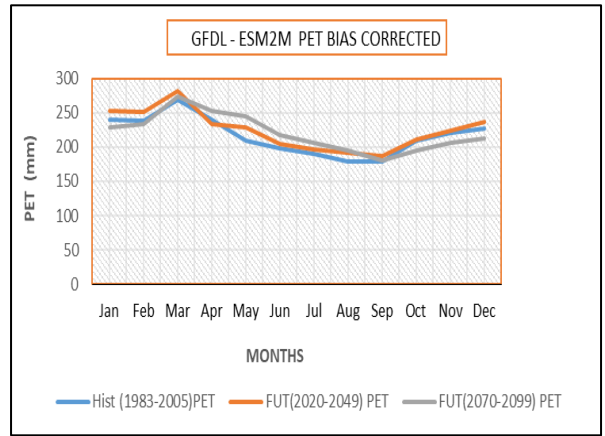
b. WASCAL bias corrected
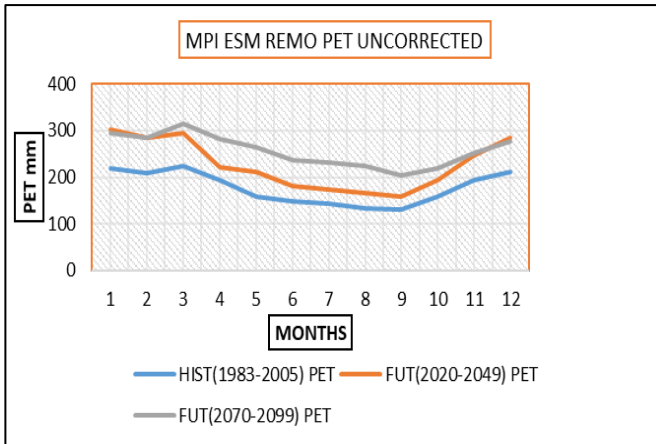
c. CORDEX non bias corrected
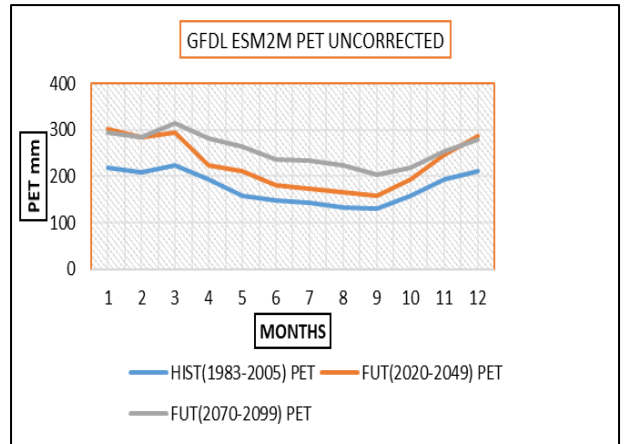
d .WASCAL non-bias corrected

Figure 5.19: PET change between the reference period (1983 -2005) and two future periods (2020-2049) and (2070 -2099) of GFD LESM 2M WASCAL and MPI ESM REMO CORDEX (corrected and uncorrected data)

The changes in PET show that by the end of century an increase of potential evapotranspiration is likely to occur in the entire basin from 1.9% to 4.03 % for GFD LESM2M –WRF (WASCAL) dataset and 2.3%   to 5.066 for MPI –ESM REMO (CORDEX) dataset for bias corrected data. Both models with uncorrected and corrected data present the same signal of increase even though there are differences in magnitude. The magnitude of changes is more pronounced in the uncorrected simulations than in the bias corrected data. As shown by the differences in the magnitude of PET change for the corrected data and uncorrected data the PET change is reduced by bias correction. The reason for the increase in PET is due to the increase in temperature in the coming years.

5.12.   SUMMARY OF CLIMATE CHANGE SIGNAL

Table 5.5: Mean annual water components per RCM-GCM for the historical (1985-2005) and

	1			2		
	MPI-ESM-REMO - CORDEX			GFDL ESM2M- WRF of WASCAL		
Climate model	Historical (1983 -2005)	Projected (2020-2049)	Projected (2070-2099)	Historical (1983 -2005)	Projected (2020-2049)	Projected (2070-2099)
Bias corrected						
Precipitation	575.483	612.137	595.37	574.483	638.6	637.24
Discharge	218.993	238.527	230.545	200.89	229.795	229.51
PET	2282.01	2338.84	2397.63	2599.9	2704.93	2649.12
AET	360.378	377.602	368.817	377.583	413.075	412.267
Non-Bias corrected						
Precipitation	1249	1295.81	1269.11	722.72	1028.69	1012.8
Discharge	673.402	769.659	775.564	314.862	485.785	424.974
PET	2282.01	1992.86	1844.21	2123.68	2716.95	3086.11
AET	581.13	529.93	497.284	411.465	546.323	591.509

5.13. CONCLUSION

The specific objective of this chapter is to assess the impact of future climate change on the hydrological regime of the catchment through scenario (RCP4.5) application comparing a reference period (1983-2005) to two future periods 2020-2049 and 2070-2099". The models mean projected a temperature increase of 0.8 and 2.8 °C by 2020-2049 and 2070-2099, respectively. Precipitation increase of 11% and 6.6 % for the 2020-2049 period and 10.9 % and 3.7 % for 2070 -2099 are projected by WASCAL and CORDEX climate dataset, respectively. Discharge is projected to increase by 11 .4 % for 2020 - 2049 period and to increase to 9.2% for the 2070-2099 period for climate models mean. This increase in discharge is likely to increase the hydropower generation in the two future periods compared to the reference period for both historical and projected discharges data obtained from this analysis will be converted to hydropower potential in Chapter six following a run-of-river hydroelectricity generation approach.

CHAPTER SIX: IMPACT OF CLIMATE CHANGE ON HYDROPOWER POTENTIAL

6.1. INTRODUCTION

This Chapter addresses the third objective of the study, i.e." to assess the impact of climate change on the hydropower potential of the investigated catchment". Following chapter 5, both historical and projected discharges corrected and uncorrected data obtained from CORDEX and WASCAL climate products scenarios will be converted to hydropower potential following a run-of-river hydroelectricity generation approach.

6.2. HYDROPOWER POTENTIAL

The current study assessed the impact of climate change on hydropower theoretical potential and briefly on the economic potential. Importantly, it should however be remembered that potentials of a hydropower resource are categorised into three types which are theoretical, technical and economic potentials. The exploitable hydropower being the part of the economic potential that can be harnessed considering the environment and other special restrictions.

❖ **Theoretical potential**: is the sum of the energy potential available at a place including losses etc.

❖ **Technical potential** is the part of theoretical potential which can be utilized with the current technology regardless of economic and other considerations.

❖ **Economic potential**: is the part of the technical potential which can be generated as economic.

6.3. EVALUATION OF THE HYDROPOWER POTENTIAL

In order to assess the impacts of climate change on hydropower potential of the Bamboi catchment a hydroelectricity production model ($P0 = \rho g Q H \eta$) was developed to simulate the energy production based on simulated discharge. The discharge (Q) for the three time periods, historical and two future periods was used as inputs to the hydroelectric production model. Power produced (hydropower potential) for historical periods 1983 -2005 and projected period 2020-2049 and 2070-2099 climate projections were compared to assess climate impact on the hydropower generation potential of the catchment. Besides discharge there are other two parameters that should be considered when evaluating hydropower potential which are effective head (H) and tail water

level. Determination of the head for a proposed hydropower plant should be done through surveying and is a surveying problem that identifies elevations of water surfaces as they are expected to exist during operation of the hydropower plant. Google earth maps and remote sensing maps provided information on the topography of the area. Conceptualization should be made of where water will be directed from a water source and where the water will be discharged from a power plant in order to design the plant.

The Bamboi gauge station does not have a hydropower plant so in order to evaluate the hydro power potential from the given discharge a conceptual mini hydro power plant was designed and all calculations were made based on the conceptual design of the plant. Details of the design of Bamboi mini hydro power plant is detailed in the following sections and energy generated after the design of the plant is well presented as well.

Methodology of hydropower evaluation
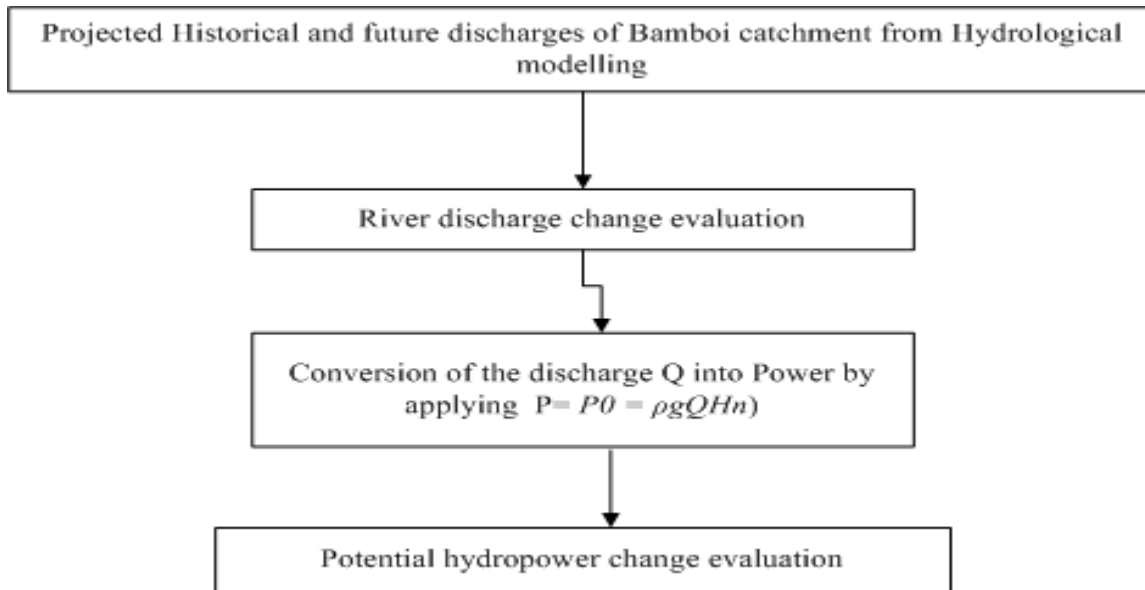
Figure 6.1 : Methodology of hydropower evaluation

6.4. HYDROPOWER PRODUCTION MODEL

The assessment of the hydropower potential of the Bamboi catchment is based on the conversion of discharges at the outlet to hydropower. The discharge data of Bamboi catchment was computed in mm per day in the HBV light model then it was converted to m^3/s using the following Equation 6.1.

Flowrate m3/s

$$Q(m^3/s) = Q(mm)\frac{CA}{24 \cdot 30 \cdot 3600 \cdot 1000},$$

Equation 6.1

CA OF Bamboi catchment = 134 200km^2 and Where CA is the catchment area.

Power-output (W)= P0 = ρgQHn)   Equation 6.2

Energy output W/h = Power output *Δt   Equation 6. 1

g= gravitational force, Q= flowrate / discharge H= effective head, P = Power output,

turbine = turbine efficiency and ρ = density of water (kgm₋₃) and Δt is time interval.

6.5. RUN OF RIVER SYSTEM

A "run-of-river" system (Okot, 2013) approach was used to evaluate the hydropower potential of Bamboi catchment. As the efficiency of the system depends among others on the type of hydropower turbines (technologies), a survey on technologies readily available in the region was carried out. Run of river system is considered an unfirm source of power because of lack of the capacity to store power, it uses water within the natural flow range to generate electricity and it requires no impoundment (Okot, 2013) . Run of river systems generate more energy during times when seasonal flows are higher and less in dry and frozen seasons. Large hydro power schemes have an efficiency of 90% and above where as small hydro power schemes their efficiency ranges from 60% to 80% (Okot, 2013).

Discharge

The discharge for Bamboi catchment was computed in Chapter 5 by HBV light model for three time periods. Historical (1983 – 2005), future mid-century (2020 – 2049) and late century (2070-2099) for two different models MPI-ESM-REMO of CORDEX-Africa project and GFDL ESM2M- WRF of   WASCAL.
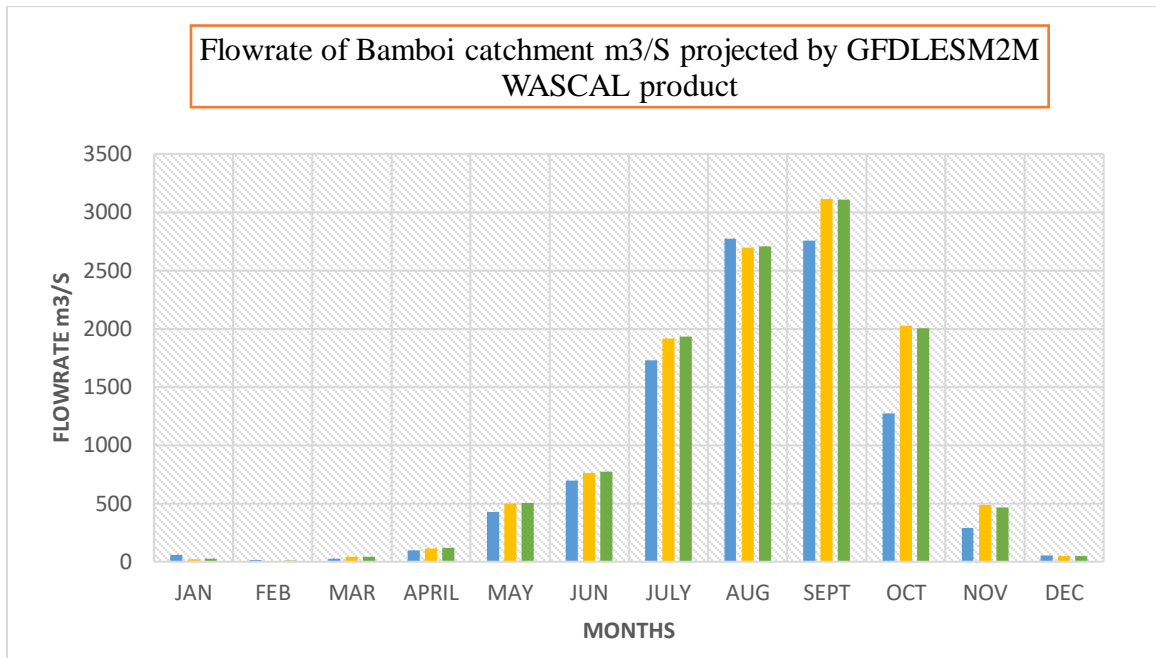
Figure 6.2 : The mean discharges for three time series projected by WASCAL climate product.
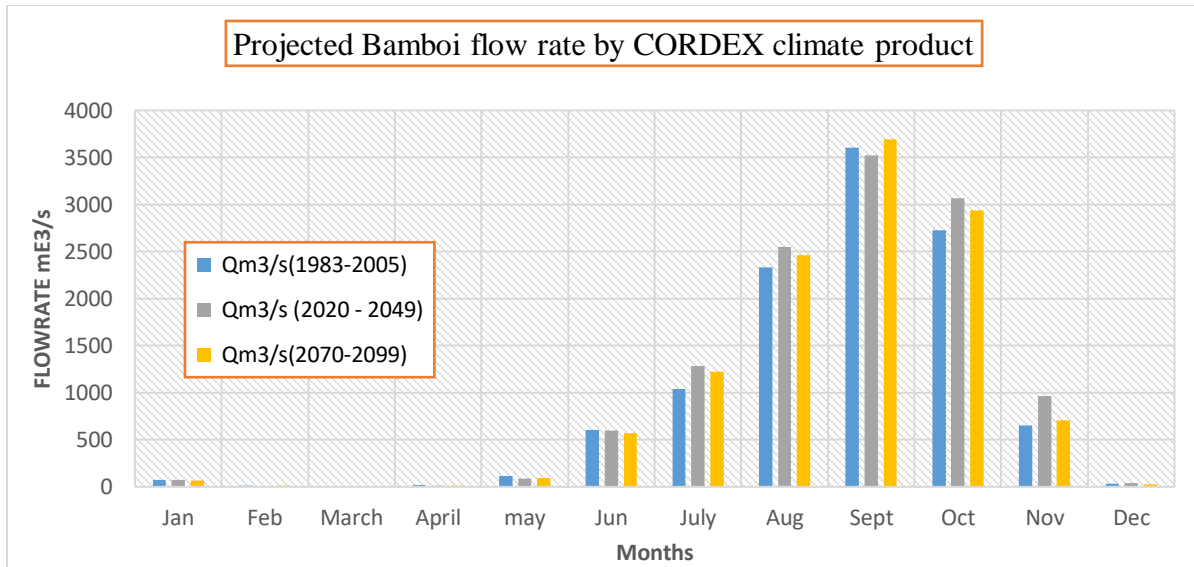
Figure 6.3 : The mean discharge calculated for the three-time series of Bamboi catchment by CORDEX climate product

6.6. FLOW DURATION CURVE OF BAMBOI CATCHMENT

A flow duration curve shows the relation between flows and lengths of time during which they are available it merely reorders the flows in order of magnitude. For the design of the hydropower plant, the average Q obtained from the historical and future discharges for both corrected and uncorrected data of CORDEX and WASCAL climate products are used.

Flow duration curve for Bamboi catchment
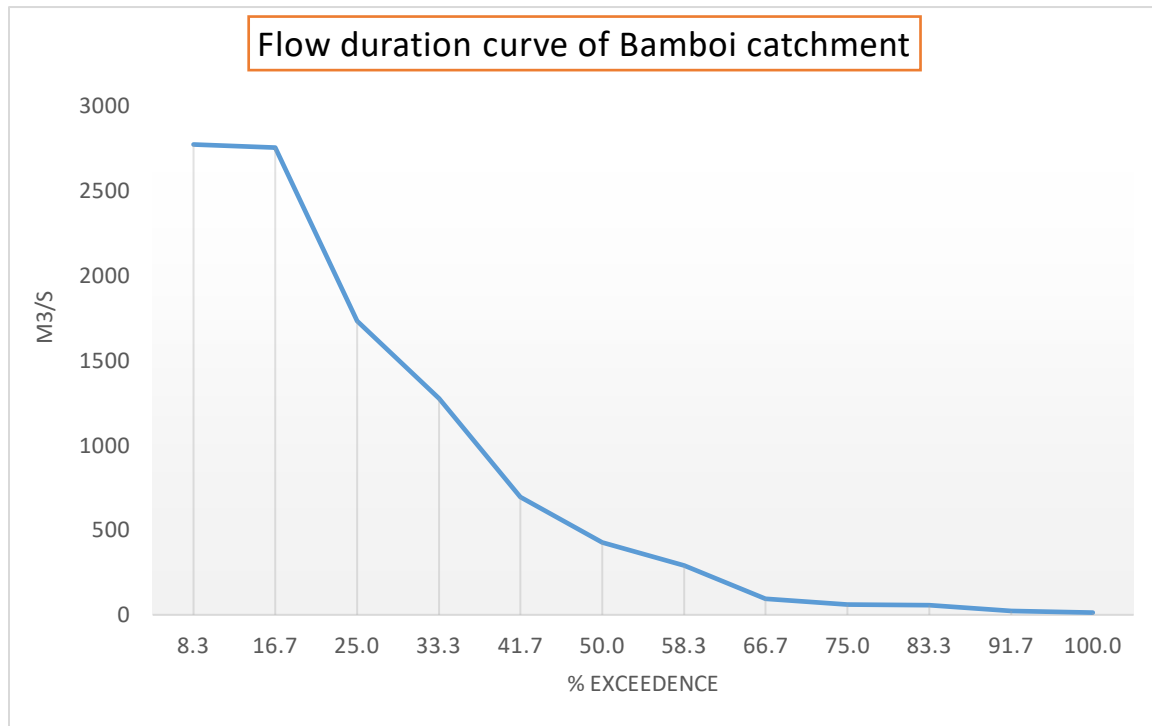
Figure 6.4 : Flow duration curve for Bamboi Catchment.

• For ecological reasons, a certain amount of flow is left in the river – residual flow Qr. Qr was calculated at Q90 to be 1.55 m3/s daily discharge.

• Residual flow Qr must be subtracted from the flow duration curve for the calculation of plant capacity, firm capacity and the available energy Qsim –Q90.

• Firm flow is the flow available p% of the time, usually equal to 80%. It is calculated from the available flow duration curve.

• 7.8 m3/s was calculated as the turbine design flow and it was used to design the Bamboi power plant and also to calculate the projected hydropower potential using the hydropower production model.

Flow duration curve
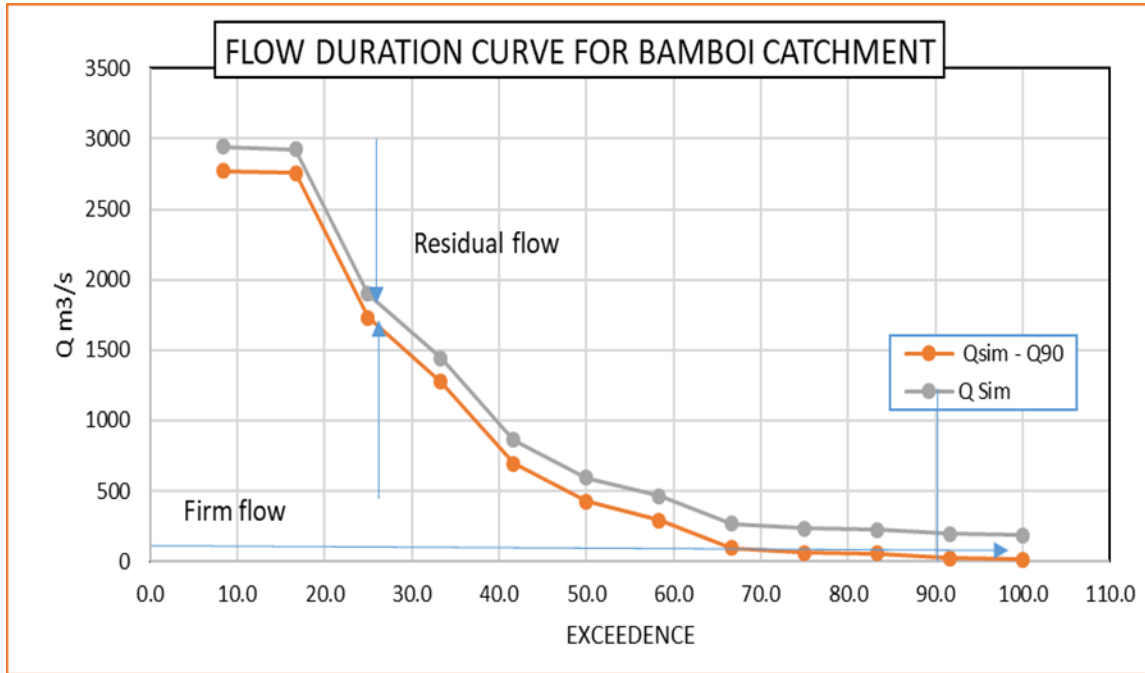
Figure 6.5 : Flow duration curve for Bamboi catchment showing residual flow and design discharge.

Residual flow is the difference between Q simulated and Q 90%. Qsim –Q90 is used for power generation. The study adopted Equation 6.2 to estimate the potential power generated from the plant using simulated discharge data. The gross hydropower generation in watts was calculated using the hydropower production model $P0 = \rho g Q H n;$ were ρ is the density of water (1000kg/m^3), g is the gravitational acceleration (9.81 m/s^2), Q is the flow discharge (7.8 m^3/s) and equals the turbine design flow. Turbines have efficiencies reaching up to 90% however, several losses are encountered during the conversion of potential and kinetic energy of water to electricity. Small turbines efficiency is lower than large turbines and typically range between 60 to 85% (Okot, 2013). Hence, an average efficiency of 85% for turbine efficiency was assumed in this study to show a more realistic impression of potential hydropower and also it was obtained from the turbine efficiency curves from Ret screen Figure 6.6). The hydropower plant effective head of 20 m was assumed in this research considering the topography of Bamboi catchment this was obtained from the Digital Elevation Maps. The estimated potential generated power was analyzed using simple graphs in order to evaluate the changes in the annual average generated power and to depict the maximum average generated power in each month of the year.

Turbine efficiency curves Ret Screen
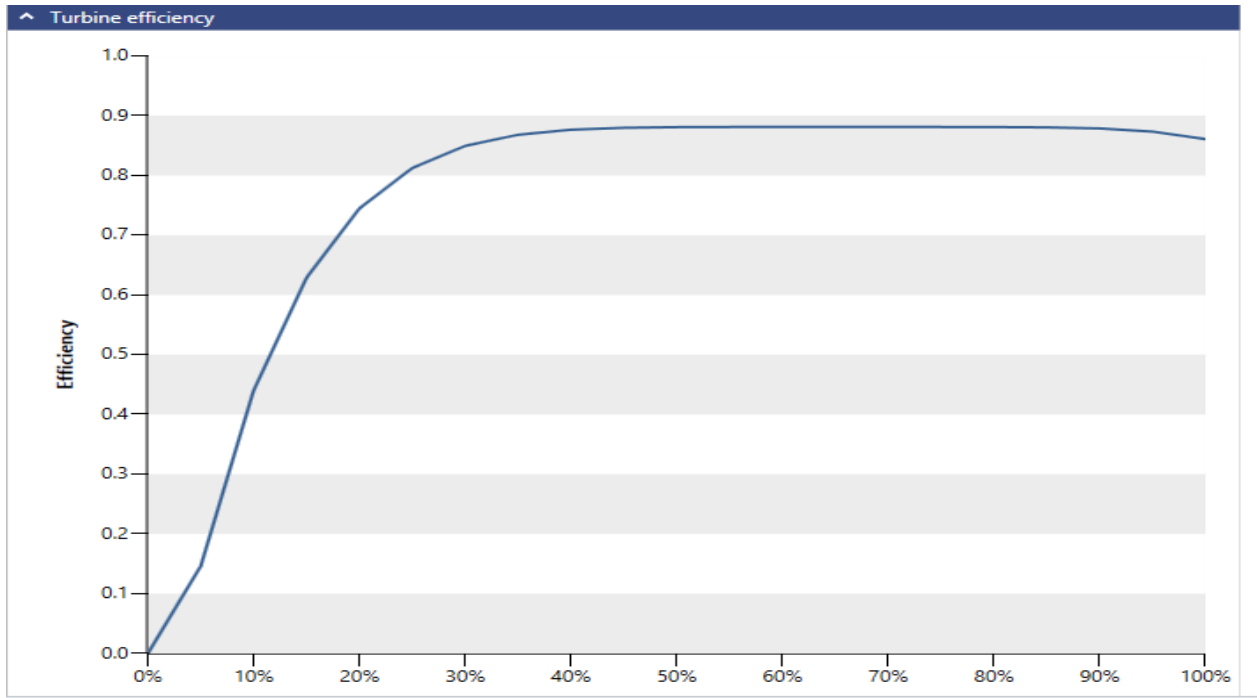
Figure 6.6 : Turbine efficiency curves by Ret screen expert software

The assumed figure of 85 % is in agreement with the turbine efficiency simulated by Ret screen displayed in Figure 6.6 : Turbine efficiency curves by Ret screen expert software

SIZING OF THE EQUIPMENT

6.7. TURBINE FULL POTENTIAL

The turbine full potential curve shows the capacity at which the selected turbine is operating for the three different projections. The turbine rated design flow in this study is 7.8 m3 obtained after averaging the discharge (Q_{80}) of three-time series projection historical and two future periods and for both climate products. The graphs show the percentage loading of the turbine for the different projections. For all three different projections it is clear the turbine will be operating at full potential every day in wet season and operating from 5 to 80% potential at least in dry season see Figure 6.7 meaning that the plant will be loaded all the time and there is high probability that every hour a kilowatt of power will be produced for the plant's lifetime provided that it is on load.

(a) Turbine full potential operating capacity for 1983- 2005

TURBINE FULL POTENTIAL CURVE FOR (1983 - 2005)
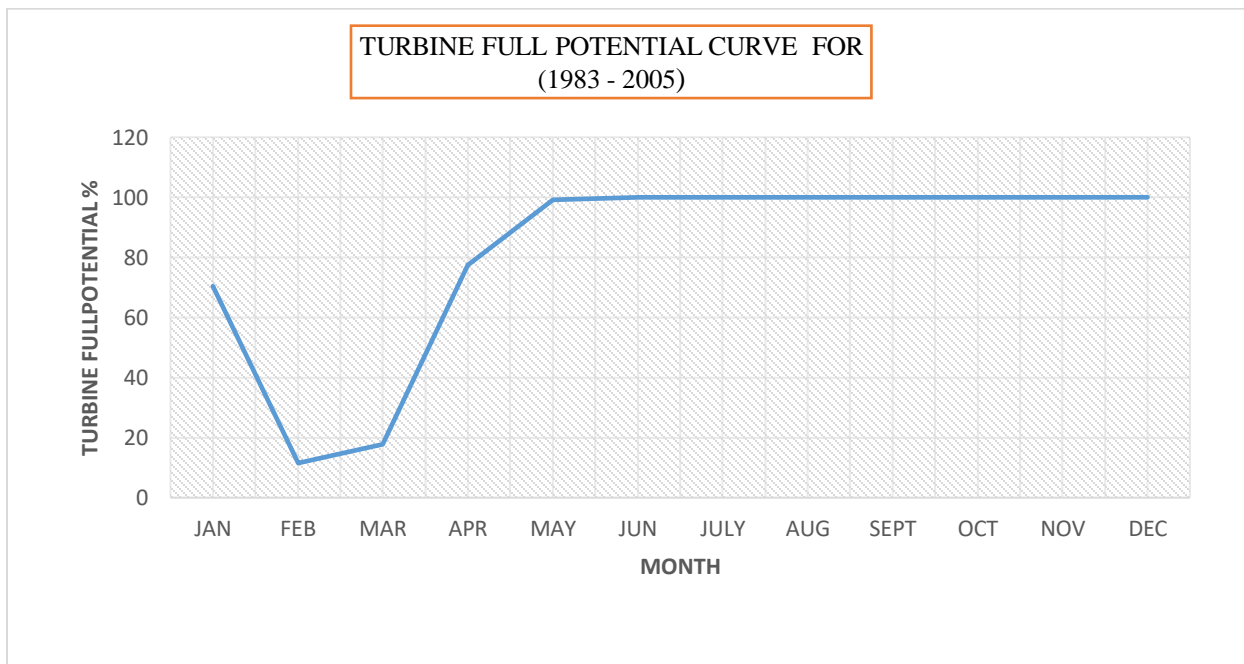
(b) Turbine full potential operating capacity for 2020-2049

TURBINE FULL POTENTIAL CURVE FOR (2020 - 2049)product
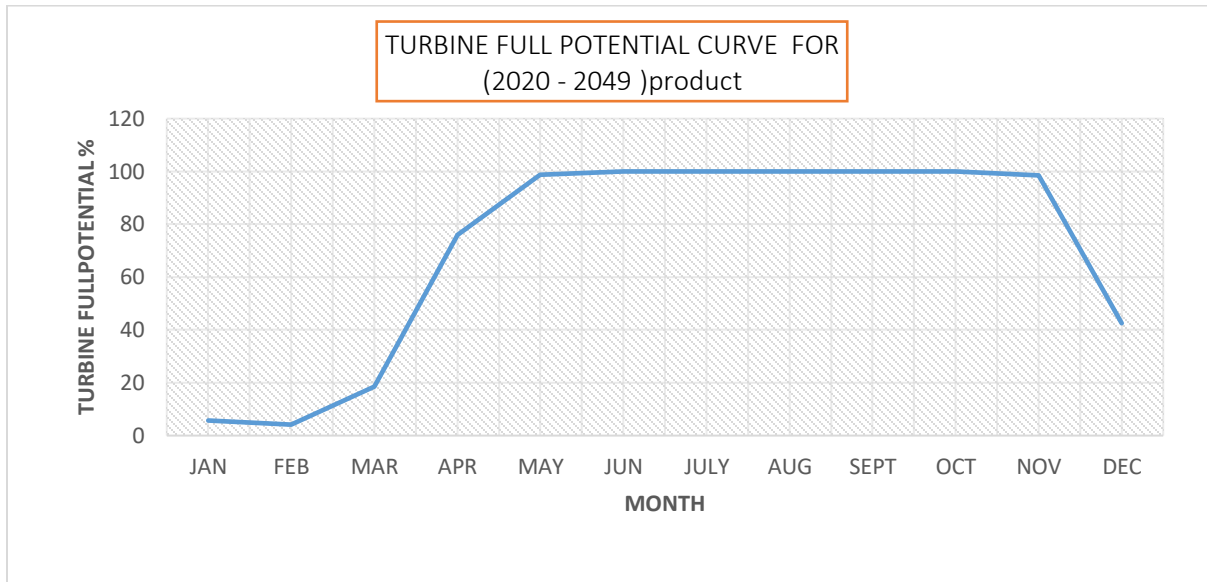
(c) Turbine full potential operating capacity for 2070- 2099

TURBINE FULL POTENTIAL CURVE FOR (2070 - 2099)
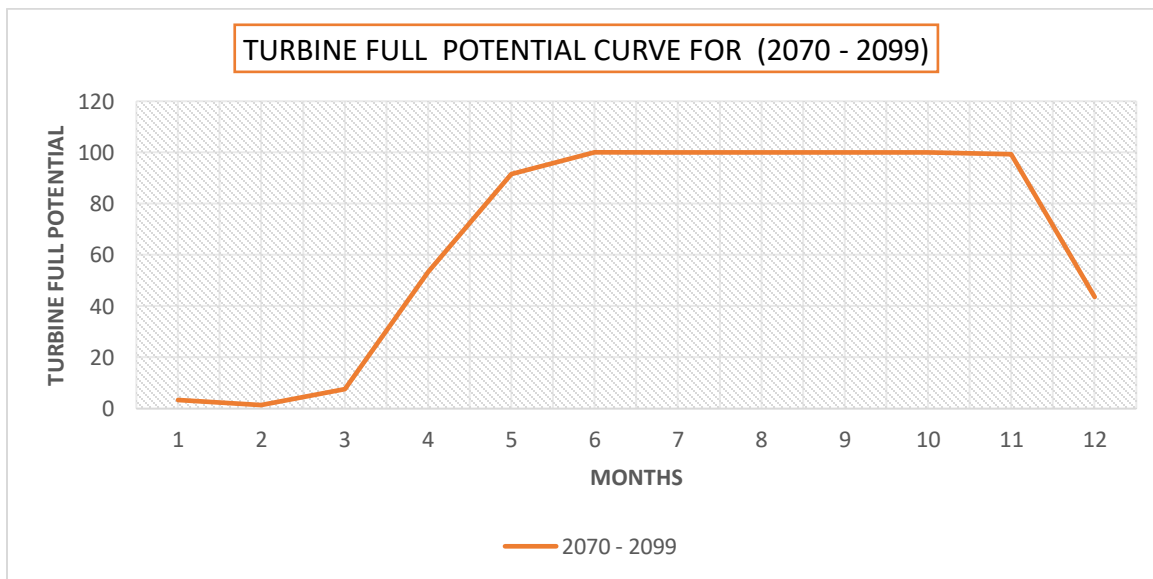
Figure 6.7: Turbine full potential curves for three different scenarios a) 1983-2005 , b) 2020 - 2049 and 2070 -2099.

All the three above turbine full potential curves support the choice of 7.8m^3/s for turbine design.

6.7.1. Turbine selection

Generally, the selection of the Turbine shall be based on:

- Available head
- Available discharge
- Power demand fluctuation

There are various parameters that need to be designed in order to ensure that turbine would work efficiently. The parameters are rotational speed, specific speed and range of discharges through turbine. The following factors have the bearing on the selection of the right type of hydraulic turbine.

Rotational speed

$$N=60*f/p$$ Equation 6.3

Where: N speed rpm; f- frequency of the generator (usually 50hz or 60 hz), p- number of pair of poles of the generator

f and p are constants thus N is constant.

Rotational speed N= $2700/(22)^{1/2}$=576 rpm

Specific speed

Specific speed of a turbine is obtained from the following equation

$N_S=1475/h^{1/3}$ for h < 18m Equation 6.4

$N_S=1750/h^{1/2}$ for h< 18<h<300m

$N_S=N(P)^{1/2}/ h^{5/4}$

Net head = Gross head –Head loss Net head

Gross head – 6% Gross head an assumed 6% assumed hydraulic losses

H_{NET} = H - (0.06 X22)

Effective head = 20 m

$$N_s = \frac{N\sqrt{P}}{H^{1.25}}$$

So the specific speed of the turbine is 145.59

Ns = 145.59

The turbine of the runner is calculated using the following formula

The specific speed corresponds well to Kaplan turbine which range from 40 <Ns< 200

Runner diameter

The runner diameter was calculated using the following formula   Equation 6.5

D runner = (41 * H_{net})/ N (rotational speed) =0.31m

Generator sizing

To size the generator

The generator output in KVA is calculated from the following equation

The sizing of the generator is following the calculation the speed and number of poles

The generator output is in KVA and is calculated from

P= ($g * H * Q * η$)/pf in KVA   Equation 6.6

g= 9.81, H =   Q =, pf = power factor

is the efficiency of the turbine, generator and the transmission.

P=   KVA

Efficiency = η turbine η generator η transmitter

$$\eta = \eta_{turbine} * \eta_{generator} * \eta_{transmitter}$$

                    Equation 6.7

Is the combined efficiency of the turbine, generator and transmitter. Taking into account the base load and the turbine, simulation in the RET screen gave a value of 85%. For power factor.

Efficiency = 0.85* 0.98*0.99

        =0.82

Generator output in KVA

$$P = \frac{g*H*Q*\eta}{pf} \quad in \ KVA$$

Equation 6.8

$$= (9.81*20 *7.8*0.85)/ 0.85$$

$$= 1530 \ KVA$$

The sizing of the generator is following the calculation the speed and number of poles. The desired speed of the generator is 579 rpm and the synchronous speed Ns= 145.5

Number poles

Therefore, number of poles = 120*f / N

$$= (120*50)/576$$

$$= 10 \ poles$$

Generator rotational speed

The rotational speed of a generator is

$$N_g = \frac{120*f}{P}*(1+s)$$

$$N_g = \frac{120*f}{P}*(1+s) \quad S =0.02$$

$$= 120*50 /10 *(1 +0.02)$$

$$=612 \ rpm$$

$$G = \frac{generator \ rpm}{Turbine \ rpm}$$

$$G = 612 /579$$

$$= 1.05$$

PROPOSED DESIGN OF BAMBOI CATCHMENT MINI HYDRO POWER PLANT.

In order to generate electricity a hydropower plant should be designed which converts the energy of water into electricity. Different designs were proposed for Bamboi catchment hydropower system and the selected option was chosen for several reasons which are:

- It utilises the full potential of the river
- High electricity production
- It ensures Q90 Ecological flow

In climate impact assessment a single value of flow rate has no significance since flow rates fluctuates considerably in a year. Therefore, it is a prerequisite to have flow rates for at least 30 years and 7.8 was chosen as the design discharge. The chosen solution hydro scheme is a run -of -river system with a diversion facility that channels a portion of a river through a canal or penstock. Channelled water will create a head that will turn the turbines to produce electricity and the used water will return back to the river. This system does not require the use of a dam. By applying the hydropower production model (Equation 6.2) to the above mentioned proposed parameters for the Bamboi hydropower plant a rated power of 1.3 MW will be obtained.

$P0 = \rho g Q H \eta$

Where

Po: the power(Watt)

ρ: density (kg/m^3=1000)

g: gravity (m/s^2= 9.8)

Q: discharge (m^3/s=7.8)

H: water level above the turbine (m=20)

Bamboi proposed mini hydro power plant

BAMBOI discharge point is located at (8.15 long, -2.033 lat) decimal degree (8° 09 '00"W Lat, 002°01 '58"W Long) degrees minutes seconds format, elevation 93 m and this the point where water will be diverted from the main stream to the Kaplan turbine through the penstock. Exhausted water from the turbine will be diverted back to the river at (8.2337 long, -0.5716) 0°34'17.74"W LONG ,8°14'1.494"N LAT point, elevation 69 m above sea level).
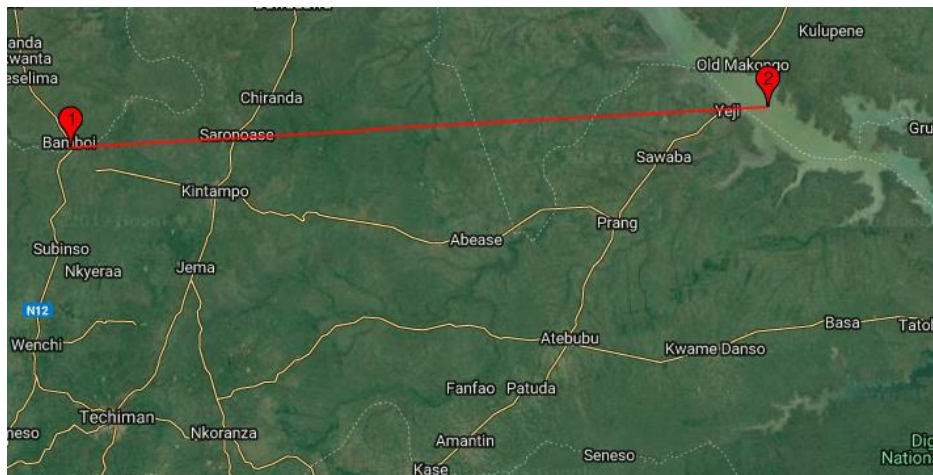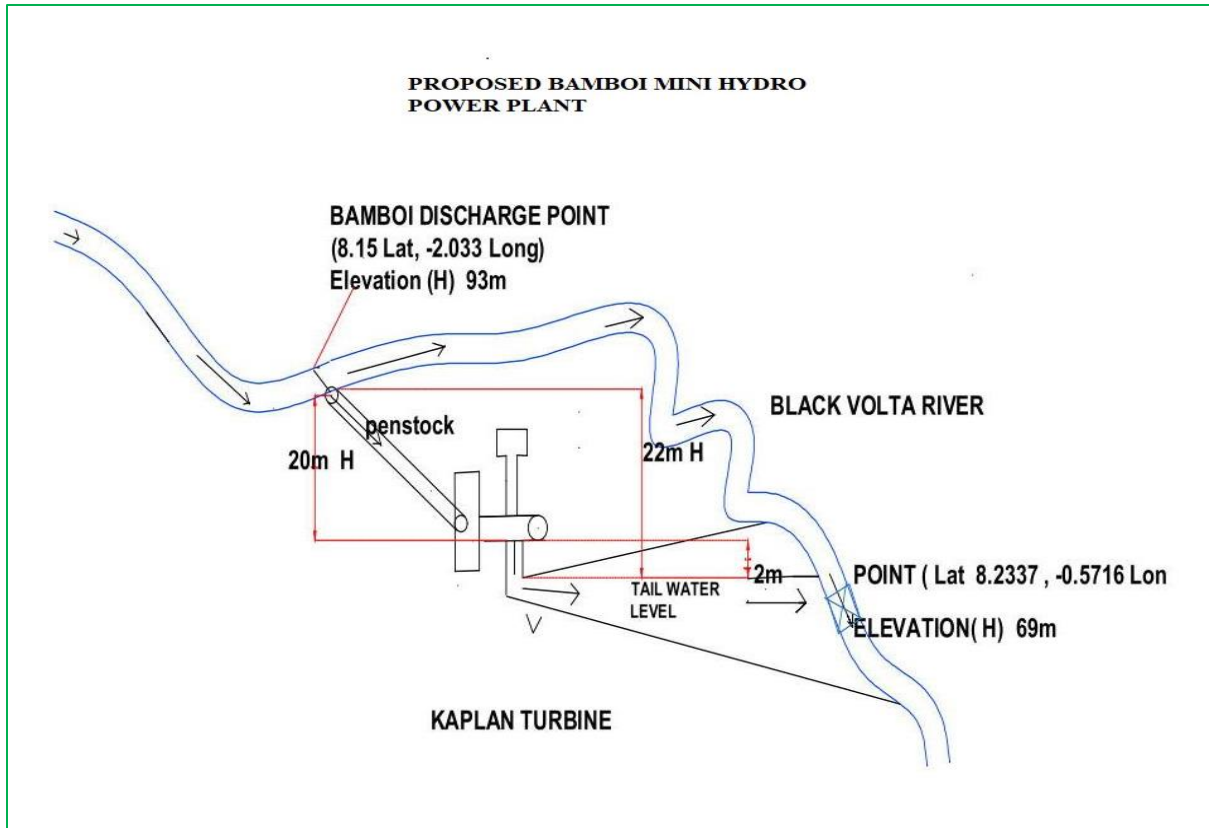
Figure 6.8 : Proposed Bamboi Mini Hydro power plant drawn with AutoCAD

Table 6.1: Proposed Bamboi Hydropower Station specification

Power output	1.3 MW
Effective H	20 m
Generator output	1530 KVA
Turbine type	Kaplan
Turbine rotational speed	576
Generator rotational speed	612 rpm
Design flowrate Q	7.8 m3
Turbine specific speed	145.59

6.7 Evaluation of Hydropower potential for historical and projected climate conditions by WASCAL and CORDEX climate product

Both historical and projected discharges corrected and uncorrected data obtained from CORDEX and WASCAL climate products scenarios were converted to hydropower potential following a run-of-river hydroelectricity generation approach Equation 6.2. The simulated discharge modelled by HBV light model in Chapter 5 is for three periods historical (1983 – 2005), mid-century 2020-2049 and late century 2070 -2099. Hydropower production for historical and future climate conditions are compared to assess the impact of climate change on the hydropower generation. WASCAL climate product projections and CORDEX climate product projections were compared to see how each of them impact the hydropower potential.

Monthly Projected power by WASCAL _GFDL ESM 2M product corrected data

Bias corrected projected power
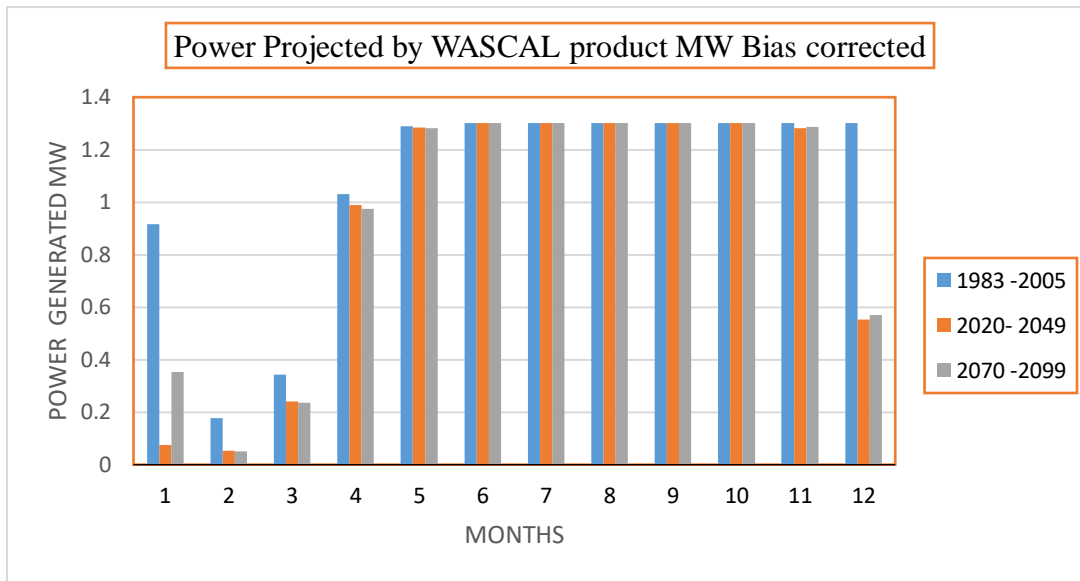
Figure 6.9: Projected power by WASCAL climate product

Projected power by WASCAL climate product GFDL ESM 2M uncorrected data
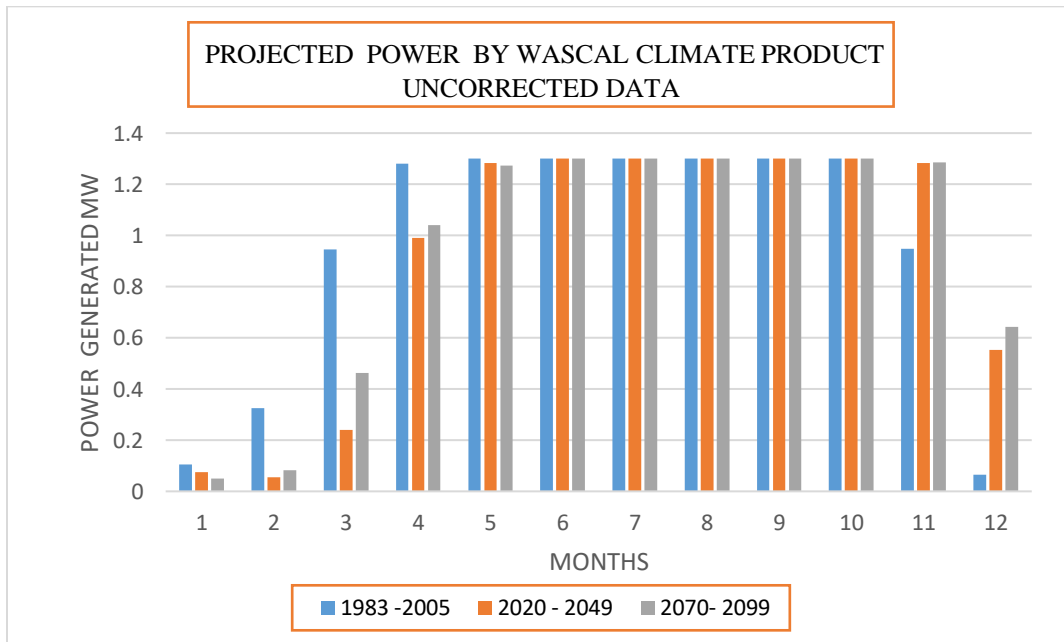
Figure 6.10 : Projected power by WASCAL climate product uncorrected data

Figure 6.9 and Figure 6.10 show that both corrected and uncorrected data predict similar trends. The maximum amount of power is generated in wet season and minimum power is generated in the dry season. Both figures indicate that the average hydropower generation will decrease in the future compared to the reference period. However, for the first three months of the year which happen to be the dry season Jan, Feb and March in the region, the corrected data is showing a greater deviation between the historical period and the future periods. More hydropower is produced during the historical period in the dry season compared to future period. These results are very consistent with the Turbine full potential graph (Figure 6.11), that shows an important turbine potential during the dry season for the historical period while this potential drops to zero for the future periods.

6.7.2. Projected monthly energy generated by WASCAL product GFDL ESM 2M Non-Bias corrected data
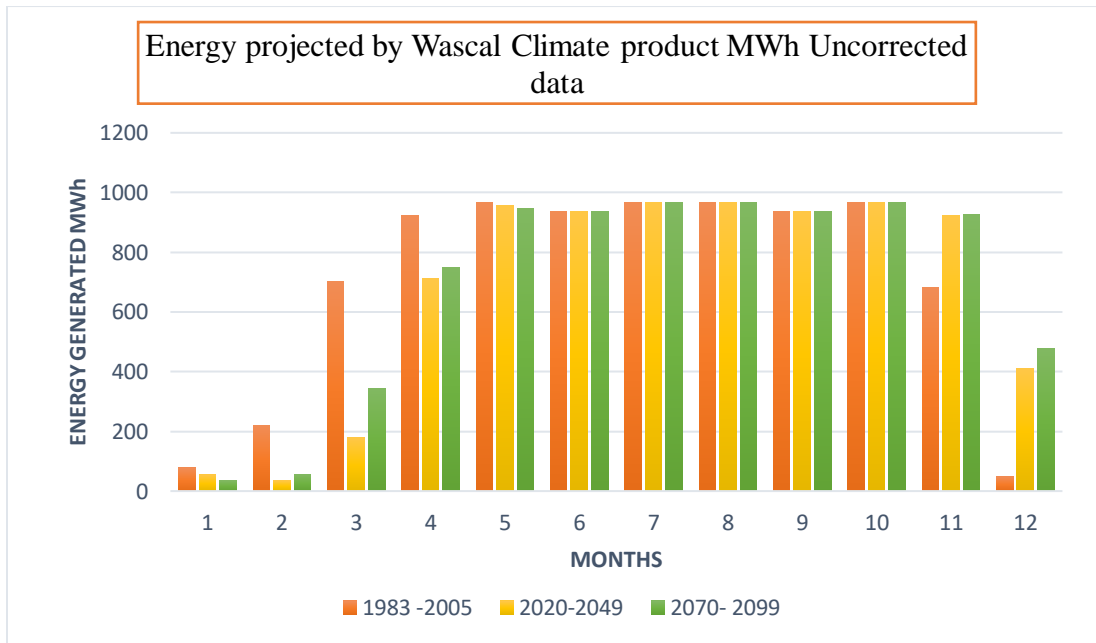
Figure 6.12 : Projected energy by WASCAL climate product un corrected data

Bias - corrected data
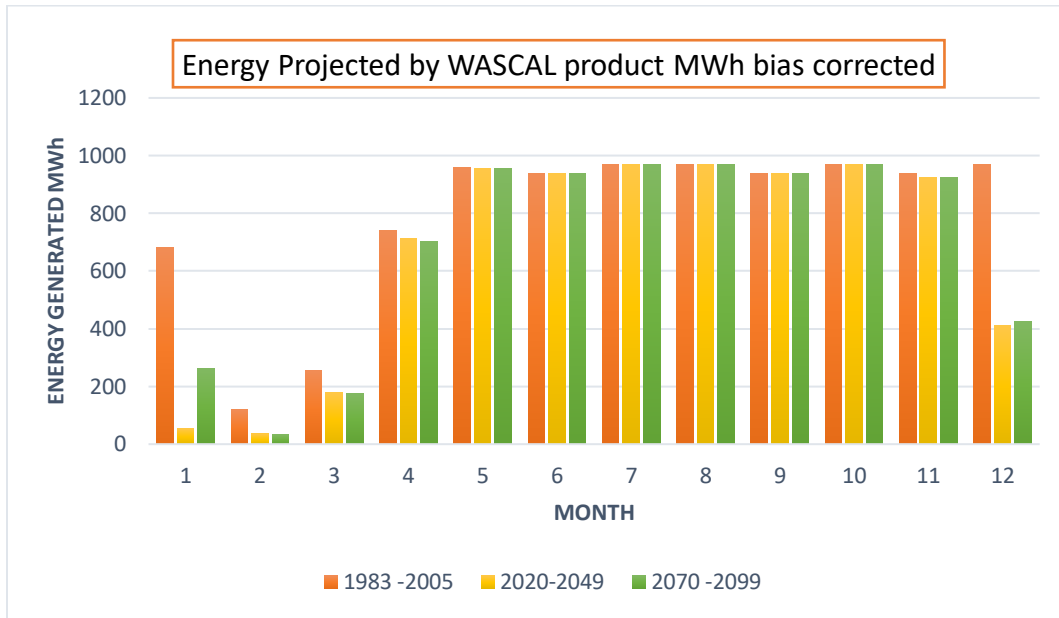
Figure 6.13 : Projected energy by WASCAL climate product bias corrected data

The maximum amount of power generation takes place in the rain season with a maximum monthly power production of 900 MWh and the lowest in the dry season with an average power production of 34MWh.

6.7.3. Monthly projected power by CORDEX MPI ESM REMO climate product

Non-Bias uncorrected data
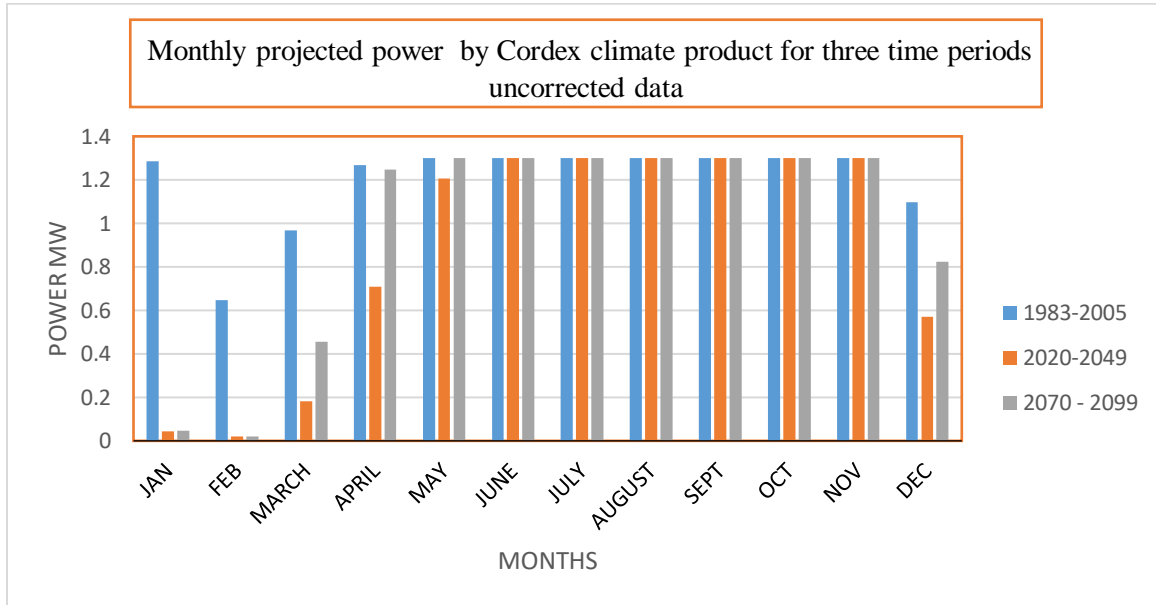
Figure 6.14 : Monthly Projected power by CORDEX climate product

Bias corrected data
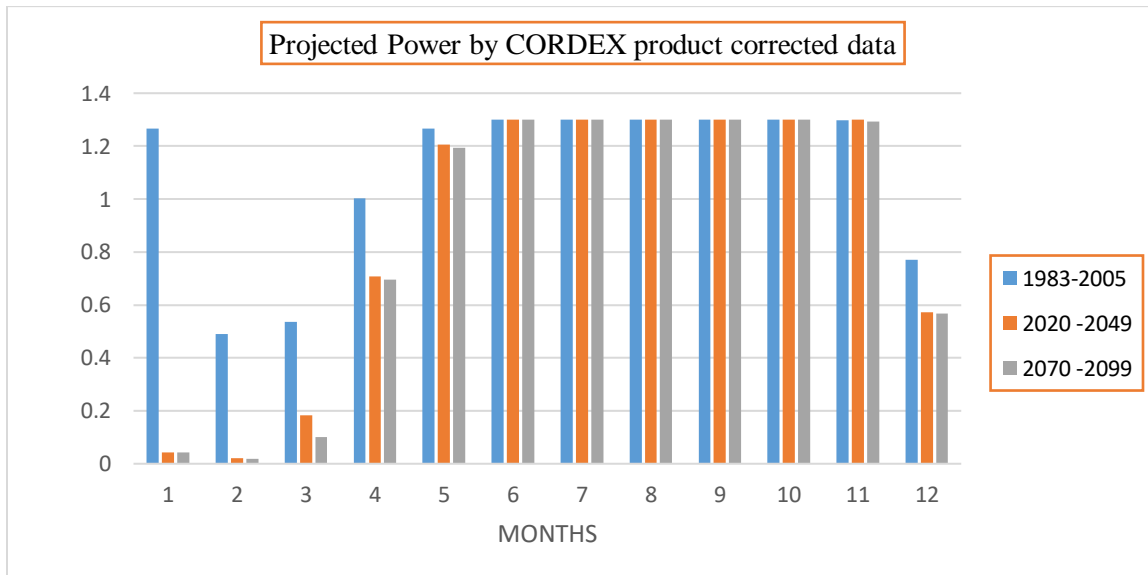
Figure 6.15 : Projected power by CORDEX climate product

The projected hydropower potential by CORDEX climate product is in agreement with the WASCAL climate product. The lowest amounts of power are generated in the dry season and the highest amount of power are generated in wet season. However, for the CORDEX product both corrected and uncorrected data shows high peaks of projected energy in the historical period of the dry season as compared to the reference. This could be attributed to high discharges in dry season in the past as compared to the future but however the peaks are too huge, it could be as a result of errors in the data or errors done during quantile mapping done in chapter 5 to correct the RCM data. For the corrected data CORDEX climate product predicts a decrease in hydropower potential in both future period as compared to the reference period which is in agreement with WASCAL climate product. Uncorrected data predicts a decrease in hydropower potential in the 2020- 2049 period as compared to the reference period, however in the late century (2070 – 2099) both climate products un corrected and corrected data except for CORDEX corrected data predicts a slight increase in hydropower potential in the late century as compared to the (2020- 2049) period.

6.7.4. Projected energy by CORDEX climate product

Bias uncorrected data
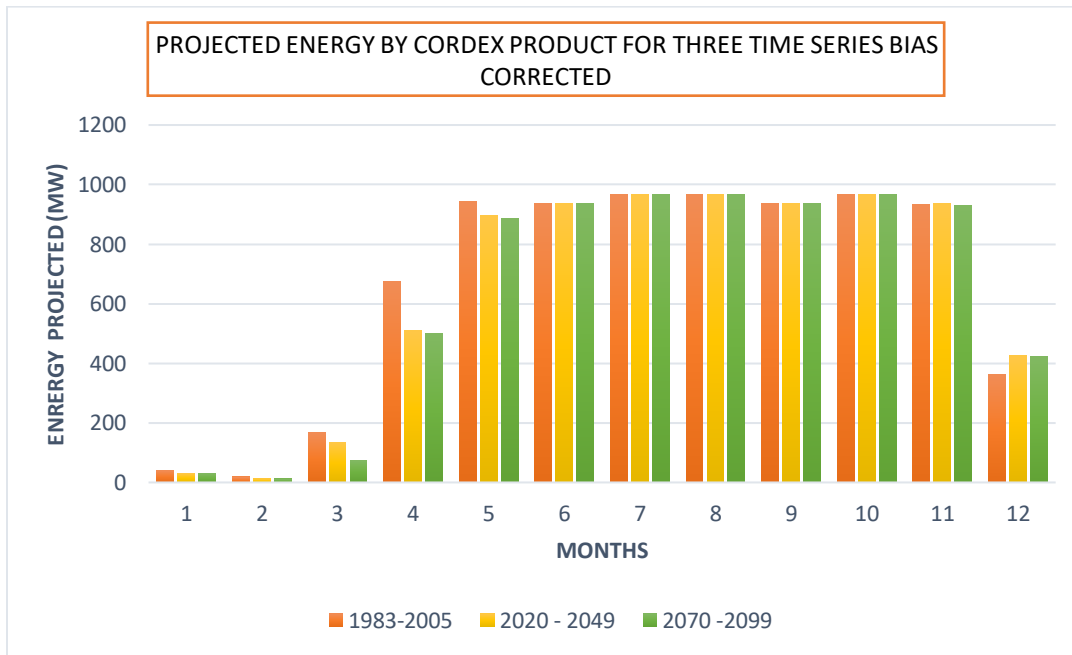
Figure 6.16: Projected energy by CORDEX MPI ESM REMO climate product

Non-Bias corrected data
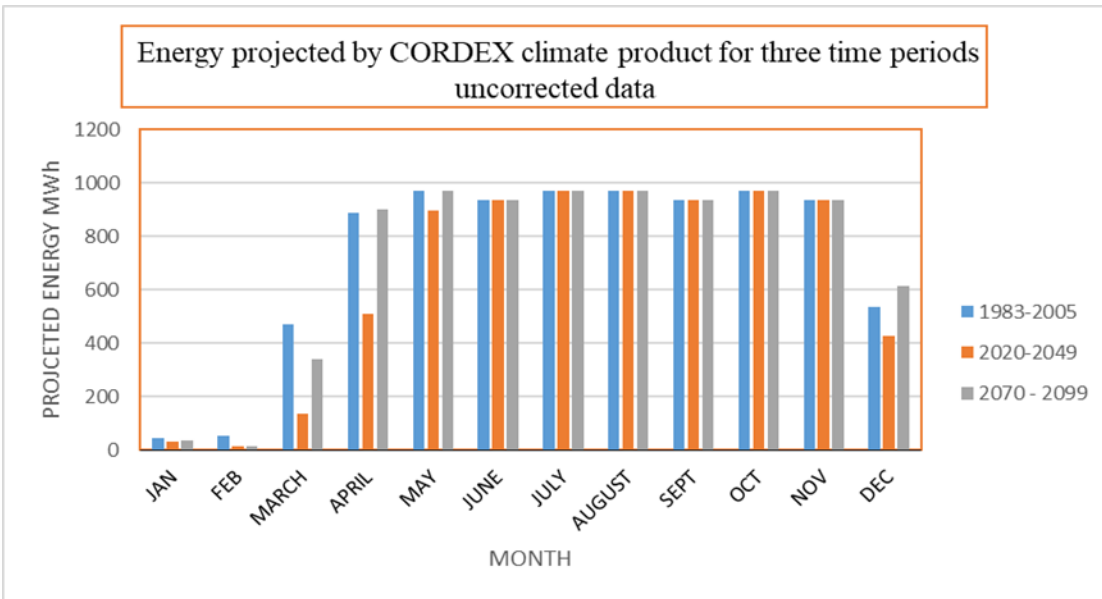
Figure 6.17 : Projected energy by CORDEX climate product un corrected data

6.7.5. Climate change vs hydropower

Climate change has the potential to affect hydropower generation by either increasing or reducing flows (discharge**).** The amount of electricity to be produced by a hydropower facility depends mainly on the volume of water passing through the turbine in a given amount of time.

6.7.6. Monthly energy generated by WASCAL climate product corrected data

Table 6.2 :Monthly power generated by WASCAL climate product

	WASCAL PRODUCT		
Month	Predicted Hydro power production MW		
	Historical Power W (1983 –2005)	Change in power production MW (%) (2020 -2049)	Change in power generation P MW (%) (2070 -2099)
January	916694.9	-48.827834	-91.765477
February	149858.2	-67.66331	-66.063113
March	230453.6	-58.48745	2.3440578
April	1008348	-7.4234275	-3.3330758
May	1290020	-0.4492507	-0.5376544
June	1301071	0	0
July	1301071	0	0
August	1301071	0	0
September	1301071	0	0
October	1301071	0	0
November	1301071	-1.4295531	-1.1635473
December	1301035	-42.452752	-56.173952

Monthly power generated by CORDEX climate product

Table 6.3 : Monthly power generated projected by CORDEX climate product

Month	Predicted Hydro power production MW (CORDEX)		
	Historical Power MW (1983 –2005)	Change in power production MW (%) (2020 -2049)	Change in power generation P MW (%) (2070 -2099)
January	59.29708	-96.6667	-96.6667
February	5.99279	-95.8793	-96.3108
March	22.97987	-65.9775	-81.2973
April	319.8257	-29.4151	-30.7138
May	2307.72	-4.88133	-5.86082
June	12025.23	0	0
July	21381.91	0	0
August	48105.07	0	0
September	72007.29	0	0
October	56293.02	0	0
November	12983.22	0.211277	-0.37162
December	350.015	-25.9435	-26.4623

From the analysis of Table 6.4.3 and 6.2 both climate scenarios WASCAL and CORDEX climate product displays that hydropower generation will increase in the wet season and decrease in the dry season as shown by positive change in hydropower potential in wet season (June to October) and negative change of hydropower in the dry season (December to April). This is due to the fact that runoff increases with precipitation in the wet season so does discharge there by increasing the hydropower potential production the opposite is true for the dry season. The wet periods will become wetter while dry periods will become drier in both future periods as compared to the reference period. During the dry season, the hydropower plant will experience a power shortage due to lack of streamflow. Both models projected a maximum decrease by -91.7% mean ensemble during the dry period as compared to the reference scenario for the WASCAL climate product while for the CORDEX product a maximum decrease by -96% in the dry season as compared to the reference period is projected

6.7.7. Mean Annual energy generated projected by WASCAL climate product

Table 6.4: Mean annual energy generated projected by the WASCAL climate product for the period 2020-2049 and 2070-2099 compared to the reference period 1983-2005.

	WASCAL CLIMATE PRODUCT MWh			% CHANGE	
Period	(1983-2005)	(2020-2049)	(2070-2099)	(2020-2049)	(2070-2099)
Corrected	9440.539	8050.63592	8257.215	-15.37963	-12.5
Uncorrected	8400 8050.635917	8050.67	8314	-4.2	-1.02

Table 6.5 : Mean annual energy generated projected by the CORDEX climate product for the period 2020- 2049 and 2070-2099 compared to the reference period 1983-2005

	CORDEX climate product MWh			% change	
Period	(1983-2005)	(2020 2049)	(2070-2099)	(2020-2049)	(2070-2099)
Corrected	7917.152	7726.577	7636.356	-2.4%	-3%
Uncorrected	8667	7726	8582	-10.9	-0.98

It is evident from Table 6.4 and Table 6.5 that the average annual hydropower generation will decrease in the future for both climate scenarios GFDLESM 2M (WASCAL) and MPI-ESM-REMO (CORDEX) climate products. For the near future part of the 21st century (2020 -2049), a decrease in the average annual power production by -15.4 %, and -2.4% for corrected data and –4.2% and - 10% for uncorrected data for scenarios GFDLESM2M(WASCAL) and MPI-ESM-REMO CORDEX respectively, compared to the reference period. By end of century (2070-2099), the average annual power production shows a slight increment as compared to the 2020 - 2049 period, however the amount is still lower compared to the reference period. A decrease in the average annual power production by – 12.5 %, and -3% for corrected data and –1.02% and – 0.98 % for uncorrected data for scenarios GFDLESM2M(WASCAL) and MPI-ESM-REMO CORDEX respectively, compared to the reference period is projected for the 2070 -2099 period. These changes are directly proportional to the discharge Qsim (m3/s). An increase in discharge increases the hydropower generation only if the discharge increase is accompanied with an increase in the flow duration and the opposite is true. In Chapter five it is mentioned that both models WASCAL and CORDEX climate products predicted an increase in precipitation and discharge in the future periods. However, this increase in discharge occurs during the wet season while the power plant already operates at its full potential. Meaning that this discharge increase does not translate in additional energy production. The presented annual discharge increase in chapter five also overshadows a decrease in monthly discharge during the dry season. However, this projected decrease in discharge during the dry months is translated in important energy losses. Precipitation, discharge, AET and PET for two future periods play a greater role in the power that will be

generated in future. The increase in PET will dry rivers quickly leading to less discharge left to turn the turbines to generate power (importantly during the dry season).

6.7.8. Change in annual discharge with response to precipitation vs hydropower

CHANGE IN ANNUAL DISCHARGE WITH RESPONSE TO PRECIPITATION for BAMBOI CATCHMENT

y = 1.2489x + 0.7338
R² = 0.987

y = 0.5989x + 7.7046
R² = 0.8453

- MPI -ESM-REMO CORDEX
- GFDL-ESM2M - WRF WASCAL
- .... Linear (MPI -ESM-REMO CORDEX)
- .... Linear (MPI -ESM-REMO CORDEX)
- .... Linear (MPI -ESM-REMO CORDEX)
- .... Linear (GFDL-ESM2M - WRF WASCAL)

CHANGE IN ANNUAL DISCHARGE %

CHANGE IN ANNUAL PRECIPITATION %
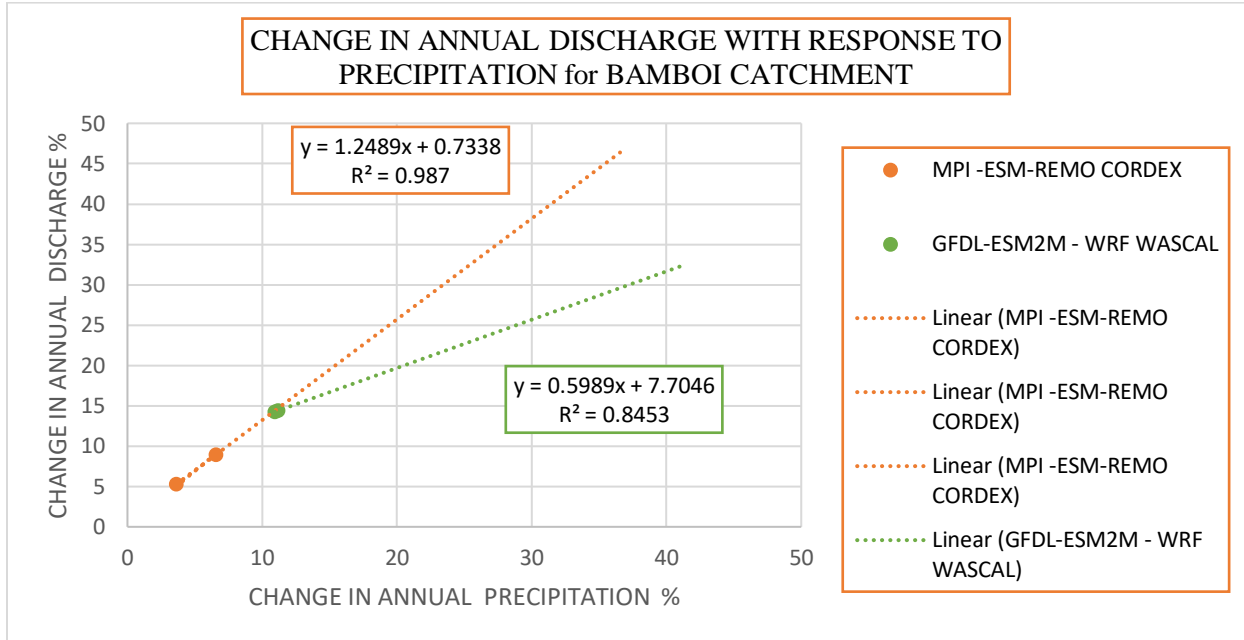
Figure 6.18 : Change in the annual discharge as a response to precipitation change under emission scenarios RCP4.5 comparing 1983–2005 to 2020–2049

Figure 6.18 that there is strong correlation between discharge and precipitation as indicated by the values of r^2 for both models which are r^2=0.987 and 0.845. If the precipitation increases the discharge also increases which is the reason why hydropower potential increases more in the wet season and decreases in the dry season provided that factors such as temperature, potential evaporation are constant.

Average projected annual energy yield MWh 2020 -2049 by CORDEX & WASCAL climate product
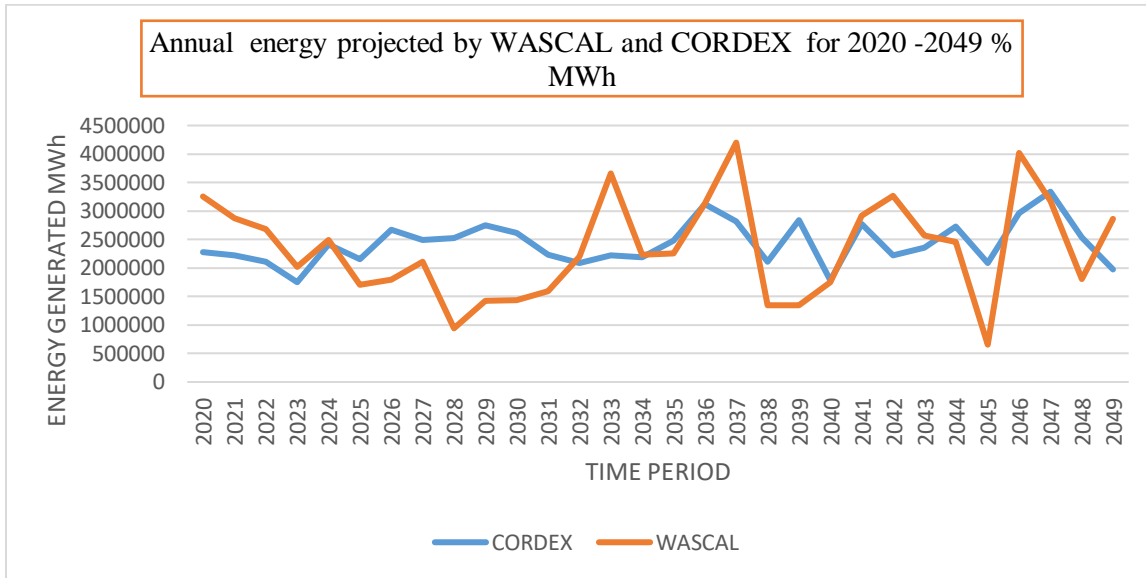
Figure 6.19: Projected annual energy yield MWh 2020 -2049 by CORDEX climate product

Projected Annual Energy yield for 2070 - 2099
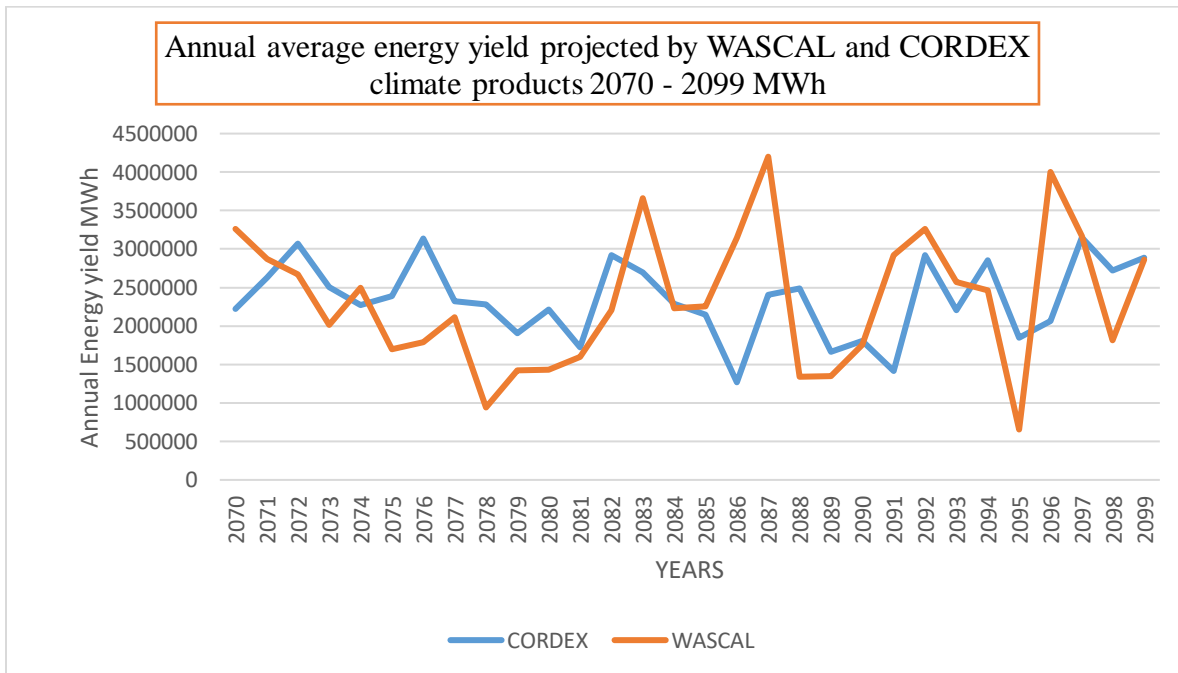
Figure 6.20 : Projected Annual Energy yield for 2070 - 2099

Figure 6.19 and Figure 6.20 and displays the annual average energy yield for two future periods 2020 – 2049 and 2070 – 2099 from both graphs it is evident WASCAL climate products projects a strong inter annual energy fluctuating as shown by maximum and minimum peaks , compared to CORDEX dataset.

6.8. ECONOMICAL POTENTIAL

How does climate change impact the hydropower economic potential?

The exploitable potential is the economic potential that can be harnessed considering the environment and other special restrictions. Assessment of hydropower potential should be done on the economic potential since it will be the exploitable hydropower to be used for actual generation. However due to lack of time and resources this research focus more on the theoretical potential of hydropower and little was done on the economic potential.

Climate change does not only affect the technical/ theoretical potential of hydropower alone rather it also affects the economic potential. Economic potential is the part of the technical potential available which can be generated as economic at a place including losses etc. Hydropower economic potential takes into consideration costs. Climate change alone affects overall system costs. Hydropower system costs increase under dry conditions and decrease under average or wet conditions (Savelsberg et al, 2018) this is due to the indirect effect of using thermal generation to substitute for reductions in hydro generation and costs of reservoirs to store water during dry season. There is enough discharge to generate electricity through run of river during wet season however in dry season discharges are very low to an extent that the power production in some months could be as low as 0 kW which results in a need to create reservoirs to store water for power generation during dry season. It should be noted that construction of reservoirs comes with a cost. In this context electricity price represent the cost of electricity supply in all countries considered in the catchment (Ghana, Burkina Faso, Ivory Coast and Mali). Therefore, changes in hydro power production have an impact on neighboring countries due to cross border trade. In order to analyse how climate change affects economic potential of hydropower a preliminary cost estimation was made based on the design discharge and the optimal engineering option on the proposed Bamboi mini hydropower plant design. The financial and economic analysis was carried out using RET screen software to evaluate the cost of the system and payback period. The model is based on the estimated feed in tariff of electricity production, the design discharges and the cost estimation of the project components.

6.8.1. Cost estimation using Ret screen

The cost estimation is done to assess the hydropower economical potential and it was computed by multiplying the quantities with the unit rates for the main construction activities of each components of the projects. Construction cost of a hydro power plant is made of civil engineering cost and manpower cost, operation and maintenance costs and other cost such as unforeseen costs. From Ret screen expert software, the proposed costs of the Bamboi mini hydropower plant is 4.160.000 $ USD and the cost includes the feasibility study, development cost, engineering and power system cost. The preliminary cost per kilowatt is 4.160 .000/1300 kW, which is 3200$/kW, which lies in the range of small hydro system cost 1200 to 6000USD per installed kilowatt.

NB: Both models are predicting a decrease in the hydropower potential in future scenarios this may affect potential as they will be need to add a reservoir to store water for power generation and these reservoirs come with a cost which will be added to the 4.160.000 $ USD which may affect the economic potential of the hydropower. From the above analysis it can be concluded that the hydropower economic potential can be impacted by climate change.
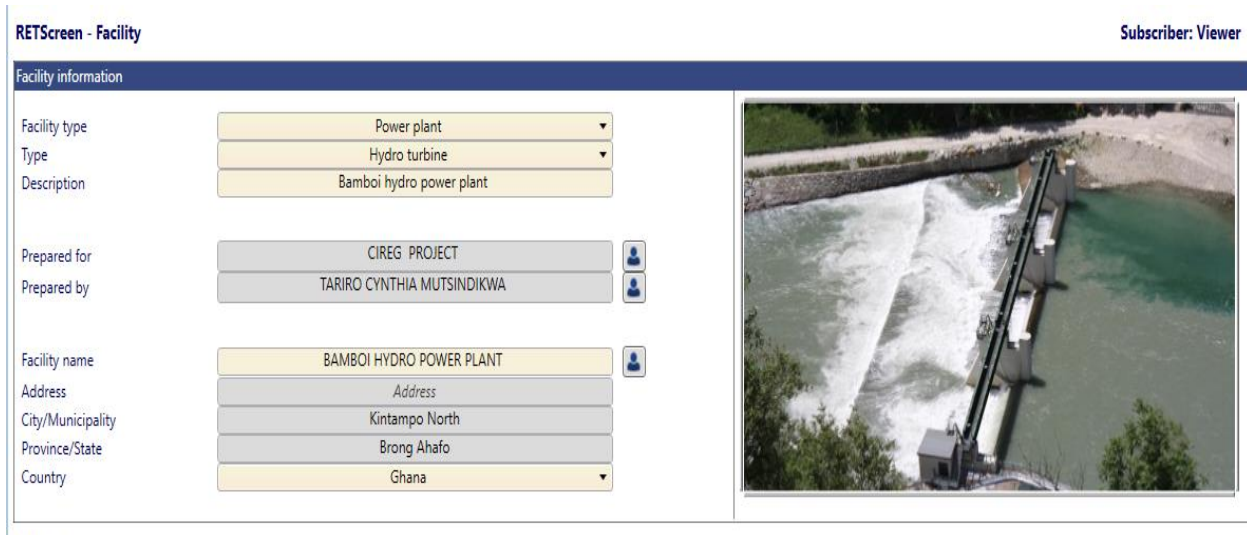
Figure 6.21 : Ret screen software screen shot

To analyse how climate change might impact the cash flows of the proposed hydropower plant, revenues for the projected plant were calculated using ret screen expert software. The installed capacity of the plant is 1.3MW. Basic export price of electricity is $ 0.18/kWh. This price was used by taking into consideration the price of electricity in the Volta basin. the electricity price

126

changes with climate change impact, in wet season the price of the unit of electricity is $ 0.18/kWh however in dry season the price can go above $0.25 kWh (World bank, 2018) .

Cash flows The Bamboi mini hydro power plant proposed cumulative cash flow

Financial analysis			Cumulative cash flows graph
Financial parameters			
Inflation rate	%	2%	
Project life	yr	20	
Debt ratio	%	70%	
Debt interest rate	%	7%	
Debt term	yr	15	
Total initial costs	$	5,330,000	
Incentives and grants	$		
Annual costs and debt payments			
O&M costs (savings)	$	100,100	
Debt payments - 15 yrs	$	409,644	
Total annual costs	$	**509,744**	
Annual savings and revenue			
Electricity export revenue	$	1,844,856	
Total annual savings and revenue	$	**1,844,856**	
Financial viability			
Pre-tax IRR - equity	%	88.3%	
Pre-tax IRR - assets	%	28.1%	
Simple payback	yr	3.1	
Equity payback	yr	1.2	

Figure 6.22 :Cumulative cash flows

Thorough analysis of the Cumulative cash flows can determine the hydropower economic potential how economically feasible is it to extract the resource considering the environment and losses. Figure 6.22 and Figure 6.22 shows positive cash flows meaning that the economic potential of the resource is positive. However, with the predicted climate change scenario by both models a decrease in hydropower it may affect the hydropower economic potential at Bamboi catchment

6.9. CONCLUSION

Both climate products WASCAL and CORDEX predict a decrease in hydropower generation. This is attributed by an increase in rainfall and discharge counter balanced by an increase in temperature and evapotranspiration as highlighted in Chapter 5. Climate Impact assessment results, this increase in evapotranspiration will decrease the flow duration in the river there by decreasing hydropower potential during the dry season. For the mid-century time period (2020- 2049),) both models predict a decrease in the hydropower generation as compared to the reference period. By late century (2070-2099) both models project a slight increase in the hydropower generation compared to the mid-century except for CORDEX corrected data. However, the potential is still lower than the reference period. From the analysis of how climate change may affect the hydropower economic potential it can be projected that climate change will affect the economic potential of hydropower.

CHAPTER SEVEN: CONCLUSION AND RECOMMENDATIONS

Hydropower is the major source of renewable energy in West Africa and it contributes significantly to climate change mitigation, however careful attention should be done to safeguard this resource in order for it to add terawatts of power to the grid. In this study a statistical bias correction was applied to two RCM-GCM models, namely the GFDL ESM 2M of WASCAL high resolution climate product and MPI ESM REMO of CORDEX Africa both of them under scenario RCP 4.5 climate scenario in order to assess the impacts of climate change on the hydropower potential of the Bamboi catchment (Black Volta) comparing two future periods 2020-2049 and 2070-2099. Non-bias corrected and bias corrected data were used as inputs to HBV light model to investigate the impact of climate change on hydropower potential over the Bamboi catchment. Bias correction was necessary for the climate models to precisely project the future climate change signal. Projected historical and future discharges data were converted to hydropower potential following a run-of-river hydroelectricity generation approach. A run of river hydro power plant was designed accordingly with an effective head of 20m and a design discharge of 7.8 m^3/s. The following conclusions were drawn from this study: Both the corrected and uncorrected simulations predict a continuous increase in projected temperatures up to 2099 when compared to the value observed during the base line period (1983-2005), i.e. 29.6 ∘C, regardless of the climate scenario. Thus, by horizon 2099, the average temperature in the catchment will be 35.17 ∘C and 36. ∘C in the hottest month of (April) and 32.8∘C and 32.3 ∘C in the coolest month (July) as predicted by GFD LESM2M –WRF (WASCAL) and MPI –ESM REMO (CORDEX) climate products, respectively. This confirms the well documented projected warming of West Africa.

Overall, the results for the two GCM RCM climate products show that precipitation is projected to increase slightly during the mid-century (2020 -2049) period and decrease slightly during the late century (2070 to 2099) for both climate products compared to the reference period (1983 - 2005). For WASCAL climate product and CORDEX climate product an increase of 11% and 6.6 % is projected for the 2020-2049 period and 10.9 % and 3.7 % for the end of century (2070 -2099) respectively. Potential evapotranspiration is projected to increase for all scenarios during the future periods due to the projected temperature increase for both scenarios relative to the observed period by 1.9% to 4.03 % for GFD LESM2M –WRF (WASCAL) and 2.3% to 5.066 % for MPI –ESM REMO (CORDEX) like wise. An increase of AET is predicted likewise.

Comparison of the observed and future simulated discharge across the study area shows that the hydrological status of the catchment is likely to change significantly. The annual mean stream flow measured at the Bamboi gauge station is also expected to increase significantly for both climate products due to the projected increase of precipitation. WASCAL climate product predicted a discharge increase of 14% and 14.2 % for 2020 – 2049 and 2070- 2099 respectively whereas the CORDEX climate product predicted a discharge increase of 8.4% and 5.27% for 2020 -2049 and 2070 – 2099, respectively. However, the discharge is expected to increase in the wet periods and decrease in the dry season.

In contrary to the above statements for both scenarios, an overall decrease of hydropower production was observed for the (2020 – 2049) and (2070- 2099) periods as compared to the reference period of 1983 – 2005 and this was brought about by a decrease in flow duration related to the projected increase in temperature in the basin coupled with an increase in potential evapo transpiration (PET) leading to an increase in the drying of rivers. For the near future part of the 21st century (2020 -2049), a decrease in the average annual power production by -15.4 %, and -2.4% for corrected data and –4.2% and - 10% for uncorrected data for scenarios GFDLESM2M(WASCAL) and MPI-ESM-REMO CORDEX respectively, compared to the reference period. By end of century (2070-2099), the average annual power production shows a slight increment as compared to the 2020 - 2049 period, however the amount is still lower compared to the reference period. A decrease in the average annual power production by – 12.5 %, and -3% for corrected data and –1.02% and – 0.98 % for uncorrected data for scenarios GFDLESM2M(WASCAL) and MPI-ESM-REMO CORDEX respectively, compared to the reference period is projected for the 2070 -2099 period.

 A significant decrease in hydropower was also projected by both climate products in the dry season. It is projected that dry season will become dryer. This season spans from December to April. For both time periods 2020- 2049 and 2070-2099, WASCAL projected a maximum decrease of – 91.7% and CORDEX a decrease of – 96 % during the dry season. However, for both climate products an increase in hydropower for both time periods is projected for the wet season.

An analysis was further done to see the effects of climate change on the hydropower economic potential. It was concluded in Chapter 6 that with the results obtained projected climate change will cause an increase of electricity prices in the dry season from an average of 0.18 $ per kilowatt

hour in the Black Volta basin (up to 0.30$). Furthermore, the proposed hydropower power plant is a run of river plant meaning there is no need of constructing a dam or reservoir to store water for power generation, however with the following projections that dry seasons will become drier and the projected decrease in hydropower potential they might be need of constructing a reservoir or small dam to store water for power generation in the dry season. Construction of reservoirs increases the capital cost of the proposed Bamboi mini hydropower plant, from the above discussion it can be concluded that climate change will affect the hydropower economic potential of Bamboi catchment.

The above mentioned results will assist the authorities to design adaptation strategies for harnessing hydropower resource in order to solve the electricity shortage in the region and improving the socio economic developments in the region. The outcome of this research could assist the authorities and the community of the Volta Basin in managing the use of water resources in the catchment.

The achieved results allow answering the research questions formulated in the general introduction as follows:

1.How efficient is the HBV hydrological model in simulating the hydrological regime of the Bamboi catchment?

The HBV model was successful in simulating the hydrological regime of the Bamboi catchment as evidenced by the statistical quality measures producing minimum values of 0.57 for Nash Sutcliffe Efficiency, 0.73 for Kling-Gupta Efficiency and 0.59 for R^2 during the calibration and validation. All these values indicate a good agreement between observed and simulated variables making the model suitable for impact assessment.

2.What is the likely trend in climate for the future period 2020- 2099 compared to the historical period 1983-2005 and how is this trend likely to impact hydro power generation in the catchment?

Temperature will increase in both future periods so is precipitation, however the hydropower potential will decrease for both future periods**.**

3.What is the expected impact of climate change on hydropower potential of the Bamboi catchment?

Hydropower is projected to decrease in the dry season December to April. Overall, both climate model predicts a decrease in hydropower in the mid-century period 2020 -2049 and late century 2070 - 2099 as compared to the reference period 1983-2005. However, all models considering uncorrected and corrected data are agreeing that hydropower production is projected to increase slightly towards the end of the century 2070 – 2099 as compared to the mid-century except for CORDEX corrected data.

Recommendations

Although the impact of climate change on hydropower generation is irreversible there are still many methods to mitigate climate change. Among others methods are the development of advanced technology, and models that can accurately predict climate change signal. Climate factor uncertainty must be considered when planning for hydropower projects and future development plans in the Volta Basin must take into account the potential effect of climate change in order to design sustainable and efficient water management strategies in order to combat climate change. Government effort should also not be underestimated, for every project to succeed it must have government support therefore Governments should be at the center of climate change adaptation strategies and promotion of long sustainability of hydropower development. Predictions of climate change impacts on hydropower potential in the Bamboi catchment gives enough warning signs that decision-makers need to be thinking of a more resilient mix of options for energy to stand up to the climate challenge in future. The results also show the importance of harnessing the potential of run-of-river hydropower systems in the region.

BIBLIOGRAPHY

1. Akpoti, K. (2016). Impacts of Rainfall Variability, Land Use and Land Cover Change on Stream Flow of the Black Volta Basin, West Africa (ABDOU MOUMOUNI; Vol. 3). https://doi.org/10.3390/hydrology3030026

2. 2. Allwaters consult, & Limited. (2012). *DIAGNOSTIC STUDY OF THE BLACK VOLTA BASIN IN GHANA Final Report*.

3. Amisigo, B. A., McCluskey, A., & Swanson, R. (2014). Modeling impact of climate change on water resources and agriculture demand in the Volta Basin and other basin systems in Ghana. In *Sustainability (Switzerland)* (Vol. 7). https://doi.org/10.3390/su7066957

4. Atulley, J. (2013). *Impact of Small Reservoirs and Dugouts in Ghana on Hydrology and Water Allocation in the Black Volta Basin* (Kwame Nkrumah University of Science and TechnologyATULLEY).Retrieved-from https://cgspace.cgiar.org/handle/10568/42166%5Cnhttp://ir.knust.edu.gh/handle/1234567 89/5380

5. Berga, L. (2016). The Role of Hydropower in Climate Change Mitigation and Adaptation: A Review. *Engineering*, *2*(3), 313–318. https://doi.org/10.1016/J.ENG.2016.03.004

6. Boadi, S. A., & Owusu, K. (2017). Impact of climate change and variability on hydropower in Ghana.AfricanGeographical *Review*, *6812*, 1–15. https://doi.org/10.1080/19376812.2017.1284598

7. Canyon Hydro. (2013). An Introduction to Hydropower Concepts and Planning Guide to Hydropower. *Guide to Hydropower*. Retrieved from http://www.asociatiamhc.ro/wp-content/uploads/2013/11/Guide-to-Hydropower.pdf

8. Climate Change and Hydropower. (2014). Climate Change and Hydropower.

9. Coulibaly, N., Coulibaly, T., Mpakama, Z., & Savané, I. (2018). The Impact of Climate Change on Water Resource Availability in a Trans-Boundary Basin in West Africa: The Case of Sassandra. *Hydrology*, *5*(1), 12. https://doi.org/10.3390/hydrology5010012

10. ENERGY FOR GROWTH HUB. (2019). ENERGY POVERTY IMPACTS THREE BILLION PEOPLE. TIME TO THINK BIG.

11. Energypedia. (2019). Energypedia.

12. FAO. (1985). Integrating crops and livestock in West Africa. In *FAO ANIMAL PRODUCTION AND HEALTH PAPER 41*. https://doi.org/ISBN 92-5-101443-4

13. Future climate change for Africa. (2019). Regional overview: A century of climate change, 1950–2050.

14. Giorgi, F., Jones, C., & Asrar, G. R. (2009). Addressing climate information needs at the regional level: the CORDEX framework. *World Meteorological Organization Bulletin*, *58*(3), 175–183. https://doi.org/10.1109/ICASSP.2009.4960141

15. Hamududu, B., & Killingtveit, A. (2012). Assessing climate change impacts on global hydropower. *Energies*, *5*(2), 305–322. https://doi.org/10.3390/en5020305

16. Harrison, G., Whittington, H., & Gundry, S. (2014). Climate change impacts on hydroelectric power. *Proc Univ Power Eng Conf*, *1*(1), 391–394. Retrieved from http://scholar.google.com/scholar?hl=en&btnG=Search&q=intitle:CLIMATE+CHANGE +IMPACTS+ON+HYDROELECTRIC+POWER#0

17. Heinzeller et al. (2018). The WASCAL high-resolution regional climate simulation ensemble for West Africa: concept, dissemination and assessment. *Earth System Science Data*, *10*(2018), 815–835.

18. IRENA. (2019). *RENEWABLE CAPACITY STATISTICS 2019*.

19. Jie Chen François P. Brissette Diane Chaumont Marco Brau. (2013). water resources research. *Advancing Earth and Space Sciences Journal*.

20. Khaniya, B., Priyantha, H.G., Baduge, N., Azamathulla, H.M., Rathnayake, U. (2018). Impact of climate variability on hydropower generation: A case study from Sri Lanka. *Journal of Hydraulic Engineering*, 1–9. https://doi.org/https://doi.org/10.1080/09715010.2018.1485516

21. Kharagpur. (2012). *Module 5 - Hydropower Engineering* (Vol. 2). Retrieved from http://nptel.ac.in/courses/105105110/pdf/m5l01.pdf

22. Maraun, D. (2016). Bias Correcting Climate Change Simulations - a Critical Review. *Current Climate Change Reports*, (10/ 06/2019), 211–220. https://doi.org/10.1007/s40641-016-0050-x

23. Masson-Delmotte, V., Zhai, P., Pörtner, H.-O., Roberts, D., Skea, J., Shukla, P. R., … Waterfield, T. (2018). Global warming of 1.5°C An IPCC Special Report. In *Report of the Intergovernmental Panel on Climate Change* (Vol. 265). Retrieved from

https://report.ipcc.ch/sr15/pdf/sr15_spm_final.pdf

24. Mbaye, M. L., Hagemann, S., Haensler, A., Stacke, T., Gaye, A. T. (2015). Assessment of Climate Change Impact on Water Resources in the Upper Senegal Basin (West Africa). *Climate Change*, *4*, 77–93. Retrieved from doi:10.4236/ajcc.2015.41008, 2015

25. Moriasi, D. N., Arnold, J. G., Liew, M. W. Van, Bingner, R. L., Harmel, R. D., & Veith, T. L. (2007). M e g s q a w s. *MODEL EVALUATION GUIDELINES FOR SYSTEMATIC QUANTIFICATION OF ACCURACY IN WATERSHED SIMULATION*, *50*(3), 885–900.

26. Mouhamadou Bamba Sylla, Pinghouinde Michel Nikiema, Peter Gibba, I. K. and N. A. B. K. (2016). Climate Change over West Africa: Recent Trends and Future Projections. In J. H. Joseph A. Yaro (Ed.), *Adaptation to Climate Change and Variability in Rural West Africa* (pp. 25–40). https://doi.org/10.1007/978-3-319-31499-0_3

27. Neumann, R., Jung, G., Laux, P., Kunstmann, H., Neumann, R., Jung, G., … Karlsruhe, F. (2010). *Climate trends of temperature , precipitation and river discharge in the Volta Basin of West Africa*. *5124*(April 2013), 37–41. https://doi.org/10.1080/15715124.2007.9635302

28. OBAHOUNDJE Salomon. (2015). *Université abdou moumouni*. ABDOU MOUMOUNI.

29. Okot, D. . (2013). Review of small hydropower technology. *Renewable and Sustainable Energy Reviews*, *26*, 515–520. Retrieved from https://doi.org/10.1016/j.rser.2013.05.006

30. Otuagoma, S. O. (2016). *Turbine Selection Criteria for Small Hydropower Development – The River Ethiope Experience . S O Otuagoma*. *02*(05), 34–40.

31. Penche, C. (2004). Guide on how to develop a small hydropower plant. *European Small Hydropower Association*.

32. Power Africa. (2018). USAID.

33. Riverso, C. (2010). *Calibration of rainfall-runoff models Summary of contents* (ALMA MATER STUDIORUM - UNIVERSITÀ DI BOLOGNA). Retrieved from https://core.ac.uk/download/pdf/11806898.pdf

34. Savelsberg, J., Schillinger, M., Schlecht, I., & Weigt, H. (2018). The impact of climate change on Swiss hydropower. *Sustainability (Switzerland)*, *10*(7). https://doi.org/10.3390/su10072541

35. Sedogo, L., Lamers, J., & Fonta, W. (2015). Climate -Smart Agriculture. *Policies and Instructions Conducive for Enehancing the Transfer to CSA in Africa*. Mont pellier France.

36. Seibert, J. (2005). HBV light version 2 User Manual. In *User's manual, Department of*

Earth Science, Hydrology, Uppsala University. New Oregon State.

37. Seibert, J., & Vis, M. J. P. (2012). Teaching hydrological modeling with a user-friendly catchment-runoff-model software package. *Hydrology and Earth System Sciences*, *16*(9), 3315–3325. https://doi.org/10.5194/hess-16-3315-2012

38. Sweden, & Jonas Olsson , Berit Arheimer , Matthias Borris , Chantal Donnelly, Kean Foster , Grigory Nikulin , Magnus Persson , Anna-Maria Perttu , Cintia B. Uvo, M. V. and W. Y. (2016). Hydrological Climate Change Impact Assessment at Small and Large Scales: Key Messages from Recent Progress in Sweden. *Climate*, *4*(3). Retrieved from https://doi.org/10.3390/cli4030039

39. Sylla, M. B., Giorgi, F., Coppola, E., and Mariotti, L. (2003). International Journal of climatology. *Uncertainties in Daily Rainfall over Africa: Assessment of Gridded Observation Products and Evaluation of a Regional Climate Model Simulation*, *33*, 1805–1817. Retrieved from https://doi.org/10.1002/joc.3551

40. TEMIZ, A. (2013). *DECISION MAKING ON TURBINE TYPES AND CAPACITIES FOR RUN-OF-RIVER HYDROELECTRIC POWER PLANTS A CASE STUDY ON EGLENCE-1 HEPP A Thesis Submitted to in Energy Engineering*. (June).

41. Thomas Poméon, Dominik Jackisch, B. D. a. (2017). Journal of Hydrology. *Evaluating the Performance of Remotely Sensed and Reanalysed Precipitation Data over West Africa Using HBV Light*, *547*(03 JUNE 2019), 222–235. https://doi.org/10.1016/j.jhydrol.2017.01.055

42. Thomson, A. M., Patel, P., Volke, A., Edmonds, J. A., Delgado-Arias, S., Wise, M. A., … Kyle, G. P. (2011). RCP4.5: a pathway for stabilization of radiative forcing by 2100. *Climatic Change*, *109*(1–2), 77–94. https://doi.org/10.1007/s10584-011-0151-4

43. Tirpack Denis, L. E. (2006). Adaptation to Climate Change: Key Terms. *Environment Directorate International Energy Agency*, 5–23. Retrieved from http://www.oecd.org/env/cc/%0A3

44. UNDP. (2019). *climate change adaptation*.

45. UNEP-GEF Volta Project. (2013). *Volta Basin Transboundary Diagnostic Analysis*. Accra.

46. Universite Catholique de Louvain. (2008). Introduction to climate dynamics and climate modelling.

47. USAID. (2017). *Climate Change Adaptation in WESTERN AFRICA*.

48. world bank. (2018). Regional Power Trade in West Africa Offers Promise of Affordable, Reliable Electricitye.

49. Yira Yacouba , Bernd Diekkruger, Gero Stepup, A. Y. B. (2017). Impact of climate change on hydrological conditions in a tropical West African catchment using an ensemble of climate simulations. *Hydrology and Earth System Sciences*, *21*, 2143–2161. https://doi.org/10.5194/hess-21-2143-2017

APPENDIX

8.1.APPENDIX 1: RCODE FOR BIAS CORRECTION

select a grid cell / column.

.libPaths('D:/R/Lib')

require(qmap)

require(stats)

require(hydroGOF)# for rmse alone

####### reshape function

read in the text files

Mod_2020_2049 = read.csv ("C:/Users/Cynthia/Desktop/New_folder_2/uncorrected intermediate/NEWHUMIDITY2020-2049.csv",sep="\t");Mod_2020_2049Mod_2070_2099 = read.csv("C:/Users/Cynthia/Desktop/New_folder_2/uncorrectedfuture/NEWHUMIDITYFUTURE2070-2099.csv",sep="\t");Mod_2070_2099obs_new = read.csv("C:/Users/Cynthia/Desktop/New_folder_2/uncorrected_data_historical/OBSERVEDRH1.csv",sep="\t");obs_newmod_new = read.csv("C:/Users/Cynthia/Desktop/New_folder_2/uncorrected_data_historical/NEWHUMIDITYWORK1983-2005.csv",sep="\t"); mod_new# select a grid cell / column.

(In reality: loop through all to correct the whole data set)

in the lab session we will only explore a few grid cells

first: check the calibration period

change the calibration period

calibration.start='1983-01-01'

calibration.end='2005-12-31'

Selecting the data column

ggg=2

Getting the index corresponding to the calibration period

find.start = which(obs_new[,1] ==calibration.start);find.start

find.end = which(obs_new[,1] ==calibration.end);find.end

now get familiar with the data set, construct qqplots

plot time seriesplot(obs_new[find.start:find.end,ggg], mod_new[find.start:find.end,ggg], xlim=c(0,60),ylim=c(0,60),ylab = 'Model Historical Period', xlab ='Observed Historical Period')

plot(sort(obs_new[find.start:find.end,ggg]), sort(mod_new[find.start:find.end,ggg]),ylab = 'Model Historical Period', xlab ='Observed Historical Period')

lines(sort(obs_new[find.start:find.end,ggg]), sort(obs_new[find.start:find.end,ggg]),col=2)

plot ecdfs

plot(ecdf(mod_new[find.start:find.end,ggg]),col=2)   # add original model data

plot(ecdf(obs_new[find.start:find.end,ggg]), add=T)   # reference data

what does the plot tell you?

is there a bias in the data set?# yes? Great, then let's start with the bias correction

now perform the quantile mapping

newfit = fitQmapQUANT(obs_new[find.start:find.end,ggg],mod_new[find.start:find.end,ggg],wet.days= T,qstep=.0001,nboot=100)

mod_corr = doQmapQUANT(mod_new[find.start:find.end,ggg],newfit)

#Saving the corrected data into a file

write.csv(data.frame(mod_corr),

     "D:/RESULTS OF R/GFDLESM_NEW_HUMIDITY_historic_corrected.csv")

For future data correction only

mod_corr_Future = doQmapQUANT(Mod_2020_2049[,2],newfit)

Saving the corrected data into a file

write.csv(data.frame(mod_corr_Future),

     "D:/RESULTS
OFR/Mod_2020_2049_GFDLESM_NEW_HUMIDITY_future_corrected.csv"

For future data correction only

```
mod_corr_2070_2099 = doQmapQUANT(Mod_2070_2099[,2],newfit)

# Saving the corrected data into a file

write.csv(data.frame( mod_corr_2070_2099),

    "D:/RESULTS
OFR/Mod_2070_2099_GFDLESM_NEW_HUMIDITY_future_corrected.csv")

#add the cdf of the bias corrected data mod_corr to the plot

lines(ecdf(mod_corr),col=3)

# Plotting the corrected values

plot(sort(obs_new[find.start:find.end,ggg]), sort(mod_corr))

lines(sort(obs_new[find.start:find.end,ggg]), sort(mod_corr), col=3)

abline(lsfit(sort(obs_new[find.start:find.end,ggg]), sort(obs_new[find.start:find.end,ggg])),col=4)

# evaluate the calibration period:

rmse(obs_new[find.start:find.end,ggg],mod_new[find.start:find.end,ggg])

rmse(obs_new[find.start:find.end,ggg],mod_corr[find.start:find.end])

plot(ecdf(obs_new[find.start:find.end,ggg]),col= 'black')

lines(ecdf(mod_new[find.start:find.end,ggg]),col='red')

lines(ecdf(mod_corr[find.start:find.end]),col='blue')

qqplot(obs_new[,ggg],mod_new[,ggg],distribution                                  =
qnorm,xlim=c(0,50),ylim=c(0,50),xlab="obs",ylab="mod")

qqplot(obs_new[,ggg],mod_corr,distribution                                       =
qnorm,xlim=c(20,50),ylim=c(20,50),xlab="obs",ylab="mod")

#check ecdfs

plot(ecdf(obs_new[,ggg]))             # reference data

lines(ecdf(mod_new[,ggg]),col=2)    # add original model data

lines(ecdf(mod_corr),col=4)          # add bias corrected model data
```

8.2. APPENDIX 2: RESEARCH BUDGET

RESEARCH BUDGET

S/No.	Item	Explanation	Unit	Quantity	Rate (Unit price)	Amount*	Comment*** (For Evaluator Only)	Time line
	(A) Material and Supplies							
1	Software License	Homer				185		April
2	Internet recharge For 6 months					600		Mar to July
3								
	Sub Total					**785**		
	(B) Equipment							
1	Meteorological Data	Climate data						April
2	GPS hiring			190		190		April
3	Hiring Weirs and strings for measuring etc			100		100		April
4	Stationery , printing and binding					300		May to July
	Sub Total					**590**		
	(C) Travel + Visa Costs							
1	Flight-from Burkina Faso to Ghana					400		May
2	Transport Tlemcen to Algiers		2	25		50		March

3	Visa		1			130		March
4	Travel insurance					75		April
	Sub Total					**675**		
		(D) Special Activities						
1	e.g. Publication	.				300		July
2	French - English translation		1			250		April
5	Field transport					400		April to May
	Sub Total					**950**		
		(E) Contingencies (%) optional l				####		
A		Personnel						
B		Material & Supplies				785		
C		Equipment				590		
D		Travel				675		
E		Special Activities				950		
F		Contingencies (%) - optional				0		
		Grand Total				3000		